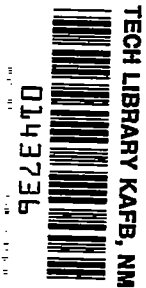


NACA



RESEARCH MEMORANDUM

INVESTIGATION OF THE CHARACTERISTICS
OF A HIGH-ASPECT-RATIO WING IN THE
LANGLEY 8-FOOT HIGH-SPEED TUNNEL

By

Richard T. Whitcomb

Langley Memorial Aeronautical Laboratory
Langley Field, Va.

CLASSIFIED DOCUMENT

This document contains classified information which, if disclosed, could be injurious to the national defense of the United States. It is to be controlled, stored, handled, transmitted, and disposed of in accordance with the provisions of the Espionage Laws, Title 18, U.S.C., and the Executive Order, No. 11652, of April 14, 1950, and any amendments or supplements thereto. It is to be controlled, stored, handled, transmitted, and disposed of in accordance with the provisions of the Espionage Laws, Title 18, U.S.C., and the Executive Order, No. 11652, of April 14, 1950, and any amendments or supplements thereto. It is to be controlled, stored, handled, transmitted, and disposed of in accordance with the provisions of the Espionage Laws, Title 18, U.S.C., and the Executive Order, No. 11652, of April 14, 1950, and any amendments or supplements thereto.

**NATIONAL ADVISORY COMMITTEE
FOR AERONAUTICS**

WASHINGTON

August 28, 1946

RM L6H28a 7064

319.9811

NATIONAL ADVISORY COMMITTEE FOR AERONAUTICS

RESEARCH MEMORANDUM

INVESTIGATION OF THE CHARACTERISTICS
OF A HIGH-ASPECT-RATIO WING IN THE
LANGLEY 8-FOOT HIGH-SPEED TUNNEL

By Richard T. Whitcomb

SUMMARY

An investigation of the characteristics of a wing with an aspect ratio of 9.0 and an NACA 65-210 airfoil section has been made at Mach numbers up to 0.925. The wing tested has a taper ratio of 2.5:1.0, no twist, dihedral, or sweepback, and 20-percent-chord 37.5-percent-semispan plain ailerons. The results showed that serious changes in the normal-force characteristics occurred when the Mach number was increased above 0.74 at angles of attack between 4° and 10° and above 0.80 at 0° angle of attack. Because of small outboard shifts in the lateral center of load, the bending moment at the root for conditions corresponding to a 3g pull-out at an altitude of 35,000 feet increased by approximately 5 percent when the Mach number was increased from 0.77 to 0.90. When the Mach number was increased beyond 0.83 the negative pitching moments for the high angles of attack increased, whereas those for the low angles of attack decreased with a resulting large increase in the negative slope of the pitching-moment curves. A large increase occurred in the values of the drag coefficients for the range of lift coefficients needed for level flight at an altitude of 35,000 feet when the Mach number was increased beyond a value of 0.80. The wakes at a station 2.82 root chords behind the wing quarter-chord line extended approximately a chord above the wing chord line for the angles of attack required to recover from high-speed dives at high Mach numbers.

INTRODUCTION

The recent development of turbine-jet units of relatively high thrust ratings has made possible the

consideration of jet-propelled airplanes with maximum speeds greater than 500 miles per hour. Until the present time, however, very little information has been available on the aerodynamic characteristics of the component parts of an airplane designed to operate at these high speeds. In order to design such a high-speed airplane properly, more information about these characteristics at high and low speeds was needed. The NACA has undertaken a broad research program to supply this additional information. In conjunction with this program a series of tests have been made on a high-aspect-ratio wing in the Langley 8-foot high-speed tunnel in order to determine the effects of compressibility on the characteristics of such a wing at Mach numbers approaching unity. Included in the series of tests were investigations of the basic wing characteristics, aileron characteristics, effects of dive brakes and a dive-recovery flap, and downwash fluctuations. The results of the first investigation are presented herein. The results of the other investigations are presented in references 1, 2, and 3, respectively.

The results presented herein include the normal-force, span-loading, pitching-moment, drag, and wake-width data for the wing alone with undeflected straight-sided ailerons. Data for Mach numbers up to 0.925 are presented.

SYMBOLS

Symbols are defined as follows:

- a speed of sound in undisturbed stream, feet per second
- a_N slope of normal-force curve (dC_N/da), per degree
- b span of model, feet (3.15)
- C effective area of tunnel cross section, square feet (49.5)
- C_L lift coefficient
- c section chord of model, feet
- \bar{c} average model chord, feet (0.35)

c'	mean aerodynamic chord (M.A.C.), feet (0.37)
ΔH	loss of total pressure in wake
L	lift on model, pounds
M	Mach number (V/a)
$M_c/4$	pitching moment about 25-percent-chord line
p_o	static pressure in undisturbed stream, pounds per square foot
p	local static pressure at a point on airfoil section, pounds per square foot
P	pressure coefficient $\left(\frac{p - p_o}{q} \right)$
q	dynamic pressure, pounds per square foot $\left(\frac{1}{2} \rho V^2 \right)$
S	area of model, square feet (1.10)
V	velocity in undisturbed stream, feet per second
x	distance along chord from leading edge of section, feet
y	distance along semispan from wing center line, feet
y'	distance from root section to center of lift, feet
α	angle of attack, degrees
γ	ratio of specific heats
ρ	mass density in undisturbed stream, slugs per cubic foot

Subscripts:

cr	critical
L	lower surface of airfoil section
U	upper surface of airfoil section

[REDACTED]

The coefficients are defined as follows:

c_n section normal-force coefficient

$$c_n = \frac{1}{c} \int_0^c (P_L - P_U) dx$$

c_m section pitching-moment coefficient about 25-percent-chord station

$$c_m = \frac{1}{c^2} \int_0^c (P_U - P_L) \left(x - \frac{c}{4} \right) dx$$

C_N wing normal-force coefficient

$$C_N = \frac{2}{S} \int_0^{b/2} c_n dy$$

$C_{m_c}/4$ wing pitching-moment coefficient about 25-percent-chord station

$$C_{m_c}/4 = \frac{2}{Sc^4} \int_0^{b/2} c^2 c_m dy$$

C_B bending-moment coefficient for root section

$$C_B = \frac{4}{Sb} \int_0^{b/2} c_n c_y dy$$

$2y'/b$ lateral position of center of load

$$\frac{2y'}{b} = \frac{C_B}{C_N}$$

C_{B60} bending-moment coefficient for 60-percent-semispan station

$$C_{B60} = \frac{4}{Sb} \int_{0.3b}^{0.5b} c_{cn}(y - 0.3b) dy$$

C_{B60}/C_N design index for bending moments at 60-percent semispan station

C_{D0} wing profile-drag coefficient

C_{D1} wing induced-drag coefficient

$$C_{D1} = 0.036C_L^2$$

C_D wing total-drag coefficient

$$C_D = C_{D0} + C_{D1}$$

APPARATUS

The Langley 8-foot high-speed tunnel, in which the tests were conducted, is of the single-return, closed-throat type. The Mach number at the throat is continuously controllable. The air-stream turbulence in the tunnel is small but slightly higher than in free air.

The wing tested has an NACA 65-210 airfoil section, an aspect ratio of 9.0, a taper ratio of 2.5:1.0, no sweepback, twist, or dihedral, a tip having ordinates given in table I, and a 20-percent-chord, 37.5-percent-semispan plain aileron that extends from the 60-percent-semispan station to the end of the straight part of the trailing edge. The wing, as tested, is shown in figure 1. The effective span of the model is 37.8 inches, the root chord is 6 inches, and the tip chord is 2.4 inches. Other dimensions are given in figure 2. The ordinates of the NACA 65-210 airfoil used for the inboard sections are presented in table II. For the sections outboard of the 40-percent-span station, the ordinates ahead of the 80-percent-chord station are the same as those given in

table II but from 80-percent chord to the trailing edge, the contours of these sections are straight lines. The wing was machined from medium hard brass. The ailerons were machined from steel and are attached to the wing by small hinges.

Twenty static-pressure orifices were placed at each of eight stations along the wing span. The approximate chordwise locations of these orifices at each station are shown in figures presenting pressure-distribution data. The spanwise locations of the stations are 11, 20, 30, 43, 56, 64, 80, and 95 percent of the semispan. The four inboard stations were placed on the left half of the wing and the four outboard stations were placed on the right half.

The model was supported in the tunnel by means of a vertical steel plate as shown in figure 1(b). The plate was designed to have zero velocity gradients in the direction of the stream and to produce minimum variations in velocity along the span near the test region at the Mach numbers scheduled. The profile of the plate is a modified ellipse, the ordinates for which are presented in table III and the dimensions and construction details of the plate are shown in figure 3. The angle of attack of the model was changed during the test by the mechanism shown in figure 3. The steel pressure tubes in the model were connected to tubes that passed through the hollow part of the plate and were connected to multiple-tube manometers. Wake surveys were made by a rake, which has 42 total-pressure tubes and 7 static-pressure tubes, placed behind the model as shown in figures 1(c) and 3. The vertical spacing of the total-pressure tubes varies from 0.1 inch at the center of the rake to 2 inches at the tips of the rake. The rake is supported in the tunnel by means of a horizontal strut, the leading edge of which is approximately 5 inches behind the trailing edge of the vertical support plate.

METHODS AND PROCEDURES

Support System

The use of a vertical steel plate as the support of the model was chosen for the following reasons:

(1) The large, unknown interference effects produced at high Mach numbers by struts of the usual type were completely eliminated.

(2) Inasmuch as the plate effectively produced a new test section, the frontal area of the model was the only factor contributing to choking of the air stream. The highest possible choking Mach number that could be obtained in an 8-foot circular tunnel with a model of the size tested was therefore realized.

(3) The necessity of having a portion of the model enveloped by a relatively thick boundary layer, as would be the case if a semispan model had been supported at the tunnel wall, was avoided.

(4) The symmetrical installation eliminated the possibility of unsymmetrical choking or of cross flows, such as would be expected if a semispan model, mounted from the tunnel wall or from a reflection plate near the wall, were employed.

Calibration Tests

A series of calibration tests of the tunnel air stream were made with the support plate installed both with and without the wake-survey-rake support strut installed. Static pressures were determined at 30 points on the plate and at 36 points on the tunnel wall at Mach numbers up to 0.95 with and without the model in place. The calibration tests with the model were made for angles of attack of 0° , 4° , and 9° and a series of tests were also made to determine the static pressures and the angles of flow at the model position. A combination of a calibrated static head and a yaw head mounted on the wake-survey-rake support strut was used for these tests.

A comparison of the static pressures measured on the surfaces of the plate and walls and by the static-pressure tube indicates that the Mach number and dynamic-pressure variations in the air stream in the region of the model are small. The variations in these values at the surfaces of the plate in the direction of the air stream are less than 0.2 percent through distances of 1 foot from the model position at all Mach numbers up to 0.90. The vertical variations are less than 0.2 percent through distances

[REDACTED]

of 2 feet from the model position. The spanwise variations are less than 1.0 percent through a distance of 20 inches from the plate and 2.5 percent from the plate to the wall at Mach numbers up to 0.90. The dynamic pressures used to obtain the coefficients were determined from averages of the pressures measured near the model position.

The angularity of the stream flow in a horizontal plane has been found to be less than 0.1° , this value being the limit of the accuracy of the calibrating instrument.

Limiting Test Mach Numbers

The tunnel choked at the support plate at a Mach number of 1.0 without the model in place. The tunnel choked at the model at an uncorrected Mach number of 0.95 with the support plate and model in place. Numerous tests have indicated that the data obtained in a wind tunnel when choking occurs at the model are not applicable to the prediction of wing characteristics for free air (reference 4). The data obtained at the choking Mach number of 0.95, therefore, have not been presented.

Static-pressure measurements made on the tunnel wall and model support plate at an uncorrected Mach number of 0.925 indicate that there is a perceptible tendency toward choking at the plane of the model at this Mach number. The results obtained at this Mach number, even if completely corrected for the usual effects of tunnel-wall interference, may not, therefore, indicate the flight characteristics. The general trends, however, are believed to be illustrated by the results obtained at this Mach number.

With the support strut for the wake-survey rake in place the tunnel choked at this strut when the uncorrected Mach number at the plane of the model was 0.882. As previously mentioned, a calibration test was made with the wake-survey strut in place. The results of this test show that no invalidating choking effects occur at the plane of the model when the tunnel chokes at the survey strut. Choking at the survey strut simply imposes a limitation on the maximum test Mach number instead of affecting the applicability of the results. The data on

the model with the wake-survey strut in place can thus be assumed to be correct up to the choking Mach number of the wake-survey strut and data up to this Mach number have been presented.

Tests

All normal-force and pitching-moment data were obtained from pressure-distribution measurements and all drag data were obtained from wake surveys. The pressure and wake measurements were made during separate test runs. Pressure-distribution measurements were made at the following uncorrected Mach numbers and angles of attack: for Mach numbers of 0.400, 0.600, 0.760, 0.800, 0.825, and 0.850 at angles of attack of -2° , 0° , 2° , 4° , 7° , and 10° ; for Mach numbers of 0.900, and 0.925, at angles of attack of 0° , 2° , 4° , and 7° . The pressures at the 160 orifices in the wing were recorded simultaneously by photographing the multiple-tube manometers.

Wake-survey measurements were made at six spanwise stations 1.40 root chords behind the 25-percent-chord line of the wing. These stations were 20, 40, 60, 80, 95, and 102 percent of the wing semispan from the wing support plate. These measurements were made for uncorrected Mach numbers of 0.400, 0.600, 0.725, 0.760, 0.800, 0.850, and 0.883 at angles of attack of 0° , 2° , 4° and 7° . In order to obtain wake-width measurements at a typical tail location, wake surveys were made at a station 2.82 root chords behind the 25-percent-chord line of the wing and 0.265 semispan from the plate.

Corrections for Tunnel-Wall Interference

Calculations using the methods of references 5 to 8 have been made to estimate the magnitude of the effect of tunnel-wall interference on the Mach number, the dynamic pressure, and the normal force, pitching moment, and drag. Three types of interference have been considered:

- (1) Model constriction
- (2) Wake constriction
- (3) Lift vortex interference

The basic formulas employed to determine the effects of solid blockage and lift vortex interference are taken from reference 5. The formulas for wake constriction have been developed from reference 6. Most of the corrections for effects of compressibility are from reference 7, and further corrections for these effects came from reference 8. The following expressions were used; For the effects of model and wake constriction,

$$\frac{\Delta V}{V} = \frac{0.0515}{c^{3/2}(1 - M^2)^2} \int_{-b/2}^{b/2} c^2 dy + \frac{(1 + 0.4M^2)}{4c(1 - M^2)^{3/2}} C_{DS}$$

and

$$\frac{\Delta M}{M} = \frac{\Delta V}{V} \left(1 + \frac{\gamma - 1}{2} M^2 \right)$$

$$\frac{\Delta q}{q} = \frac{\Delta V}{V} (2 - M^2)$$

For the effects of lift vortex interference,

$$\Delta C_L = \frac{\pi^2}{48} \frac{L\bar{c}}{qc^{3/2}(1 - M^2)}$$

$$\Delta C_{mc}/4 = \frac{\pi^2}{192} \frac{L\bar{c}}{qc^{3/2}(1 - M^2)}$$

$$\Delta \alpha = \frac{0.598\pi(L\bar{c} + 4M_c/4)}{qc^{3/2}\sqrt{1 - M^2}} + 7.16 \frac{s}{c} C_L$$

The magnitudes of the corrections obtained by the use of these expressions have been found to be very small even at test Mach numbers up to and including 0.90. At this Mach number, the corrections to the Mach number vary

from 0.4 percent at an angle of attack of 0° to 1 percent at 10° . The corrections to the coefficients for the lift vortex interference are even smaller. The corrections, the greater part of which arise from wake constriction, have been applied to all data obtained at test Mach numbers up to and including 0.90. The results obtained by the use of the aforementioned expression for the wake-constriction corrections have been compared with wake-constriction corrections determined by use of static pressures measured at the tunnel wall and the results of the two methods have been found to be substantially in agreement at test Mach numbers up to and including 0.90. It may be assumed, therefore, that no significant errors exist in the results for these Mach numbers as a consequence of tunnel-wall interference.

Corrections obtained by the indicated expressions for data obtained at a Mach number of 0.925 are much larger than the corrections for the lower Mach numbers; the corrections to the Mach numbers amount to as much as 2.5 percent, whereas those to the coefficients amount to 3.0 percent. Because of the close proximity of this Mach number to choke and to the speed of sound, these corrections are possibly unreliable. No corrections have been applied to the results obtained at this Mach number.

Corrections for Model Inaccuracies

During the construction of the model a washout of 0.3° developed in the right half of the wing. In addition, the wing was inadvertently tested with approximately a 0.3° negative aileron angle. The effects of these inaccuracies were indicated by the results of the tests made at an angle of attack of -2° , which is very close to the zero-lift condition at low Mach numbers. The distributions for this angle at low Mach numbers were not zero across the span but showed a slightly negative normal force at the tip. All the span load distributions have been corrected for these inaccuracies by the use of cross plots of section normal-force coefficient against angle of attack. The moment coefficients have also been similarly corrected.

Because of its relatively great torsional stiffness, the twist of the model due to air loads was small at all Mach numbers; calculations indicate that the twist was

less than 0.05° for all conditions. No corrections have been made for the effect of this twist.

RESULTS

Effects of Reynolds Number

The Reynolds numbers obtained during the tests varied from 900,000 at a Mach number of 0.400 to 1,400,000 at a Mach number of 0.907. These values are considerably lower than those for an airplane wing in flight. An indication of the effects of such a difference in Reynolds number on the characteristics of the NACA 65-210 airfoil section with and without ailerons may be obtained by referring to the two-dimensional data obtained for this section at various Reynolds numbers in the Langley two-dimensional low-turbulence pressure tunnel (references 9 and 10). The effects of Reynolds number variations at supercritical Mach numbers have not been fully established; however, the results of tests made on airfoils at supercritical Mach numbers for various Reynolds numbers (reference 11) indicate that at these Mach numbers the effects of variations in the Reynolds number are of secondary importance in comparison with the predominating effects of compressibility.

Pressure-Distribution Measurements

In order to illustrate the changes in the chordwise pressure distributions caused by compressibility effects, representative pressure distributions for the 30-percent-semispan station are presented in figure 4 and similar data for the 95-percent-semispan station are shown in figure 5. The chordwise pressure-distribution diagrams for all the spanwise stations have been integrated to determine section normal-force coefficients and pitching-moment coefficients. These coefficients have been used to determine the spanwise variations in section loadings and moments. The spanwise variations in section loadings are presented in figure 6. The spanwise-load distributions have been integrated to determine the total normal forces and the moments of these forces about the root chord. The variations of the normal-force coefficient with Mach number and angle of attack are presented in

figures 7 and 8, respectively. Because the accuracy of the results obtained at a Mach number of 0.925 is affected to an unknown extent by choking tendencies and tunnel-wall interference, all curves obtained by the use of these results are shown as broken lines. (See fig. 7.)

The slopes of the normal-force curves measured at values of the normal-force coefficient corresponding to a wing loading of 60 pounds per square foot at an altitude of 35,000 feet are presented in figure 9 as a function of Mach number. The lateral positions of the centers of the load on the wing in terms of the semispan are presented in figure 10. These values were obtained by dividing the values of the bending-moment coefficient by the corresponding values of normal-force coefficient. The lateral centers of load on the wing in terms of the semispan have been determined for an approximate 3g dive recovery and were obtained for the various Mach numbers at the angles of attack corresponding to a wing loading of 180 pounds per square foot at an altitude of 35,000 feet. (See fig. 11.) The critical stresses may not occur at the root but at some outboard station. To illustrate the changes in the bending moments that occur at the outboard stations, the bending-moment coefficients about the 60-percent-semispan station were computed by obtaining moments of the areas of the section-loading diagrams from the 60- to the 100-percent-semispan stations and dividing the moments thus obtained by the total area of the wing. The results were divided by the corresponding normal-force coefficients for the complete wing to obtain design indices for the bending moments at the 60-percent-semispan station. Values of these indices are presented in figure 12. The variation of section normal-force coefficients for the 30- and 95-percent-semispan stations with Mach number at angles of attack of 0° and 4° is presented in figure 13.

For all angles of attack and Mach numbers, the spanwise variations in section moment factor are presented in figure 14. The wing pitching-moment coefficients based on the mean aerodynamic chord have also been determined. The variations of these coefficients with Mach number for various values of angle of attack are presented in figure 15. The pitching-moment coefficient is plotted against normal-force coefficient for various values of Mach number in figure 16.

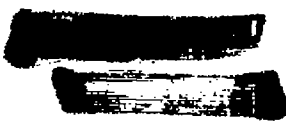
In all figures that include data for several angles of attack at a given Mach number (figs. 4, 5, 6, 8, 14, 16, 18, 20, and 21), the average values of the corrected Mach numbers for the several angles of attack are listed. The actual values of the corrected Mach numbers for the various angles of attack vary by less than 0.003 from this average at a Mach number of 0.907.

Wake-Survey Measurements

The total-pressure and static-pressure measurements made during the wake surveys at the six spanwise stations have been reduced to total wing profile-drag coefficients by use of the expressions presented in reference 12. The results are presented in figures 17 and 18.

The profile-drag coefficients at normal-force coefficients corresponding to wing loadings of 60 and 80 pounds per square foot at an altitude of 35,000 feet for the various Mach numbers have been determined. The induced-drag coefficients for the same normal-force coefficients have been computed. The variations of the total-drag coefficients with Mach number for the two wing loadings are presented in figure 19. For a wing loading of 60 pounds per square foot the induced-drag coefficient is 0.0083 at a Mach number of 0.600 and 0.0017 at a Mach number of 0.890. For a wing loading of 80 pounds per square foot the induced drag coefficient is 0.0147 at a Mach number of 0.600 and 0.0031 at a Mach number of 0.890.

The vertical variations of $\Delta H/q$ at a typical horizontal-tail location, a station 2.82 root chords behind the 25-percent-chord line and 0.265 semispan from the plate are presented in figure 20. Part of the wake-survey results obtained 1.40 root chords behind the 25-percent-chord line of the 40-percent-semispan station are presented in figure 21 to show the rate of the vertical spread of the wing wake with distance from the wing trailing edge. All wake dimensions are given in terms of the chords behind which the measurements were made.



DISCUSSION

Normal-Force Characteristics

No erratic changes in the normal-force characteristics are caused by compressibility effects at Mach numbers below the point of force break, which varies from a Mach number of about 0.74 at angles of attack between 4° and 10° to about 0.80 at 0° angle of attack. Beyond this Mach number, the normal force for a given angle of attack decreases rapidly (fig. 7). As a result there is an increase in the angle of zero lift and a decrease in the slope of the normal-force curve as shown in figure 9.

At angles of attack near the design condition, the changes in the normal-force characteristics occur at Mach numbers that are approximately 0.06 or 0.07 above the critical values, that is, the Mach numbers at which the local speeds of sound are exceeded at some point on the wing (fig. 7). At the angles of attack at which a negative pressure peak exists near the leading edge, however, the changes in the normal-force characteristics occur at Mach numbers 0.08 to 0.25 greater than the critical values. The Mach numbers at which the break in the normal-force coefficients occurs at the various angles of attack agree quite closely with the unpublished results obtained during tests of a two-dimensional NACA 65-210 airfoil section at Reynolds numbers approximately the same as those of the present tests in the Ames 1- by $3\frac{1}{2}$ -foot high-speed tunnel. This agreement indicates that the three-dimensional relieving effect, described in reference 13, was limited to the tip sections of the wing tested and the effect of this relief on the over-all characteristics is therefore negligible.

The data obtained at a Mach number of 0.925 indicate sharp increases in the normal-force coefficients for all angles of attack when the Mach number is increased beyond a value of 0.907. Results obtained in an open-throat tunnel where choking effects were considerably different from those present during these tests indicate similar increases for other airfoil sections in the same range of Mach numbers (reference 11).

[REDACTED]

The changes occurring above the points of force break will produce severe effects on the trim and stability characteristics of an airplane with the wing tested.

Span Loadings

The spanwise load distributions measured for low Mach numbers are nearly the same as those predicted by use of the charts presented in reference 14. (See fig. 6(a).) Figure 10 indicates that at angles of attack of 2° , 4° , 7° , and 10° the lateral centers of load move outboard when the Mach number is increased from about 0.77 to 0.90. When the Mach number is increased beyond 0.90, the center of load moves inboard. At a Mach number of 0.925, the center of load is approximately at the same position as it is at a Mach number of 0.80.

Figure 11 indicates that, as a result of the general outboard shift in the load, the bending moment produced at the root of the wing with a loading of the magnitude that would occur during a rapid recovery from a dive (approx. 3g at an altitude of 35,000 ft) is increased by 5 percent when the Mach number is increased from 0.77 to 0.90. This increase produces bending moments that are only 2.5 percent greater than those predicted by the charts of reference 14. A comparison of figure 10 and figure 12 indicates that for a given change in Mach number the bending moments at the 60-percent-semispan station increase more rapidly than do those at the root section. If the maximum stresses in the wing structure occur at this station, this fact must be considered.

At the lower angles of attack corresponding to level-flight conditions, the outboard movements of the lateral center of load are relatively large. Inasmuch as the stresses that occur at these angles of attack are not critical, such outboard shifts do not alter the structural requirements of a wing. These shifts would produce considerable changes in the downwash at the tail for a given lift coefficient, however, and thus would cause changes in the trim and stability characteristics of an airplane in addition to the changes in these characteristics produced by the reductions in lift coefficients and the changes in pitching-moment coefficients.

Pitching-Moment Characteristics

Extremely large and, in some cases, erratic changes occur in the pitching moments when the Mach number is increased beyond the point of force break as indicated in figure 15. Large increases occur in the negative pitching moments for all angles of attack when the Mach number is increased to 0.83. At this Mach number the negative pitching-moment coefficients for the angles of attack corresponding to design lift coefficients are more negative. When the Mach number is increased beyond 0.83, the negative pitching-moment coefficients for the high angles of attack continue to increase, whereas those for the low angles decrease. At a Mach number of 0.907 the pitching-moment coefficient for an angle of attack of 7° is -0.117, whereas that for an angle of attack of 2° is 0.012. Figure 16 indicates that there are only slight differences in the pitching-moment coefficients about the 25-percent-chord line at Mach numbers up to about 0.76. At Mach numbers greater than 0.76 the slope of the pitching-moment curve becomes negative. When the Mach number is increased beyond 0.83, the negative slope of the pitching-moment curve increases rapidly and this change produces a large increase in the stability of the airplane. The data obtained at a Mach number of 0.925 indicate sharp increases in the negative pitching moments for all angles of attack when the Mach number is increased beyond a value of 0.90 (fig. 15).

The neutral axis of most wing structures passes through points near the 40-percent-chord stations of the wing sections. The maximum measured twisting moment about this 40-percent-chord axis occurs at a Mach number of 0.600 for an angle of attack of 7° . The changes in the twist due to the variations in the pitching moments will further change the distributions of lift on a wing with resulting changes in the trim and stability characteristics of an airplane.

Drag Characteristics

The drag coefficient for a given angle of attack remains essentially unchanged when the Mach number is increased up to the critical value (fig. 17). At angles of attack near the design condition the drag starts to rise when the critical Mach number is reached and rises

[REDACTED]

abruptly at a Mach number about 0.06 greater than the critical value (fig. 17). At an angle of attack of 0° the critical Mach number is approximately 0.74; the drag coefficient starts to rise at about the same Mach number and rises abruptly at a Mach number of approximately 0.80. The data are insufficient to define exactly the Mach numbers at which the drag rises at higher angles of attack. A rough interpolation of the data obtained at these angles of attack indicates, however, that the drag does not start to rise until the critical Mach number is exceeded by at least 0.08 and the drag does not rise abruptly until the critical Mach number is exceeded by at least 0.12.

Figure 19 indicates that for a level-flight wing loading of 60 pounds per square foot at an altitude of 35,000 feet the drag rises abruptly when the Mach number is increased beyond a value of 0.80. An increase in the wing loading from 60 to 80 pounds per square foot does not change the Mach number at which the drag rise occurs by an appreciable amount. A comparison of the data for the two wing loadings indicates that, even for the supercritical Mach numbers, the increase in drag coefficient produced by increasing the wing loading is less than the resulting decrease in area. The drag for a given lift would therefore be smaller for the higher wing loading.

The results indicate that an airplane with a wing similar to the one tested cannot fly at Mach numbers greater than about 0.80 without a considerable margin of power above the value calculated to be needed at this Mach number by use of low-speed drag coefficients. In order to obtain level-flight Mach numbers appreciably greater than 0.80 without the use of excessively high amounts of power, the wing design must be changed radically. Until the present time the usual method of increasing the Mach number at which the rapid rise in drag coefficient occurs has been to change the wing section, in particular, the section thickness ratio. A reduction in the thickness of a wing with a plan form similar to that of the model tested to a value less than 10 percent would result in only a relatively small increase in the Mach numbers at which the rapid rise in drag coefficient occurs and would at the same time result in serious structural difficulties and, as shown in reference 10, in a large decrease in the maximum lift coefficient of the wing. The results presented herein indicate,


consequently, that a Mach number of 0.80 is the practical maximum that can be obtained with a wing having a conventional high-aspect-ratio plan form without the use of excessive amounts of power.

The data presented in reference 13 indicate that the Mach number at which the drag rise occurs on a wing with a given airfoil section can be increased by a considerable margin by decreasing the aspect ratio. A reduction in aspect ratio obviously also permits a higher structural efficiency if the same sections are used or it allows the use of thinner sections for a given structural efficiency. The use of a thinner section would result in a further increase in the Mach number at which the rise in the drag coefficient occurs. References 15, 16, and 17 indicate that the use of sweepback or sweepforward also delays the Mach number at which the drag rise occurs by large increments. The use of lower aspect ratios, sweepback, or sweepforward therefore offers possibilities for efficiently attaining flight Mach numbers greater than 0.80.

Section Characteristics

The chordwise pressure distributions measured for spanwise stations of 11-, 20-, 30-, 43-, 56-, 64-, and 80-percent semispan are similar at all test conditions up to those at which the wing begins to stall. The pressures obtained at the 30-percent-semispan station are presented as typical of the distributions obtained at these seven stations (fig. 4). When the Mach number is increased up to the critical value, the pressure coefficients for the various angles of attack increase at rates that are nearly equal to those predicted by the Glauert-Prandtl approximation.

When the Mach number is increased beyond the critical value at a given positive angle of attack, the pressures near the leading edge of the upper surface become more positive and the pressures near the trailing edge of this surface become more negative. The pressure coefficients on the lower surface continue to increase in magnitude gradually. (See fig. 4(d) to fig. 4(f).) The changes in the pressures on the upper surface, which are associated with the presence of supersonic velocities and separation on this surface, result in the reductions of the wing normal-force coefficients, the increases in the negative wing pitching-moment coefficients, and the large increases



in the wing drag coefficients shown in figures 8, 15, and 17, respectively. When the Mach number is increased beyond approximately 0.853 at angles of attack from 0° to 4° the critical Mach number for the lower surface is exceeded. The pressures near the leading edge of the lower surface then become more positive and the pressures near the trailing edge become more negative. The pressure coefficients on the upper surface continue to change in the same manner as at lower Mach number (fig. 4(f) and fig. 4(g)). As a result of the changes on the lower surface, the wing pitching-moment coefficients become much more positive. When the Mach number is increased beyond a value of approximately 0.907, a large increase in the negative pressure coefficients on the rear part of the upper surface occurs. The mean negative pressure coefficient on the lower surface decreases at the same time (fig. 4(h)). Because of these changes the wing normal-force coefficients increase (fig. 7) and the pitching-moment coefficients become more negative (fig. 15).

A comparison of figures 4 and 5 indicates that at a given Mach number the chordwise pressure distributions measured at the 95-percent-semispan station differ considerably from those measured at the 30-percent station which is typical of the seven inboard stations. At subcritical Mach numbers these differences in the pressure distributions are due to two factors. The primary factor is that the sections near the tip operate at local angles of attack that are considerably smaller than the local angles of attack of the inboard sections. A secondary factor is that the three-dimensional relieving effects, described in reference 13, are stronger near the tip than at the inboard stations and consequently the pressure coefficients at the outboard stations for a given local angle of attack are considerably more positive than at the inboard stations. As a result of these large spanwise variations in the chordwise pressure distributions the critical Mach numbers for the 95-percent-semispan station are considerably greater than the critical values for the inboard stations. For an angle of attack of 0° the critical Mach number is approximately 0.74 at the 30-percent-semispan station and approximately 0.78 at the 95-percent-semispan station. For an angle of attack of 4° the critical Mach number is approximately 0.58 at the 30-percent-semispan station and approximately 0.65 at the 95-percent-semispan station.

Because of the higher critical Mach numbers at the 95-percent-semispan station, the changes in the pressure distributions and section characteristics produced by the onset of shock occur at higher stream Mach numbers at this station than at the inboard station. The Mach number at which the normal-force coefficient for a given angle of attack starts to decrease is, however, approximately the same for both the 95- and 30-percent-semispan stations (fig. 13). This fact is at least partly due to the reductions of the local angles of attack at the outboard stations that result from changes in the induced velocities associated with the reductions of the normal-force coefficients at the inboard stations. A comparison of the pressure recoveries at the trailing edges of the 30- and 95-percent-semispan station (fig. 4(g) and fig. 5(c)) indicates that when the Mach number is increased to high supercritical values the increase in separation at the outboard stations is less severe than at the inboard stations. As a result, at these Mach numbers, the reductions in the normal-force coefficients are less pronounced at the outboard stations than at the inboard stations (fig. 13). Since these variations are limited to the tip of the wing they have little effect on the over-all characteristics of a wing with an aspect ratio similar to that of the wing tested.

Wake Widths

Figure 20 indicates that for all angles of attack the wake width at a station near the probable tail location increases rapidly when the Mach number is increased beyond the critical value. For an angle of attack of 2° at a Mach number of 0.890, the wake extends to a point 0.35 chord above the wing chord line extended. The wake extension is not beyond the region of tail locations used on present-day airplanes. For the higher angles of attack used to recover from high-speed dives, the wakes extend approximately a chord above the wing chord line. In order to reduce the probability of tail buffeting and severe losses in tail effectiveness, the tail should be placed above the wake.

A comparison of the results of figure 21 with those in figure 20 indicates that the wake widths behind the wing spreads rapidly at supercritical Mach numbers. At an angle of attack of 7° at a position 1.40-root chords

behind the 25-percent-chord line, the wake width is equal to approximately 0.50 chord for a Mach number of 0.853. For the same angle of attack and Mach number, but at a station 2.82 root chords behind the 25-percent-chord line, the wake width is equal to approximately 0.75 chord. The divergence of the edges of the wake is about 10° for this condition. At a Mach number of 0.890 the divergence is about 12° ; at 0.760 it is only 3° .

CONCLUSIONS

The results of the tests of a tapered wing with an aspect ratio of 9.0, an NACA 65-210 airfoil section, and undeflected ailerons indicated the following conclusions:

1. Serious changes occurred in the angles of zero lift and the slopes of the normal-force curves when the Mach number was increased above 0.74 at angles of attack between 4° and 10° and above 0.80 at 0° angle of attack.

2. Outboard shifts occurred in the lateral centers of load at angles of attack of 2° , 4° , 7° , and 10° when the Mach number was increased from 0.77 to 0.90. The outboard shifts produced approximately a 5 percent increase in the bending moment at the root section for conditions corresponding to a 3g pull-out at an altitude of 35,000 feet.

3. When the Mach number was increased beyond 0.83, negative pitching-moment coefficients for the high angles of attack increased whereas those for the low angles of attack decreased with a resulting increase in the negative slope of the pitching-moment curve.

4. A large increase occurred in the values of the drag coefficients for the approximate lift coefficients needed to maintain level flight at an altitude of 35,000 feet when the Mach number was increased beyond a value of 0.80.

5. The wakes at a station 2.82 root chords behind the wing quarter-chord line extended approximately a chord

above the wing chord line for the angles of attack required to recover from high-speed dives at high Mach numbers.

Langley Memorial Aeronautical Laboratory
National Advisory Committee for Aeronautics
Langley Field, Va.

REFERENCES

1. Luoma, Arvo A.: An Investigation of a High-Aspect-Ratio Wing Having 0.20-Chord Plain Ailerons in the Langley 8-Foot High-Speed Tunnel. NACA RM No. L6H28d, 1946.
2. Mattson, Axel T.: Investigation of Dive Brakes and Dive-Recovery Flap on a High-Aspect-Ratio Wing in the Langley 8-Foot High-Speed Tunnel. NACA RM No. L6H28c, 1946.
3. Ferri, Antonio: Preliminary Investigation of Downwash Fluctuations of a High-Aspect-Ratio Wing in Langley 8-Foot High-Speed Tunnel. NACA RM No. L6H28b, 1946.
4. Byrne, Robert W.: Experimental Constriction Effects in High-Speed Wind Tunnels. NACA ACR No. L4L07a, 1944.
5. Glauert, H.: Wind Tunnel Interference on Wings, Bodies and Airscrews. R. & M. No. 1566, British A.R.C., 1933.
6. Thom, A.: Blockage Corrections and Choking in the R.A.E. High Speed Tunnel. Rep. No. Aero 1891, British R.A.E., Nov. 1943.
7. Goldstein, S., and Young, A. D.: The Linear Perturbation Theory of Compressible Flow, with Applications to Wind-Tunnel Interference. 6865, Ae. 2262, F.M. 601, British A.R.C., July 6, 1943.
8. Allen, H. Julian, and Vincenti, Walter G.: Wall Interference in a Two-Dimensional-Flow Wind Tunnel with Consideration of the Effect of Compressibility. NACA ARR No. LK03, 1944.
9. Underwood, William J., Braslow, Albert L., and Cahill, Jones F.: Two-Dimensional Wind-Tunnel Investigation of 0.20-Airfoil-Chord Plain Ailerons of Different Contour on an NACA 651-210 Airfoil Section. NACA ACR No. L5F27, 1945.

10. Abbott, Ira H., von Doenhoff, Albert E., and Stivers, Louis S., Jr.: Summary of Airfoil Data. NACA ACR No. L5C05, 1945.
11. Ferri, Antonio: Completed Tabulation in the United States of Tests of 24 Airfoils at High Mach Numbers (Derived from Interrupted Work at Guidonia, Italy, in the 1.31- by 1.74-Foot High-Speed Tunnel). NACA ACR No. L5E21, 1945.
12. Baals, Donald D., and Mourhess, Mary J.: Numerical Evaluation of the Wake-Survey Equations for Subsonic Flow Including the Effect of Energy Addition. NACA ARR No. L5H27, 1945.
13. Stack, John, and Lindsey, W. F.: Characteristics of Low-Aspect-Ratio Wings at Supercritical Mach Numbers. NACA ACR No. L5J16, 1945.
14. Anon.: Spanwise Air-Load Distribution. ANC-1(1), Army-Navy-Commerce Committee on Aircraft Requirements. U.S. Govt. Printing Office, April 1938.
15. Jones, Robert T.: Wing Plan Forms for High-Speed Flight. NACA TN No. 1033, 1946.
16. Mathews, Charles W., and Thompson, Jim Rogers: Comparative Drag Measurements at Transonic Speeds of Rectangular and Swept-Back NACA 651-009 Airfoils Mounted on a Freely Falling Body. NACA ACR No. L5G30, 1945.
17. Ludwig, H.: Versuchsergebnisse. Pfeilflügel bei hohen Geschwindigkeiten. Bericht 127 der Lilienthal-Gesellschaft, 1940, pp. 44-52.

TABLE I
 DIMENSIONS OF WING-TIP SHAPE IN INCHES
 [See fig. 2]

Plan-form contour		
Distance from tip, y_t	Distance forward of 25-percent-chord line, x_f	Distance rearward of 25-percent-chord line, x_r
0	-0.360	0.360
.026	.041	.963
.053	.176	1.168
.079	.268	1.307
.105	.337	1.413
.158	.436	1.565
.236	.529	1.710
.341	.595	1.817
.473	.623	1.868
Section contour		
Distance from tip, y_t	Lower-surface ordinate, z_L	Upper-surface ordinate, z_U
0.026	0.024	0.076
.053	.041	.093
.079	.052	.105
.105	.061	.113
.158	.074	.126
.236	.086	.138
.341	.094	.147
.473	.098	.151

NATIONAL ADVISORY
 COMMITTEE FOR AERONAUTICS

CONFIDENTIAL

TABLE II

ORDINATES FOR NACA 65-210 AIRFOIL

[Stations and ordinates in percent of wing chord]

Upper surface		Lower surface	
Station	Ordinate	Station	Ordinate
0	0	0	0
.435	.819	.565	-.719
.678	.999	.822	-.859
1.169	1.273	1.331	-1.059
2.408	1.757	2.592	-1.385
4.898	2.491	5.102	-1.859
7.394	3.069	7.606	-2.221
9.894	3.555	10.106	-2.521
14.899	4.338	15.101	-2.992
19.909	4.938	20.091	-3.346
24.921	5.397	25.079	-3.607
29.936	5.732	30.064	-3.788
34.951	5.954	35.049	-3.894
39.968	6.067	40.032	-3.925
44.984	6.058	45.016	-3.868
50.000	5.915	50.000	-3.709
55.014	5.625	54.986	-3.435
60.027	5.217	59.973	-3.075
65.036	4.712	64.964	-2.652
70.043	4.128	69.957	-2.184
75.045	3.479	74.955	-1.689
80.044	2.783	79.956	-1.191
85.038	2.057	84.962	-.711
90.028	1.327	89.972	-.293
95.014	.622	94.986	.010
100.000	0	100.000	0
L.E. radius: 0.687. Slope of radius through end of chord: 0.084			

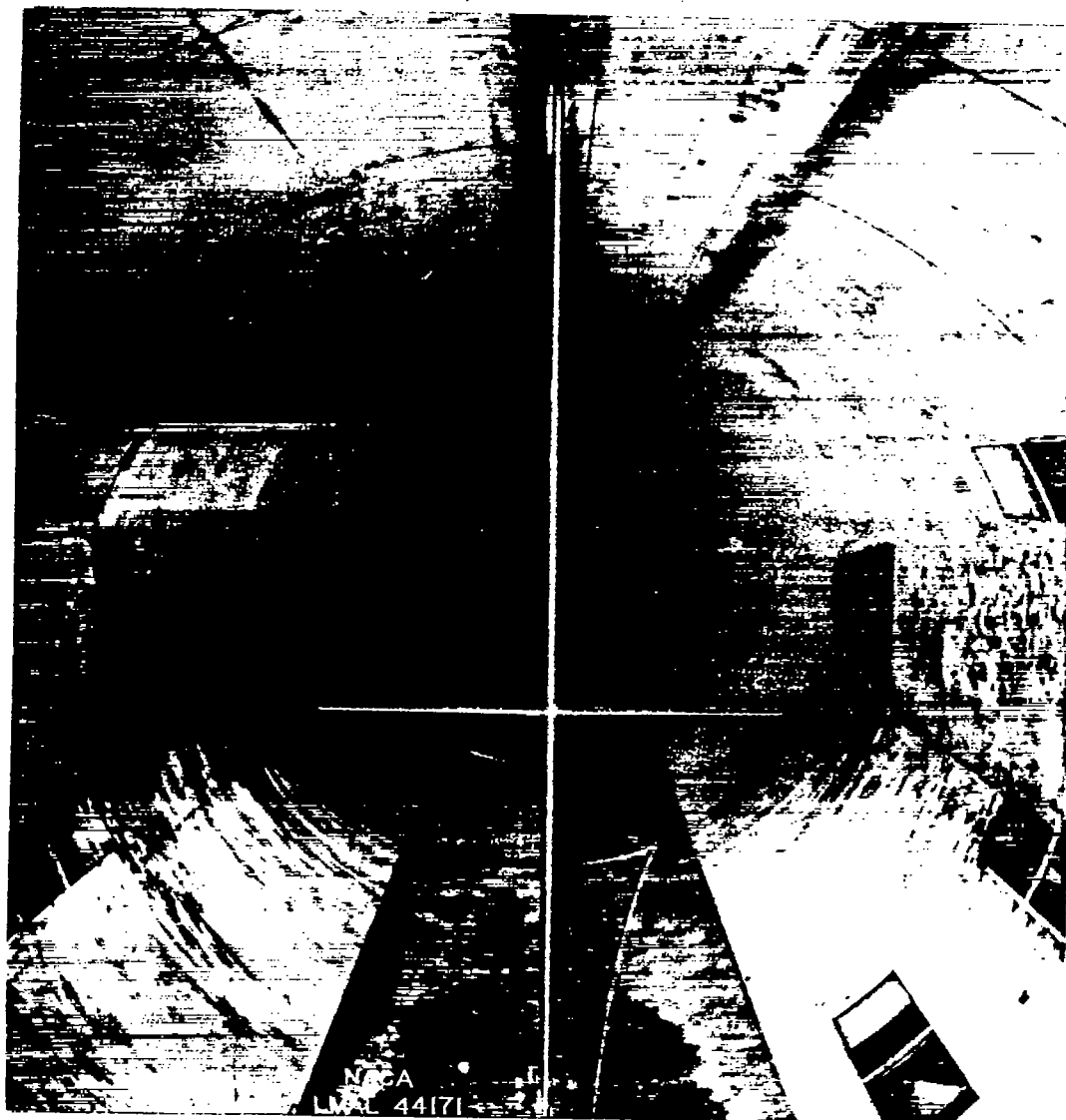
NATIONAL ADVISORY
COMMITTEE FOR AERONAUTICS

CONFIDENTIAL

TABLE III

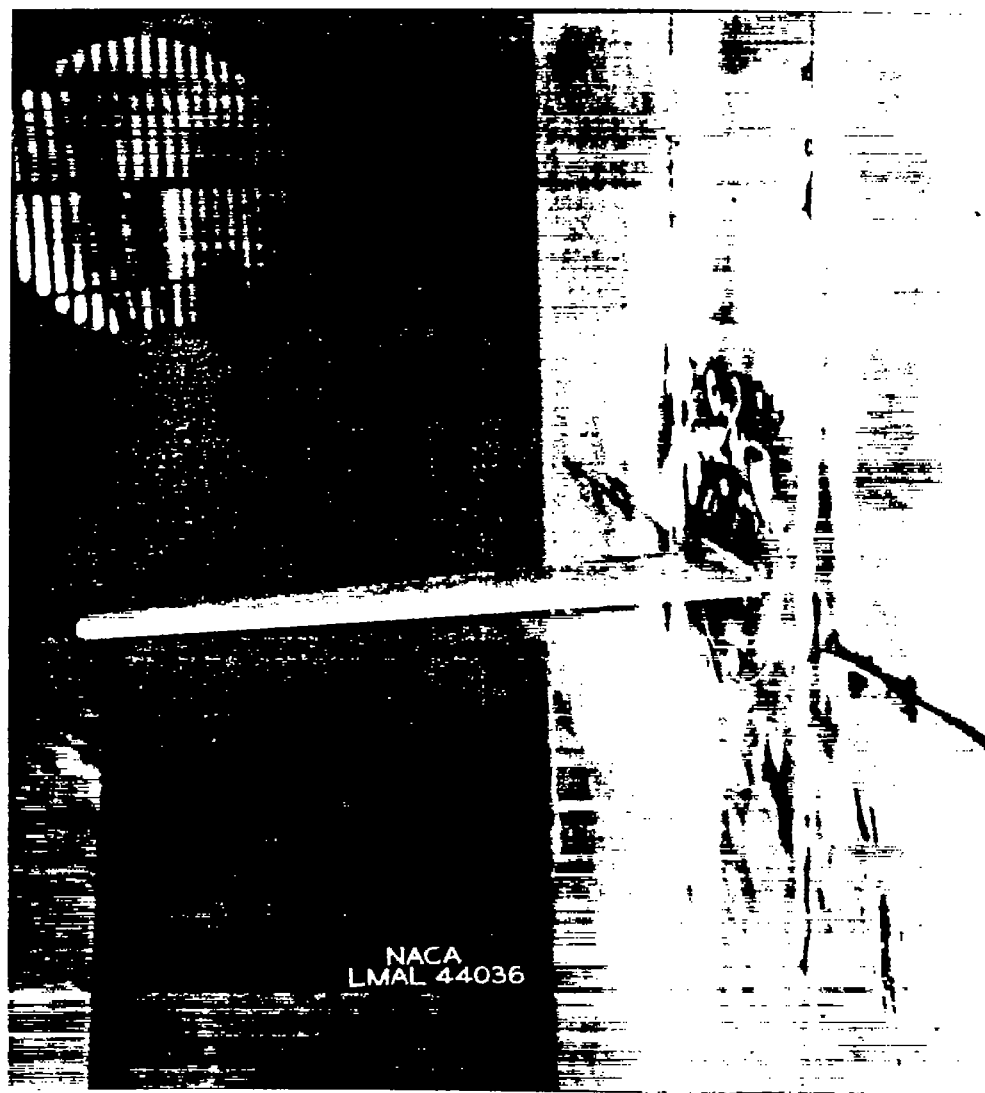
ORDINATES FOR CROSS SECTION OF SUPPORT PLATE

Station	Ordinate
Distance from leading edge (in.)	Distance from chord line (in.)
0	0
.05	.025
.12	.038
.25	.054
.32	.060
.62	.085
1.25	.119
1.88	.144
2.50	.165
3.12	.187
3.75	.200
5.00	.227
6.25	.250
7.50	.269
10.00	.301
12.50	.325
15.00	.344
17.50	.358
20.00	.367
22.50	.373
25.00	.375
27.50	.373
30.00	.367
32.50	.358
35.00	.344
37.50	.325
40.00	.301
42.50	.269
43.75	.250
45.00	.227
46.25	.200
46.88	.187
47.50	.165
48.12	.144
48.75	.119
49.37	.085
49.68	.060
49.75	.054
49.87	.038
49.95	.025
50.00	0
L.E. radius: 0.005	



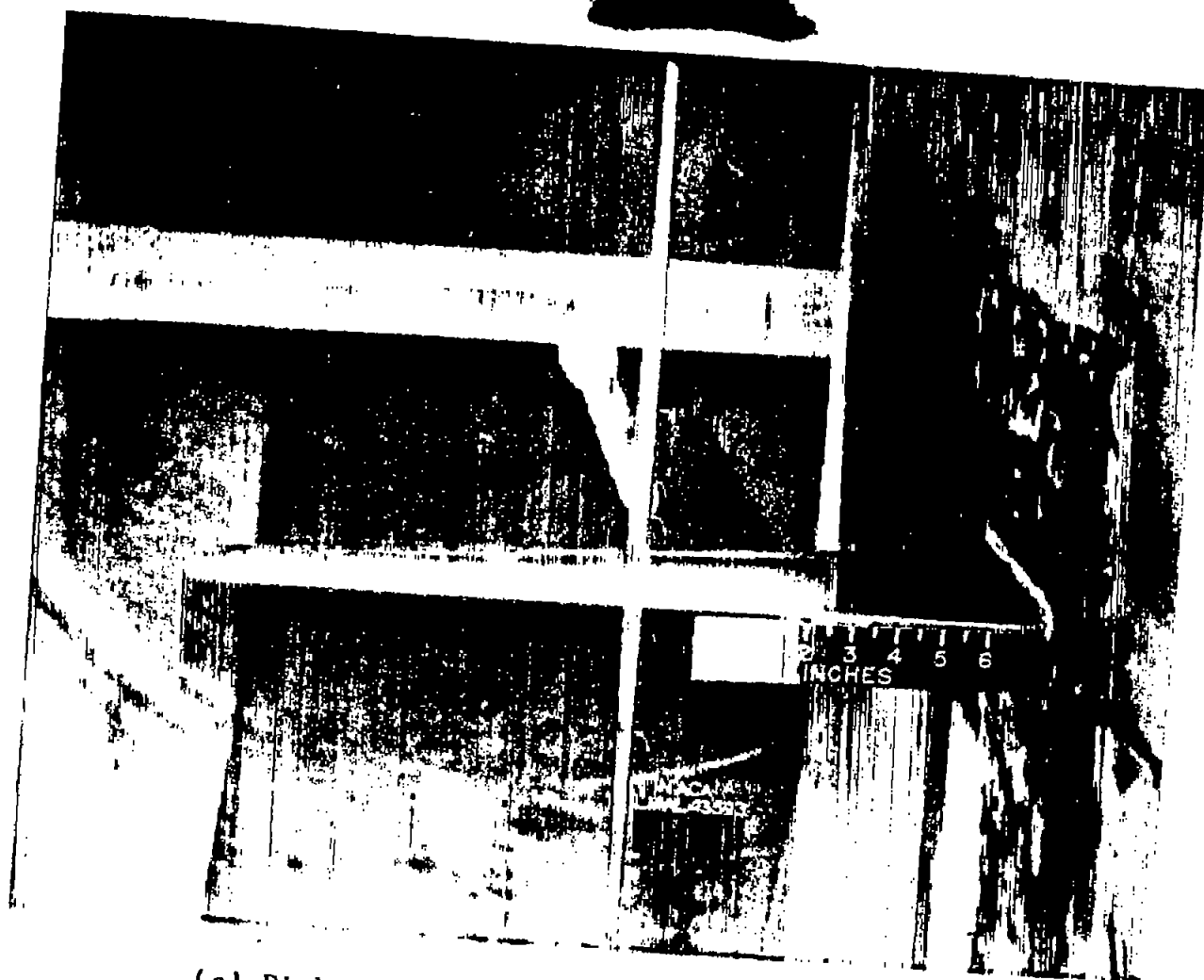
(a) Front view.

Figure 1.- High-aspect-ratio wing mounted on vertical support plate in Langley 8-foot high-speed tunnel.



(b) Three-quarter view of right half of wing.

Figure 1.- Continued.



(c) Right half of wing and wake-survey rake.

Figure 1.- Concluded.

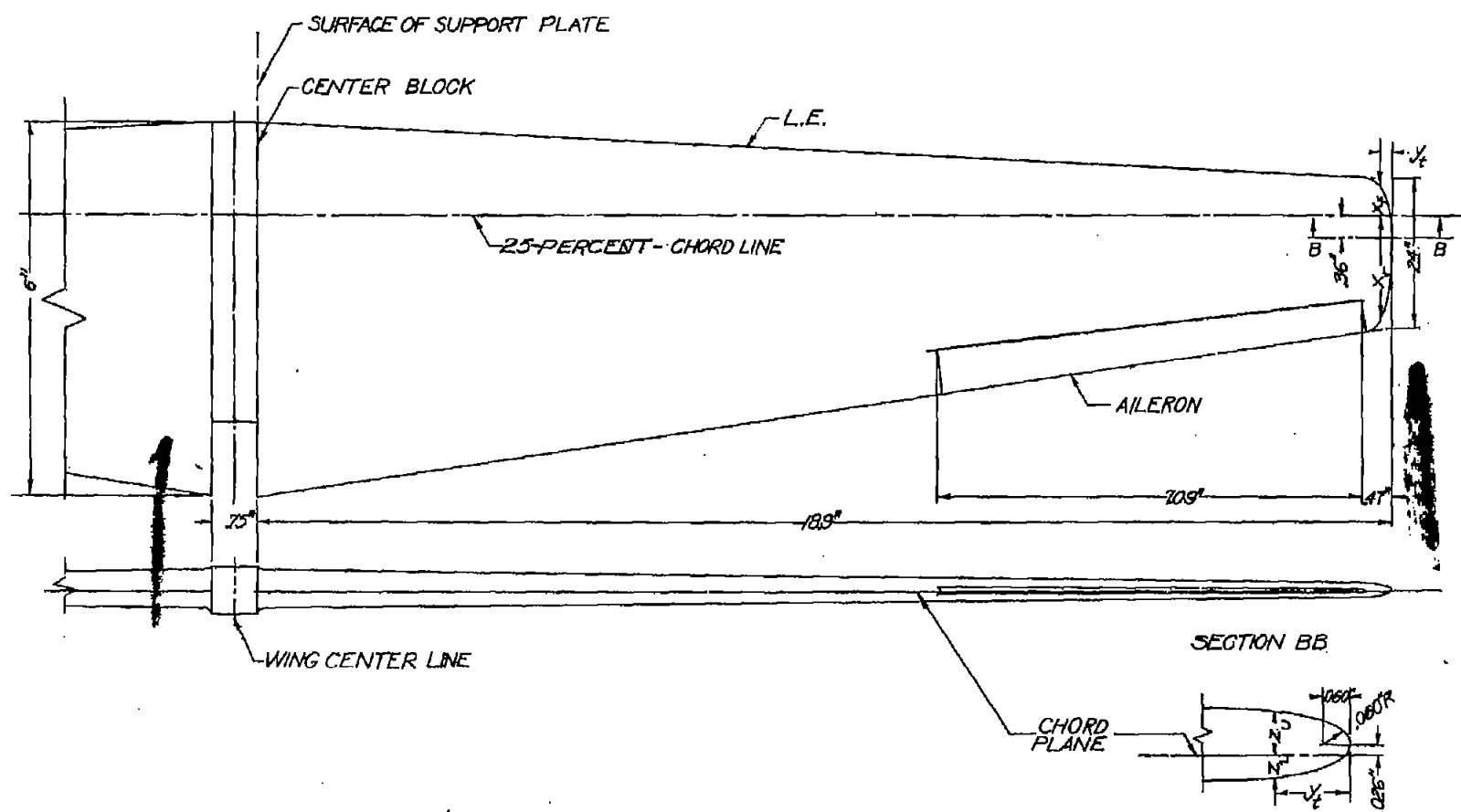


FIGURE 2.-WING DIMENSIONS.

NATIONAL ADVISORY
COMMITTEE FOR AERONAUTICS

Fig. 3

NACA RM No. L6H28a

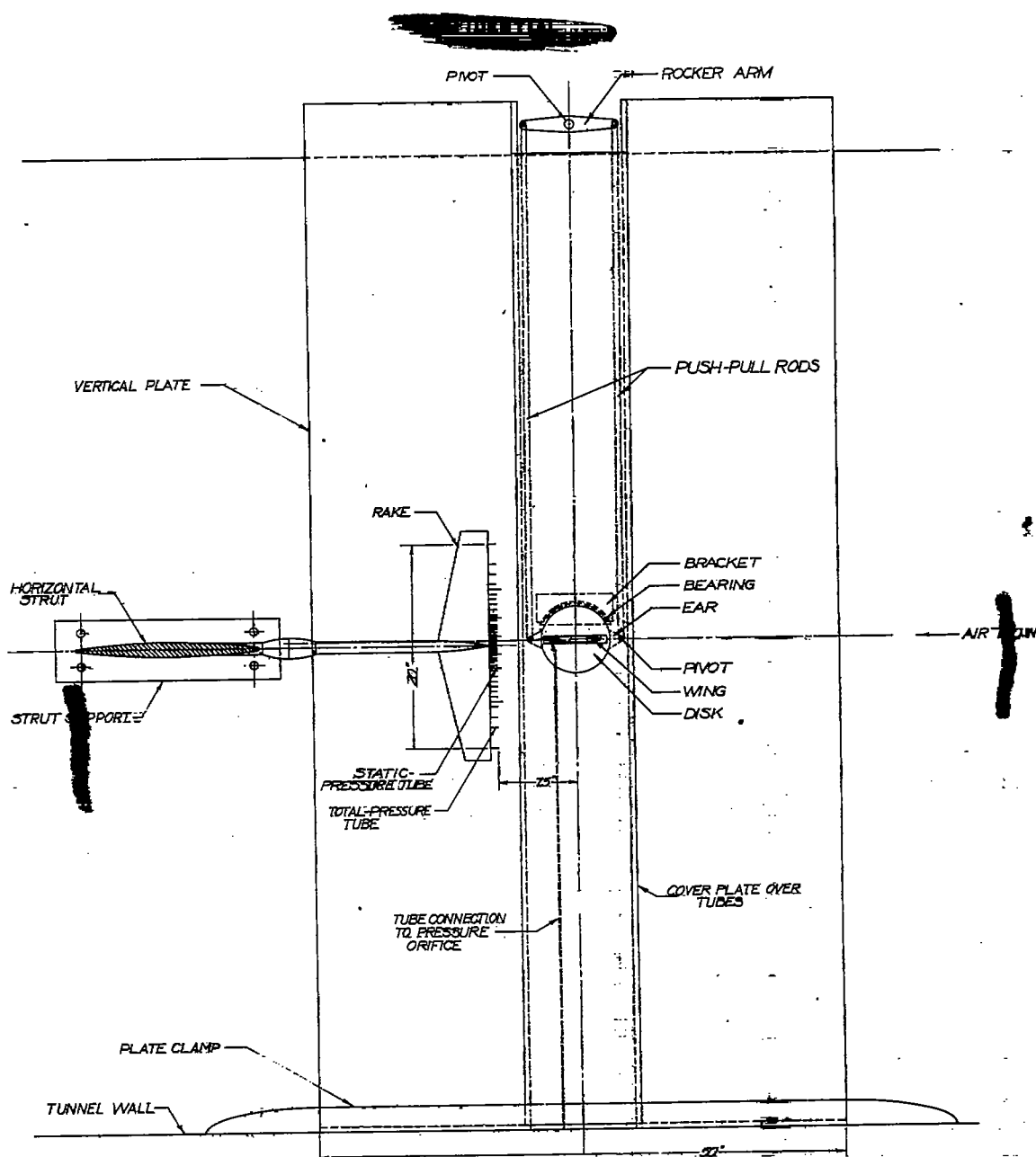


FIGURE 3.—COMPLETE TEST APPARATUS.

NATIONAL ADVISORY
COMMITTEE FOR AERONAUTICS.

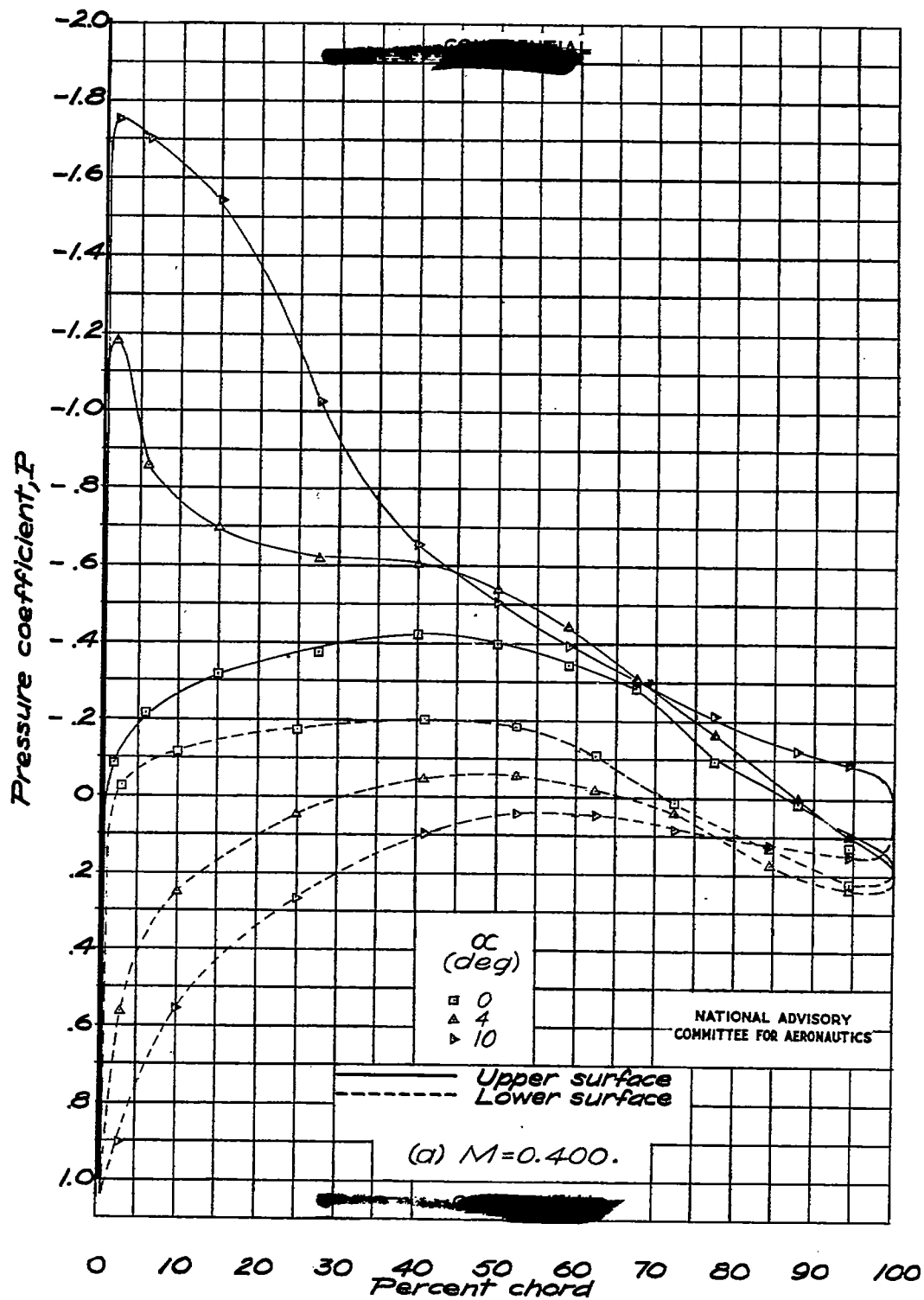


Figure 4 .- Chordwise pressure distribution at the 30-percent-semispan station.

Fig. 4b

NACA RM No. L6H28a

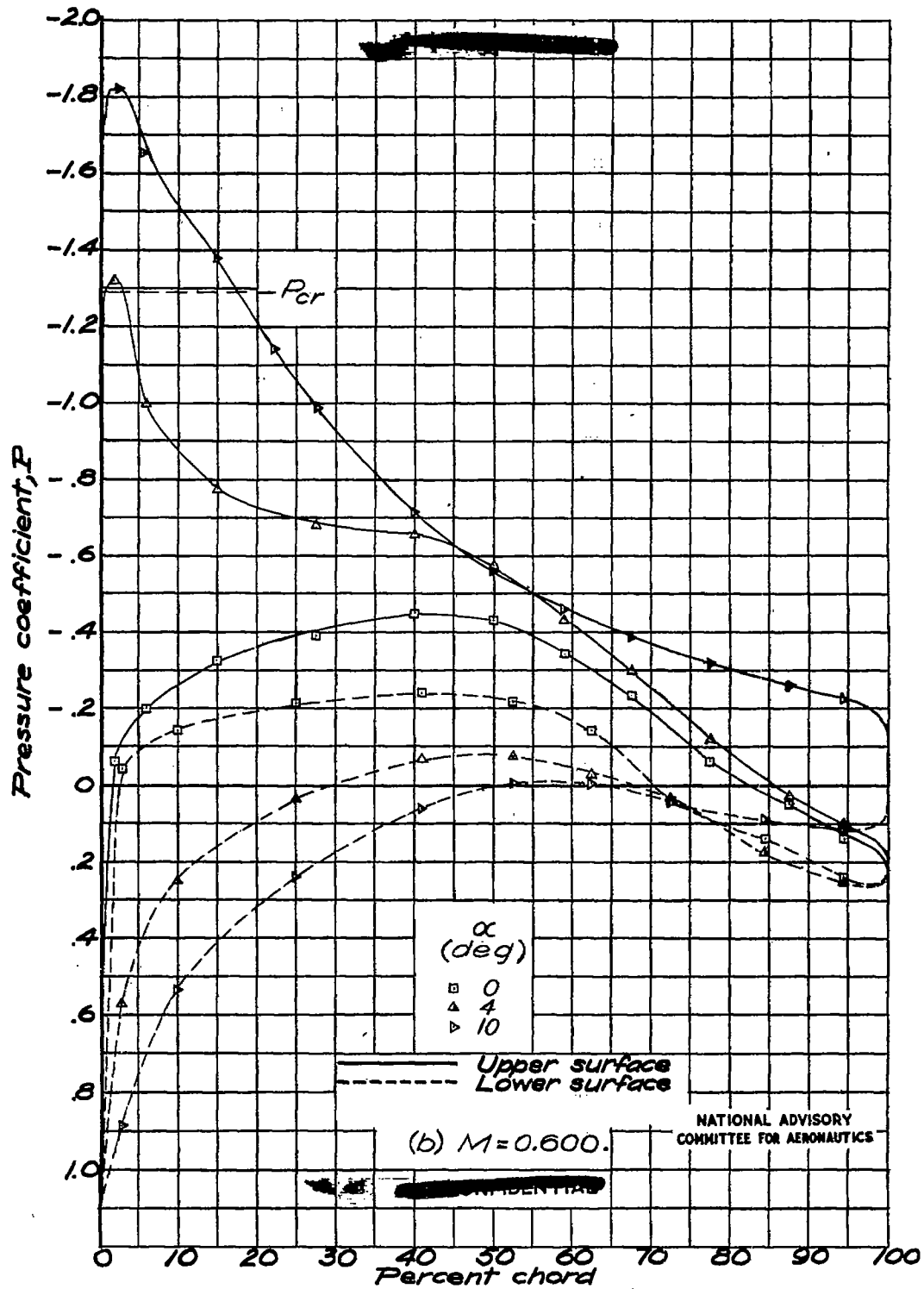


Figure 4. - Continued.

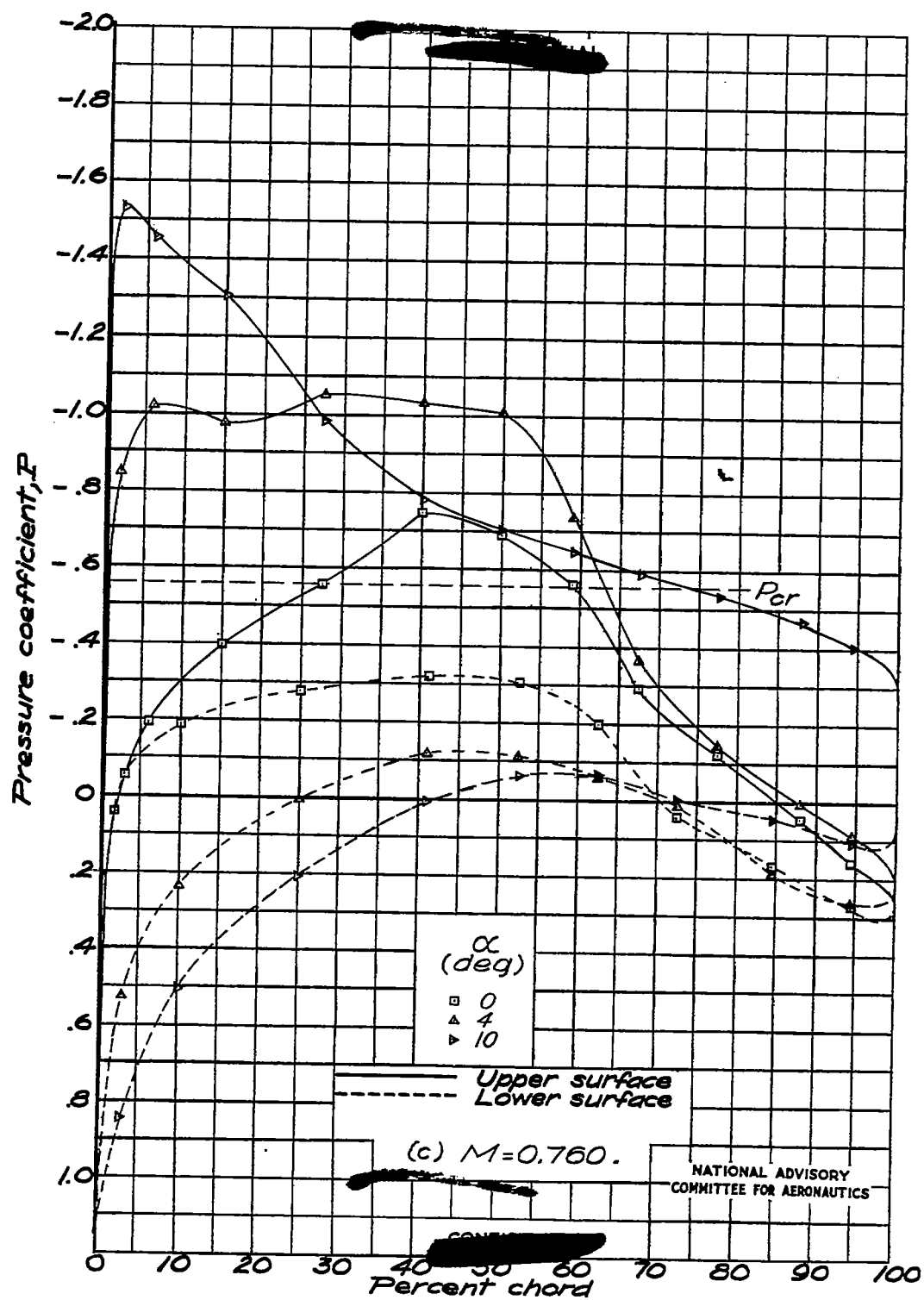


Figure 4. - Continued.

Fig. 4d

NACA RM No. L6H28a

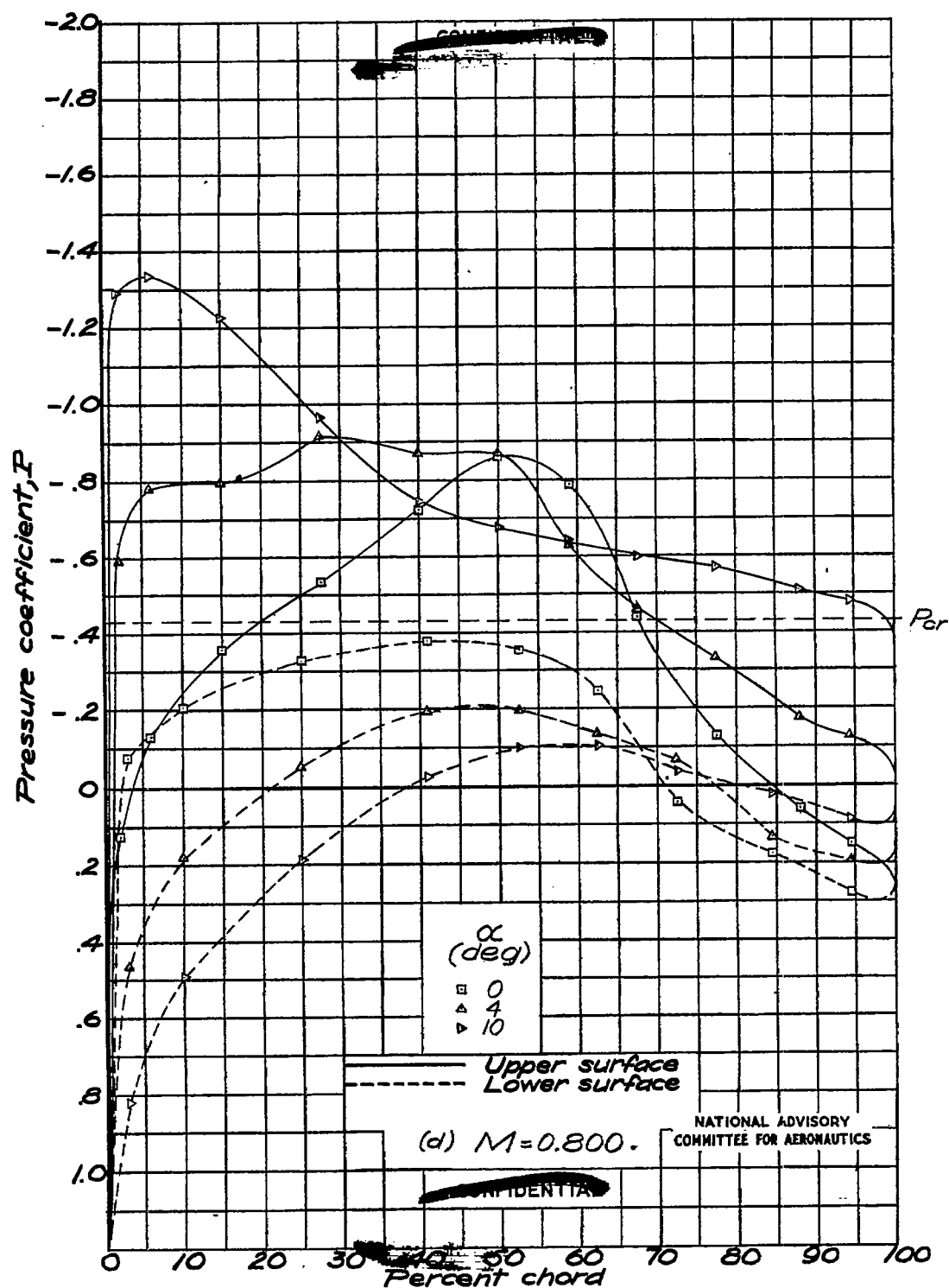


Figure 4. - Continued.

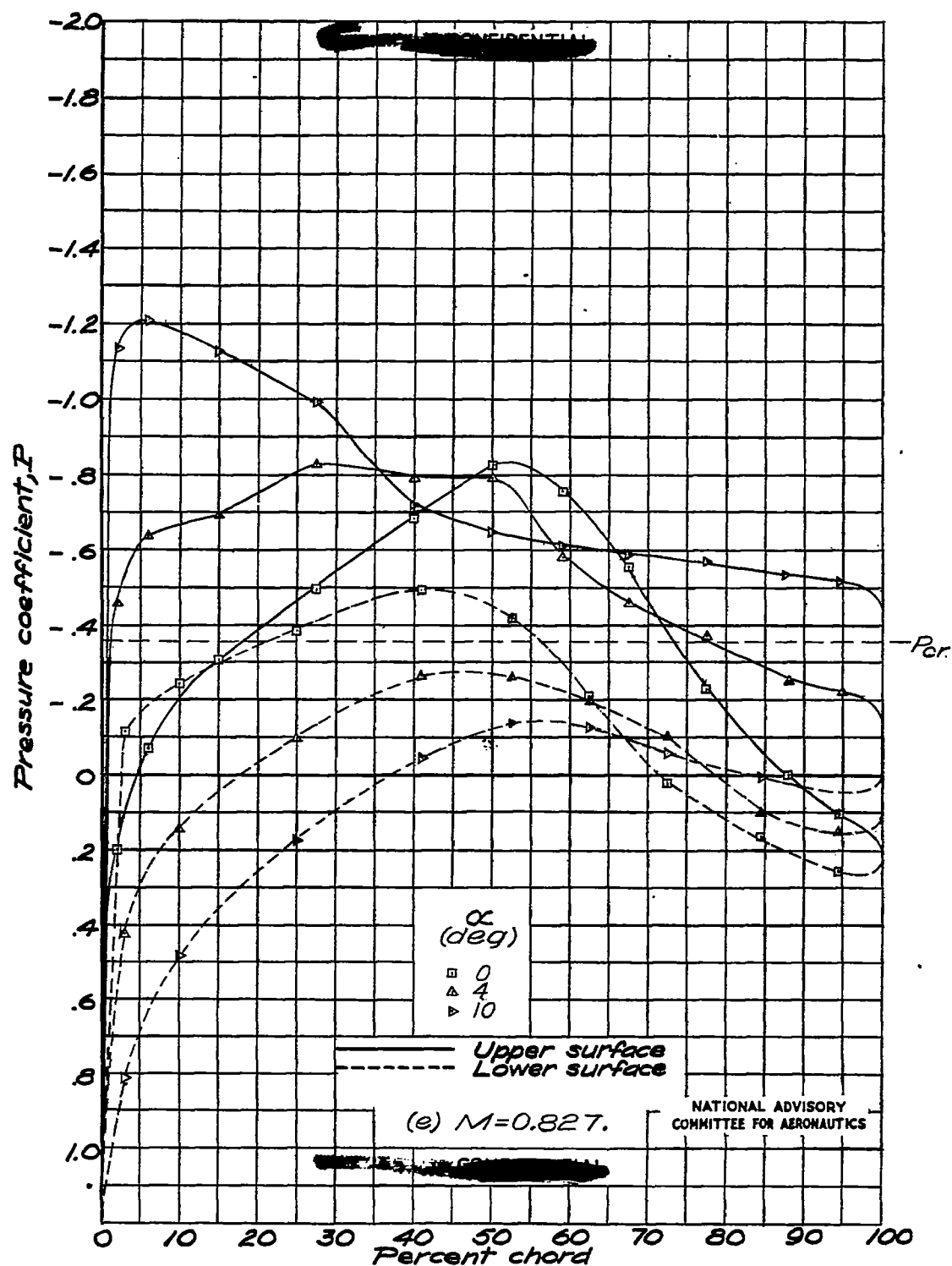


Figure 4. - Continued.

Fig. 4f

NACA RM No. L6H28a

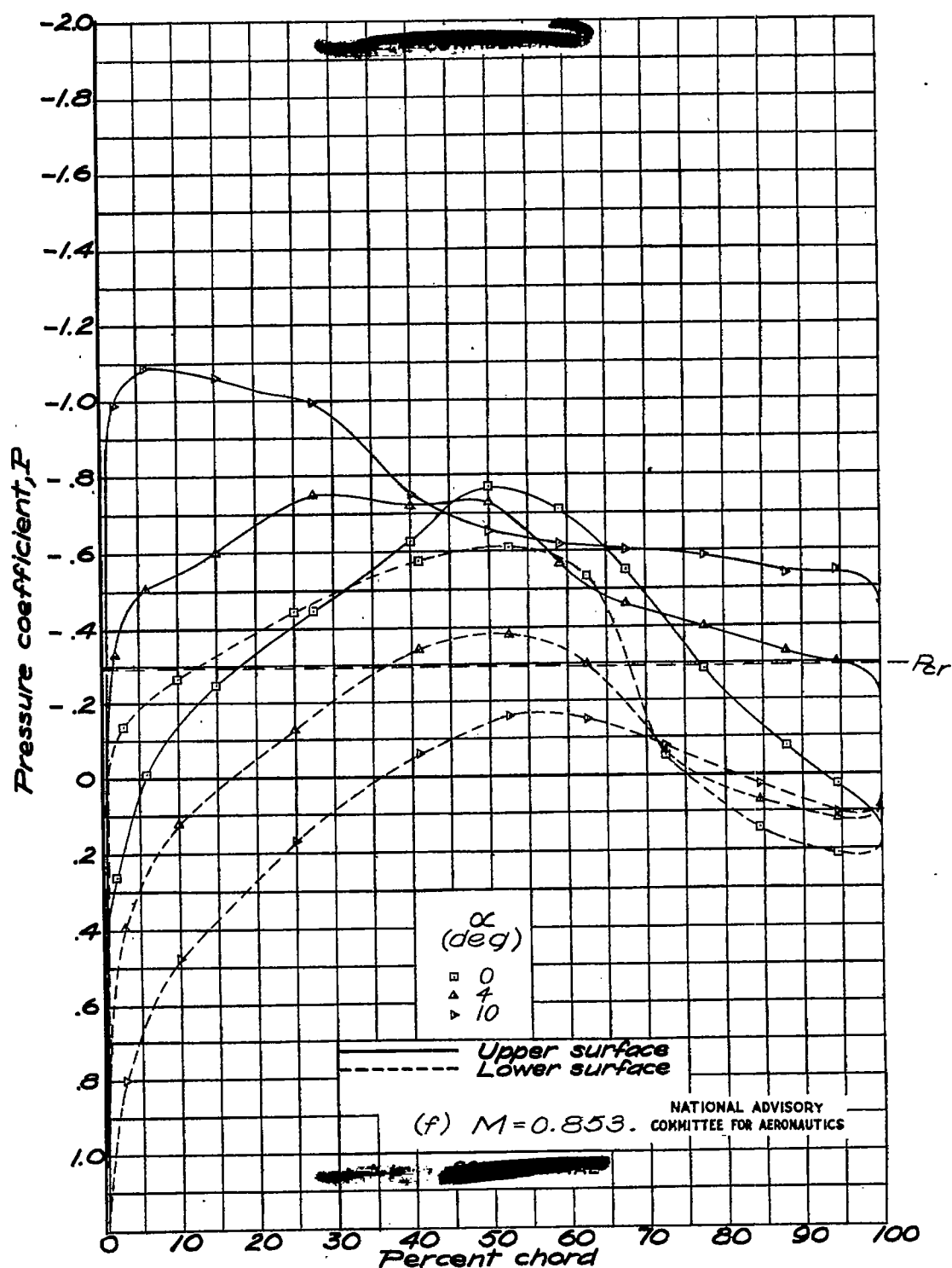


Figure 4. - Continued.

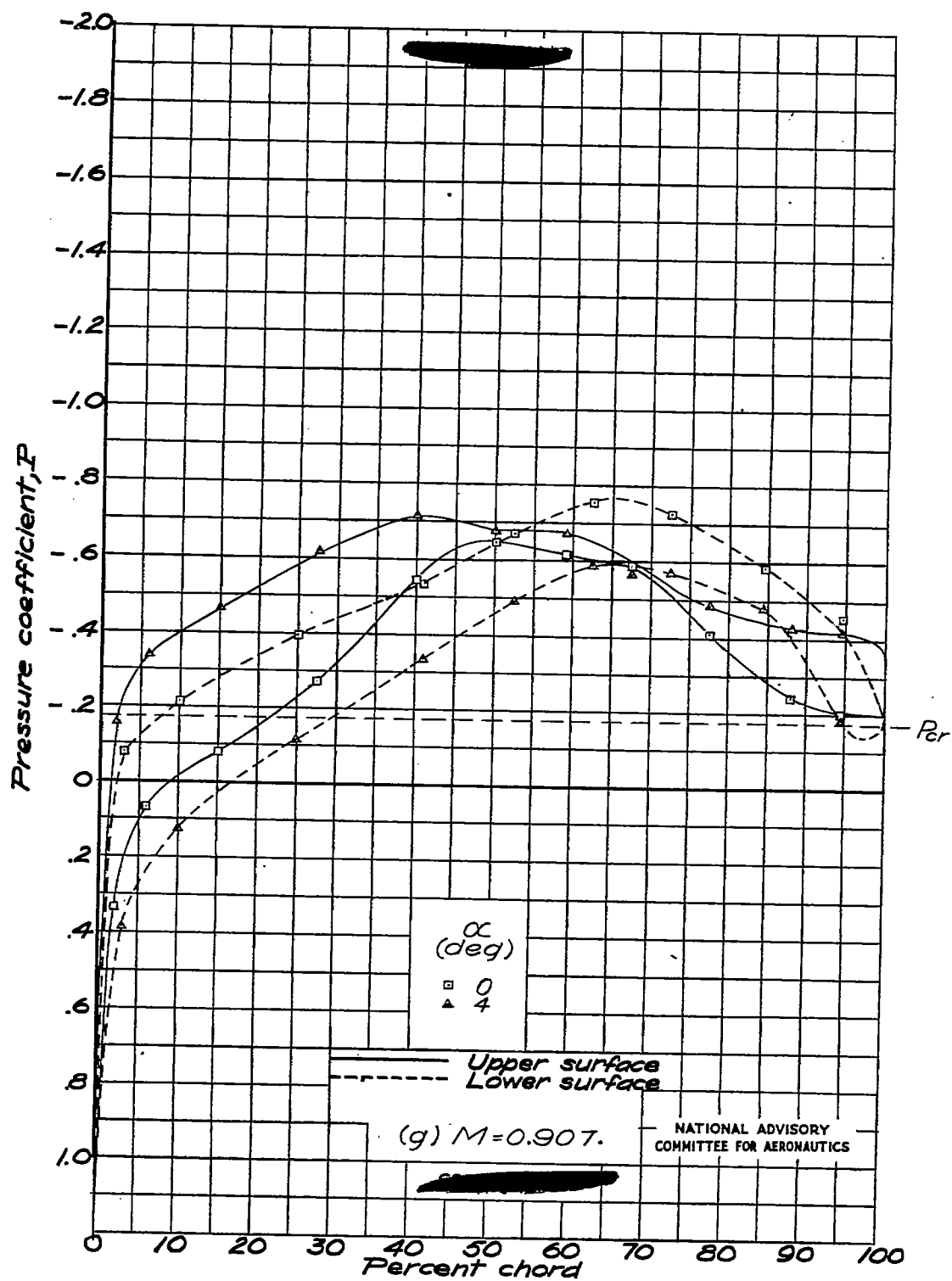


Figure 4, - Continued.

Fig. 4h

NACA RM No. L6H28a

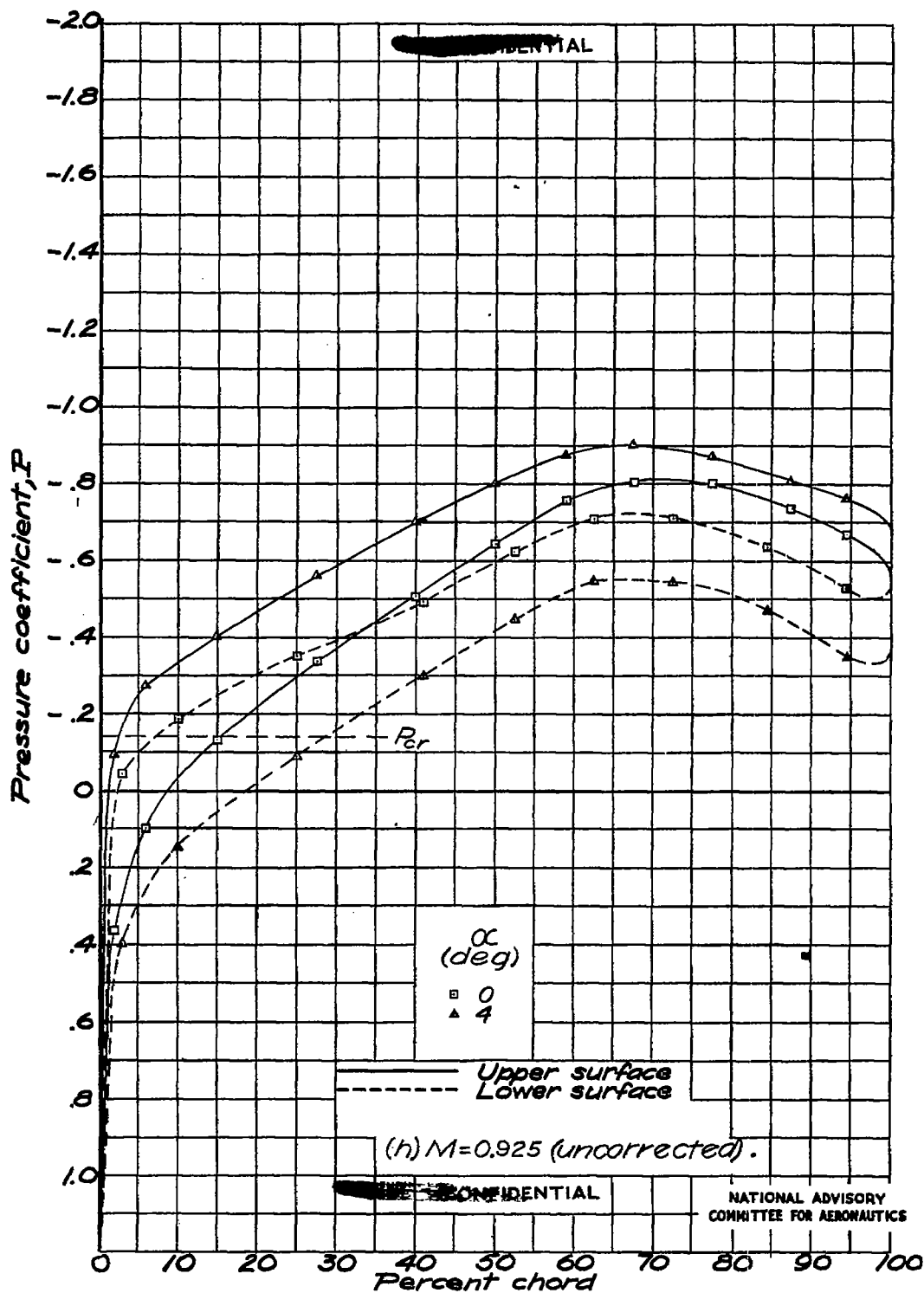


Figure 4. - Concluded.

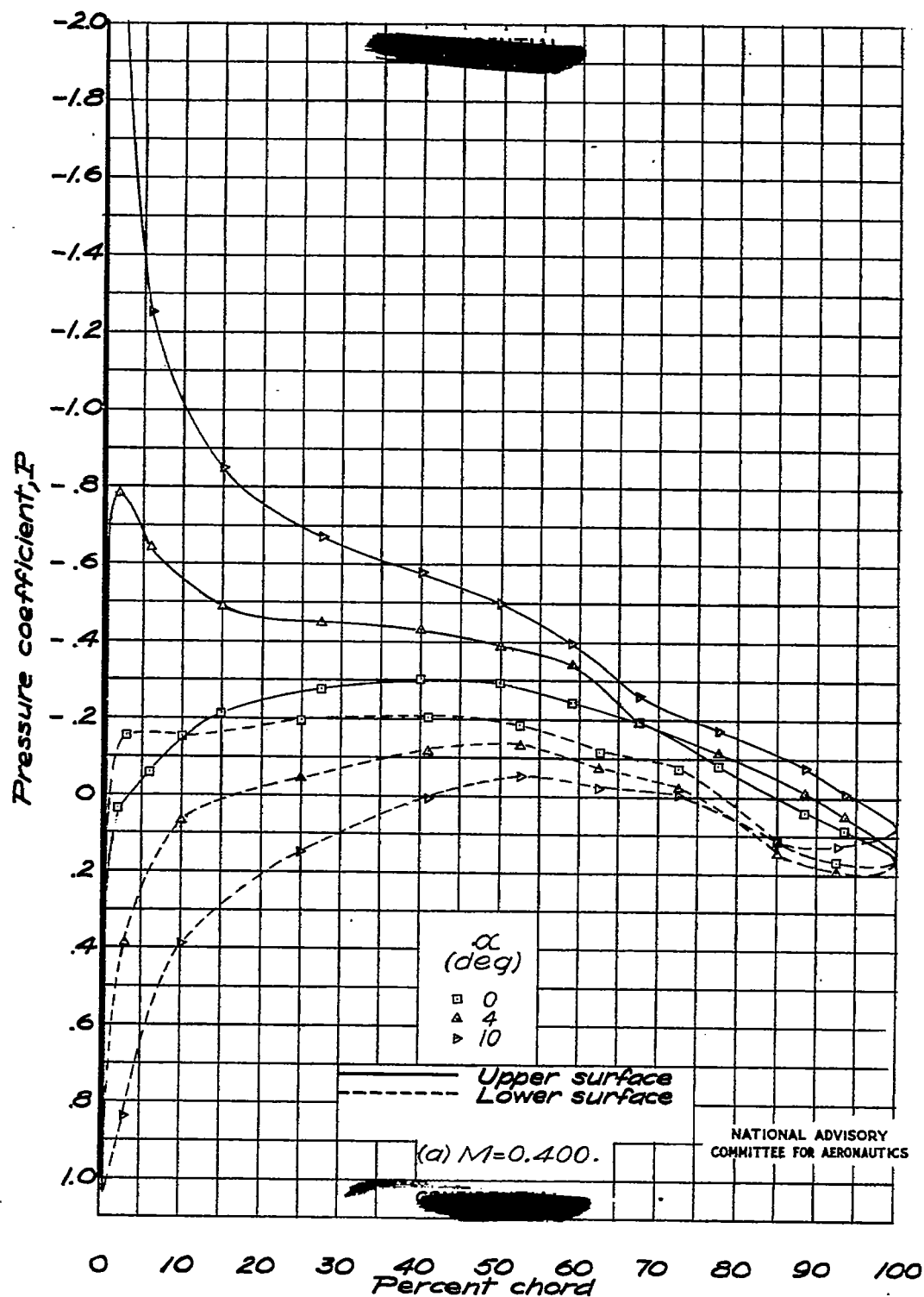


Figure 5.- Chordwise pressure distribution at the 95-percent-semispan station

Fig. 5b

NACA RM No. L6H28a

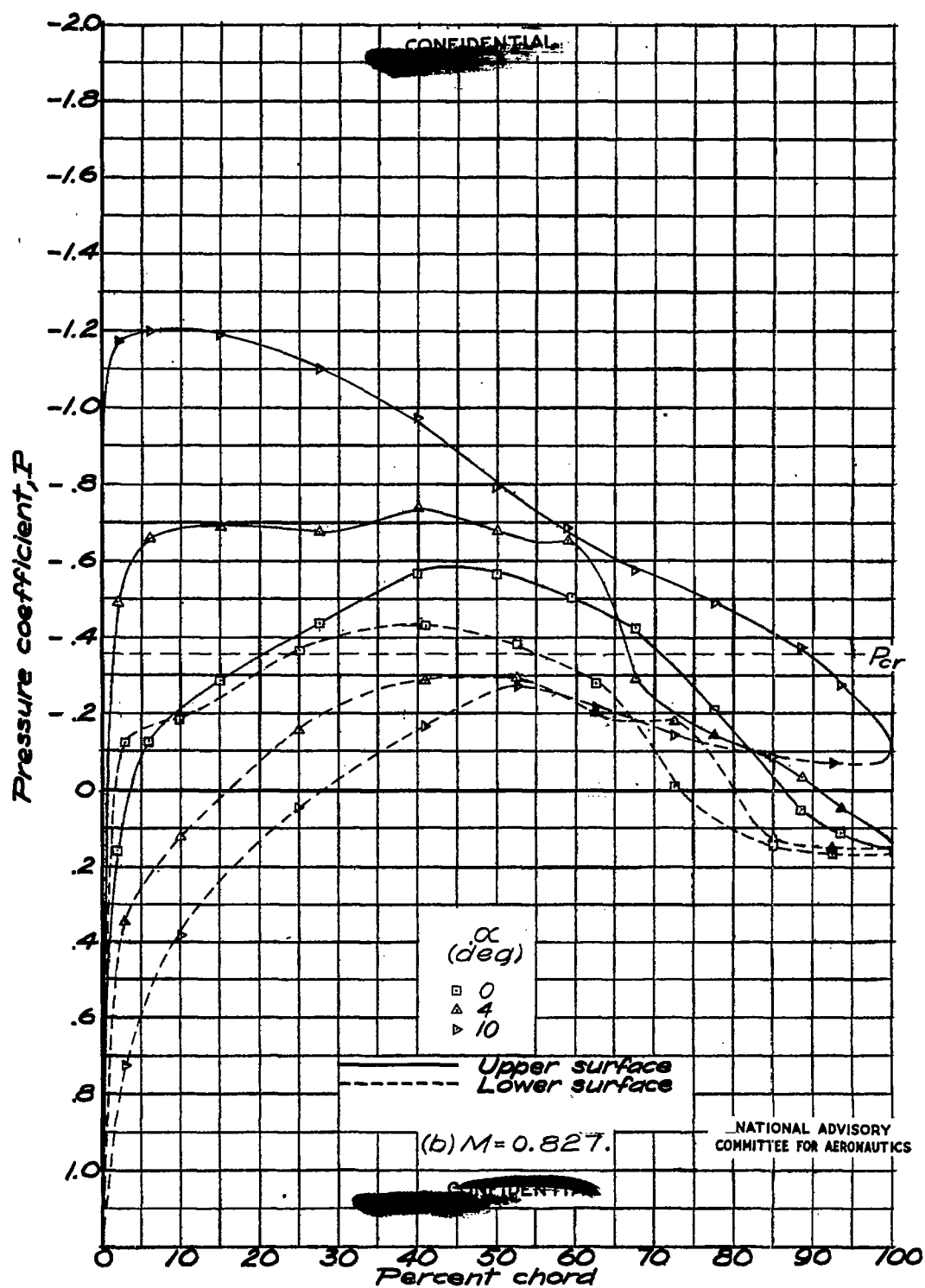


Figure 5. - Continued.

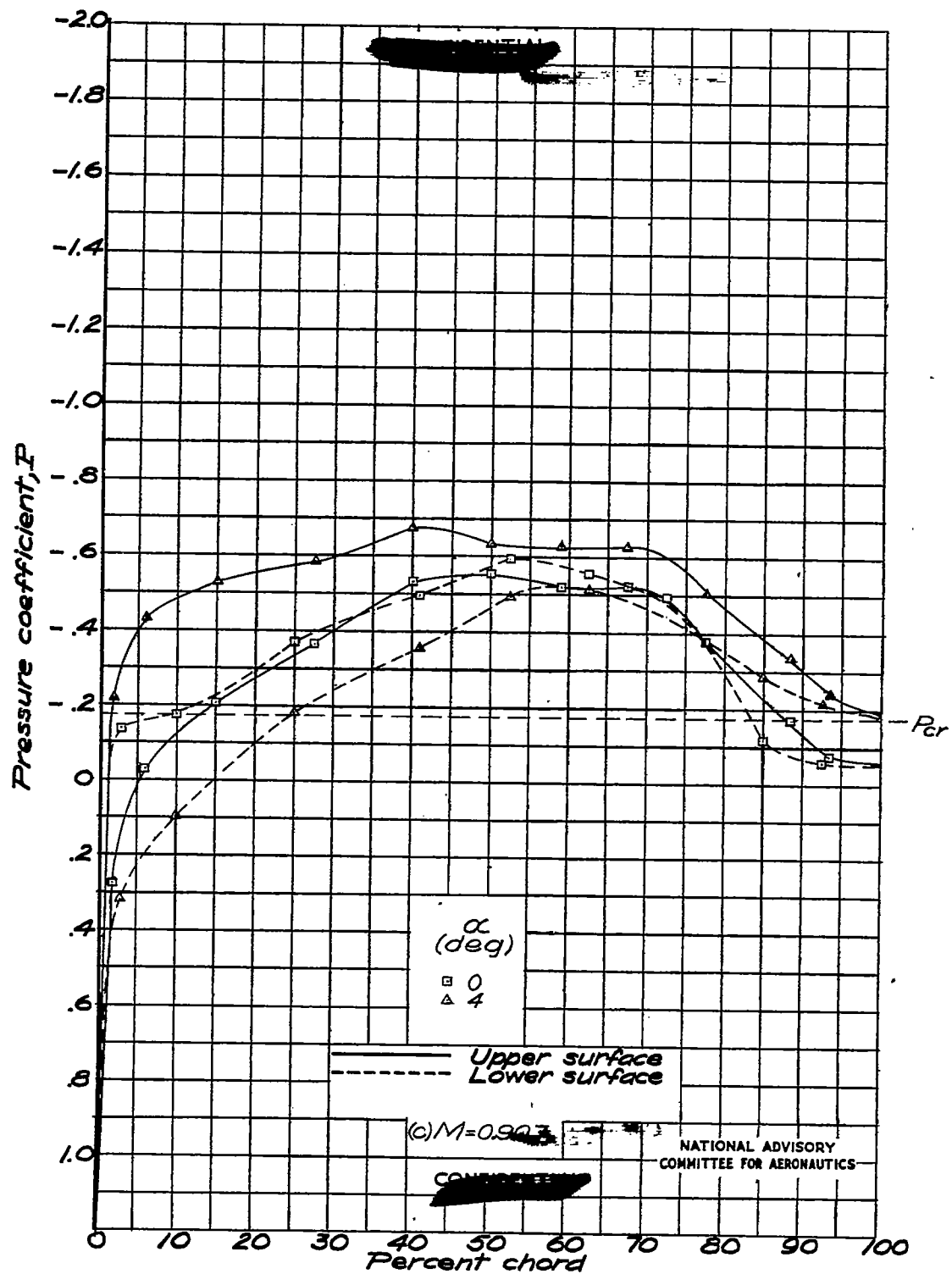


Figure 5. - Concluded.

Fig. 6a

NACA RM No. L6H28a

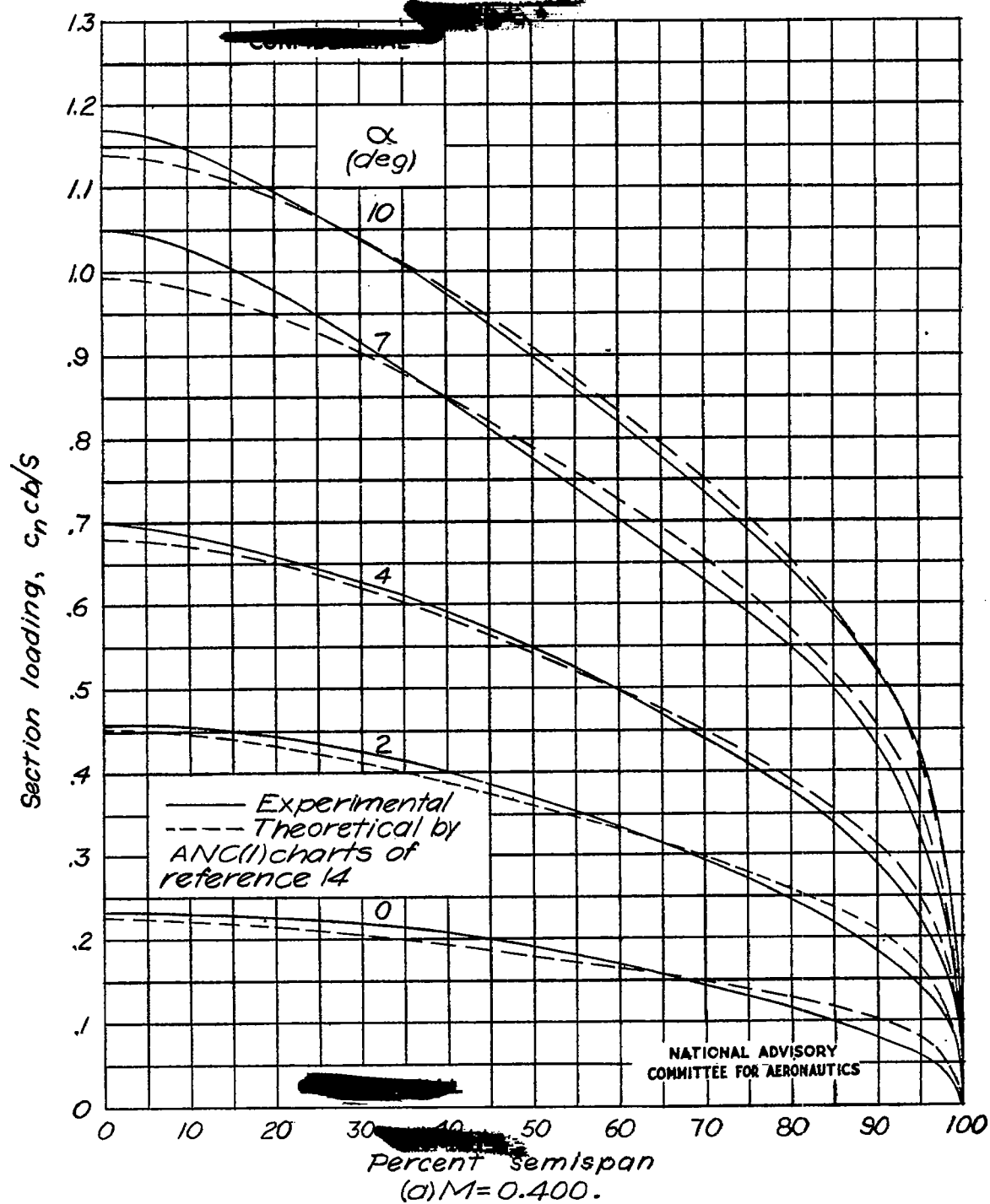


Figure 6.- Spanwise variation in section loading.

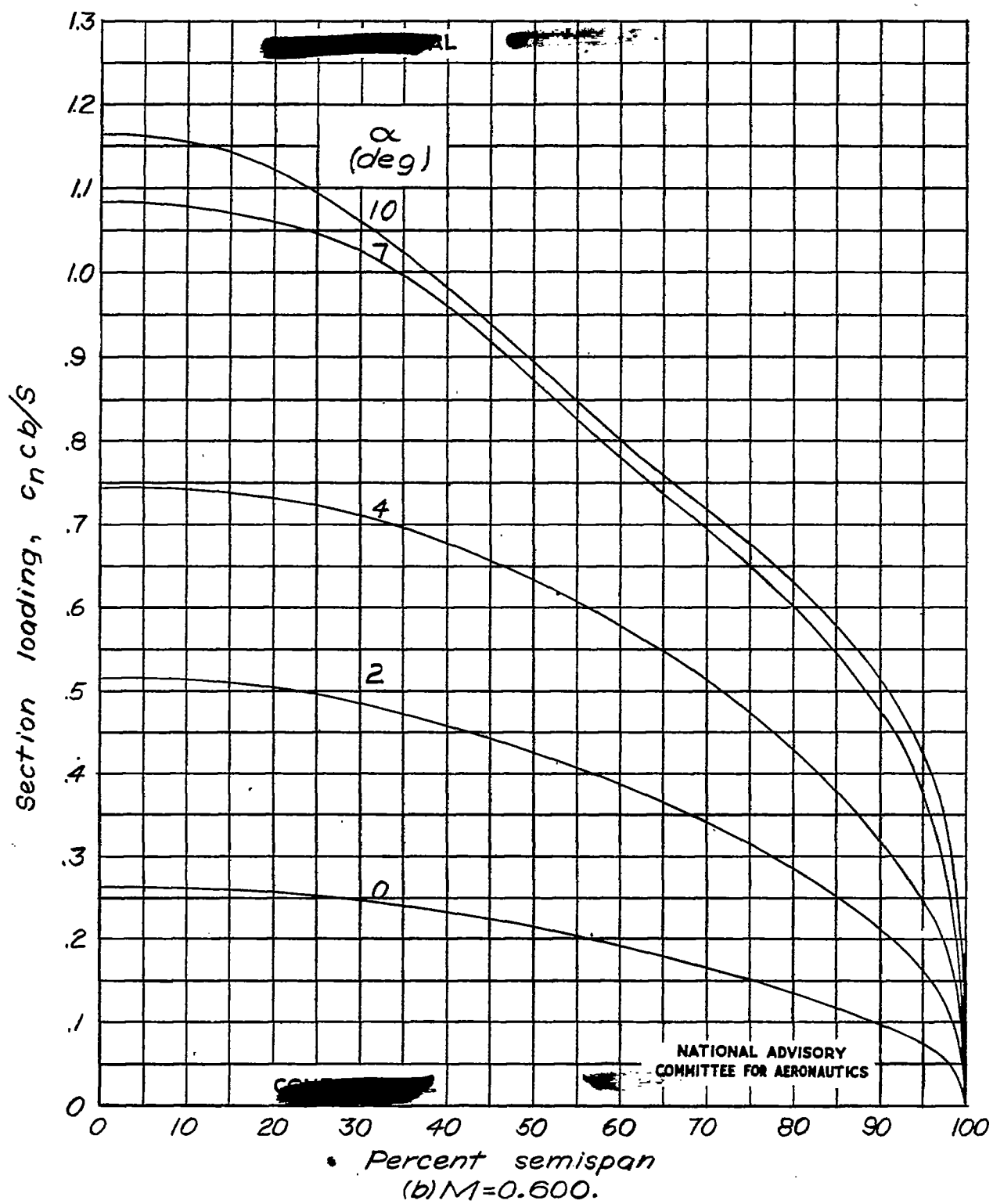


Figure 6.-Continued.

Fig. 6c

NACA RM No. L6H28a

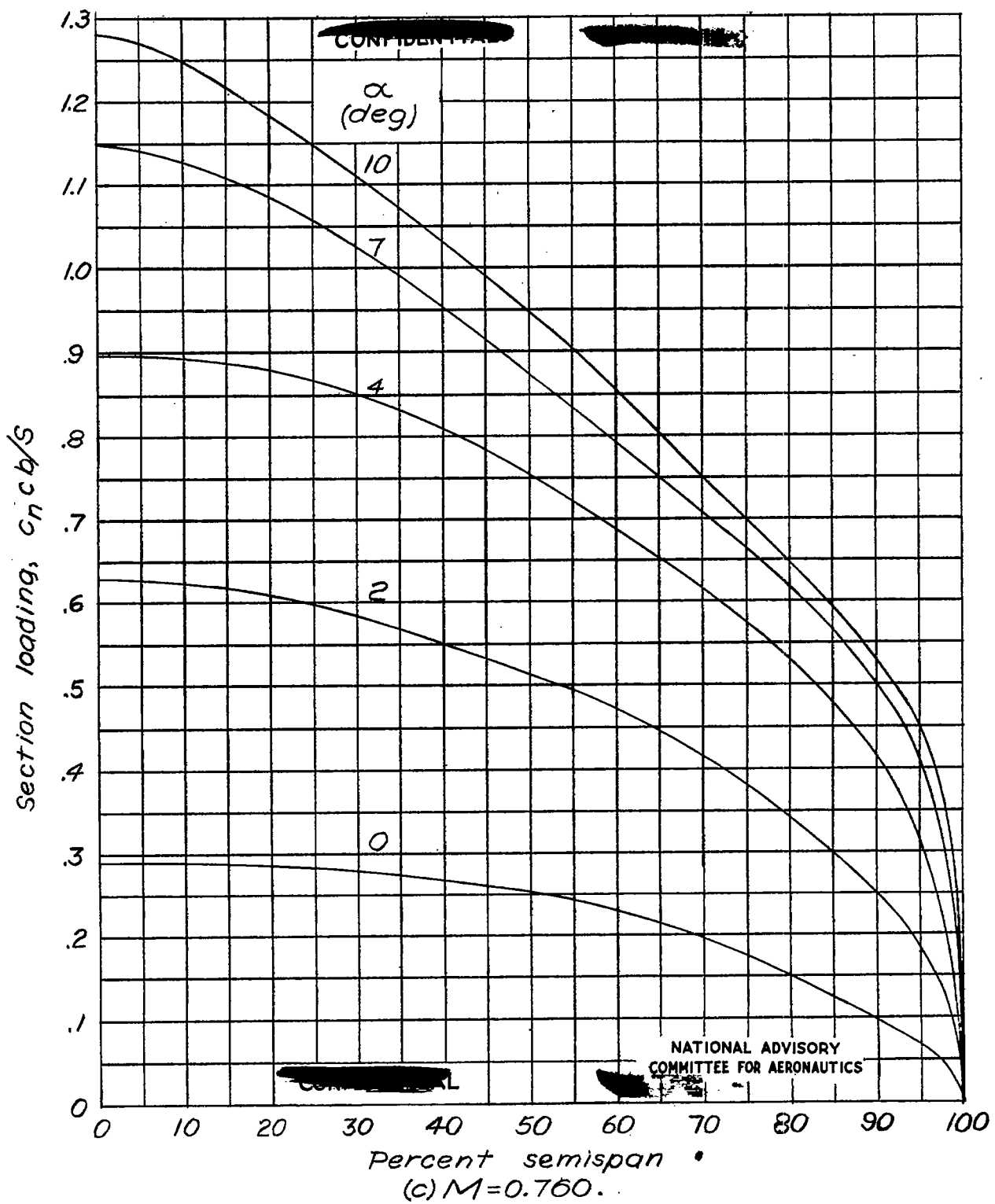


Figure 6.-Continued.

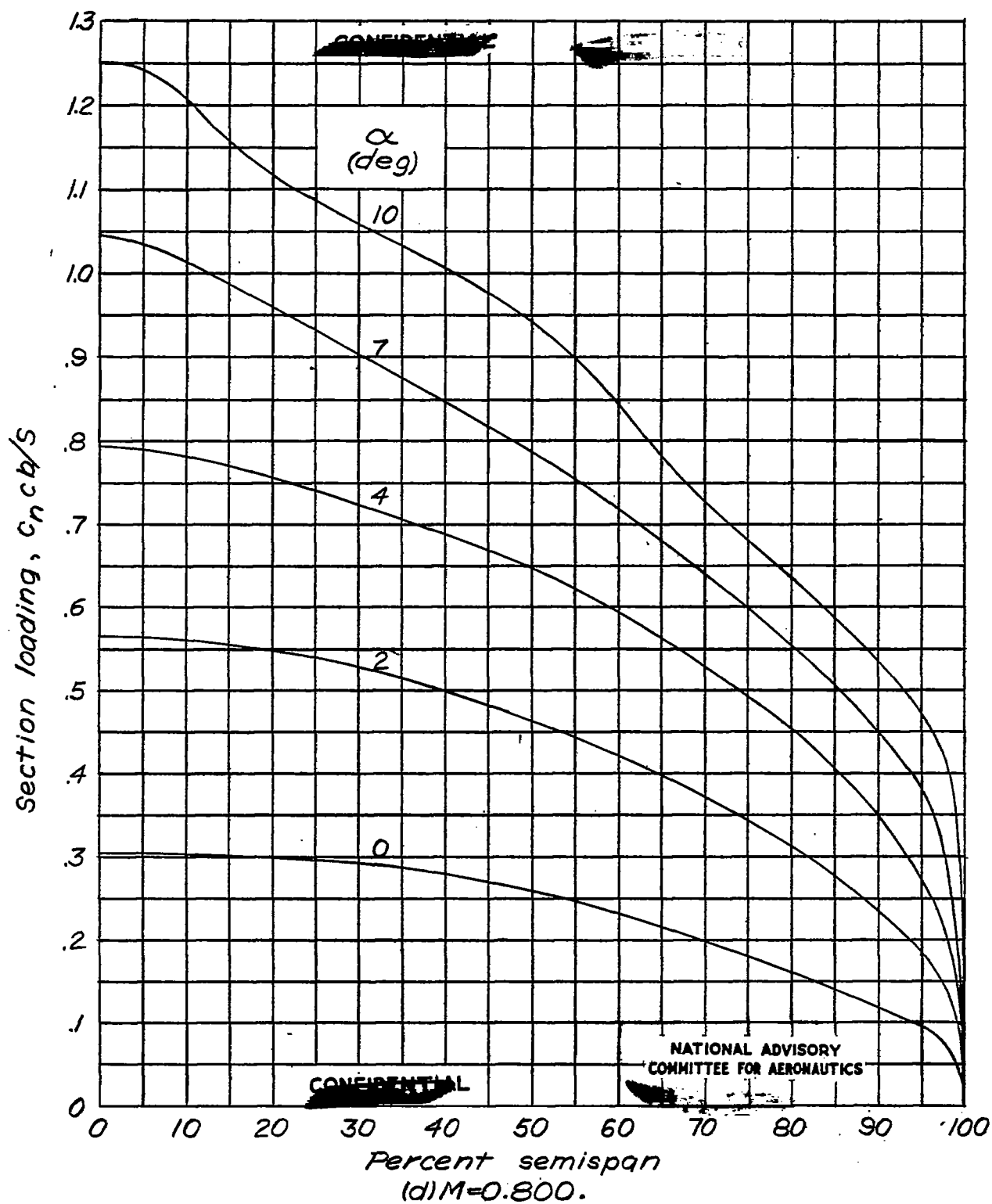


Figure 6.- Continued.

Fig. 6e

NACA RM No. L6H28a

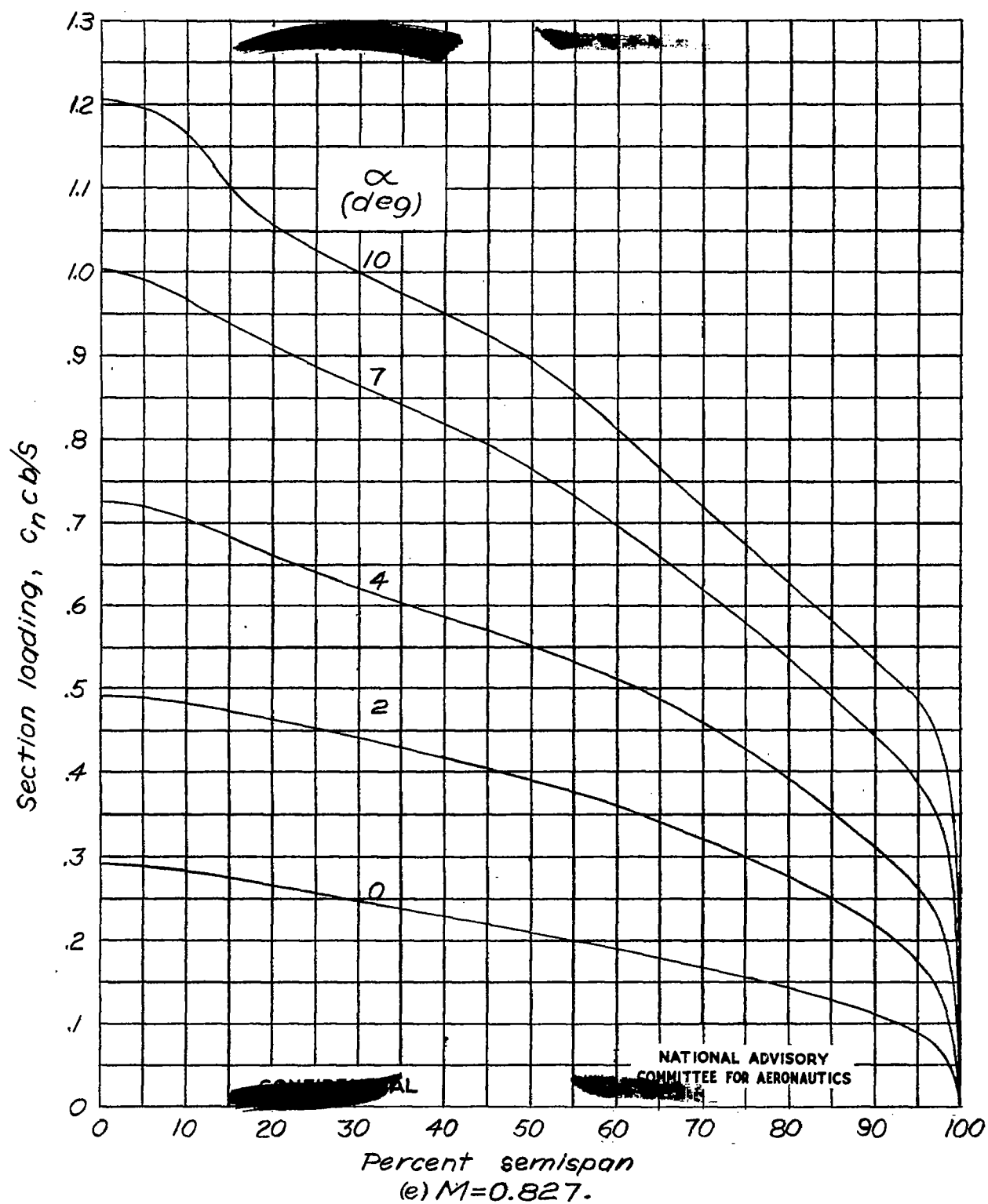


Figure 6.- Continued.

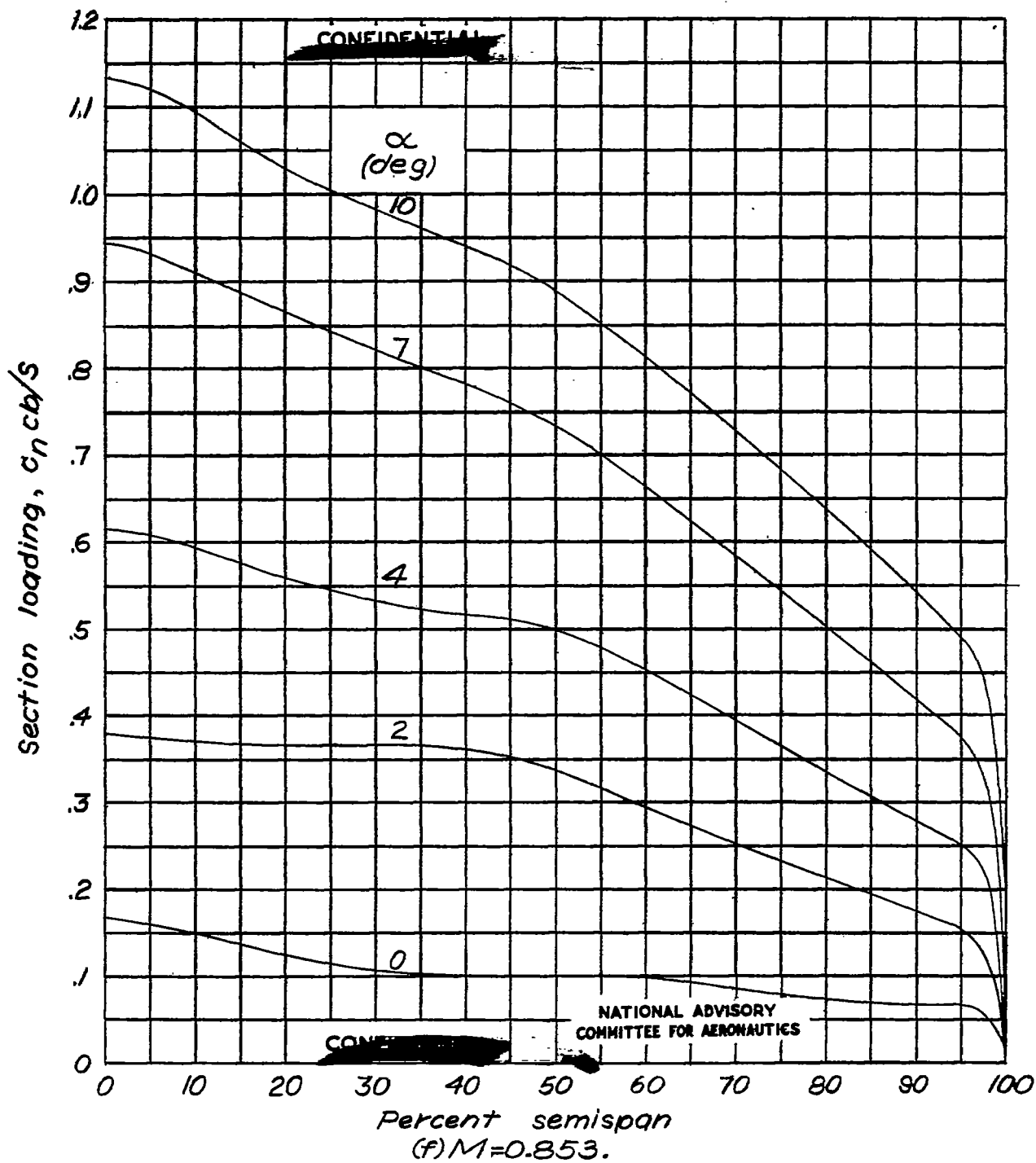


Figure 6.-Continued.

Fig. 6g

NACA RM No. L6H28a

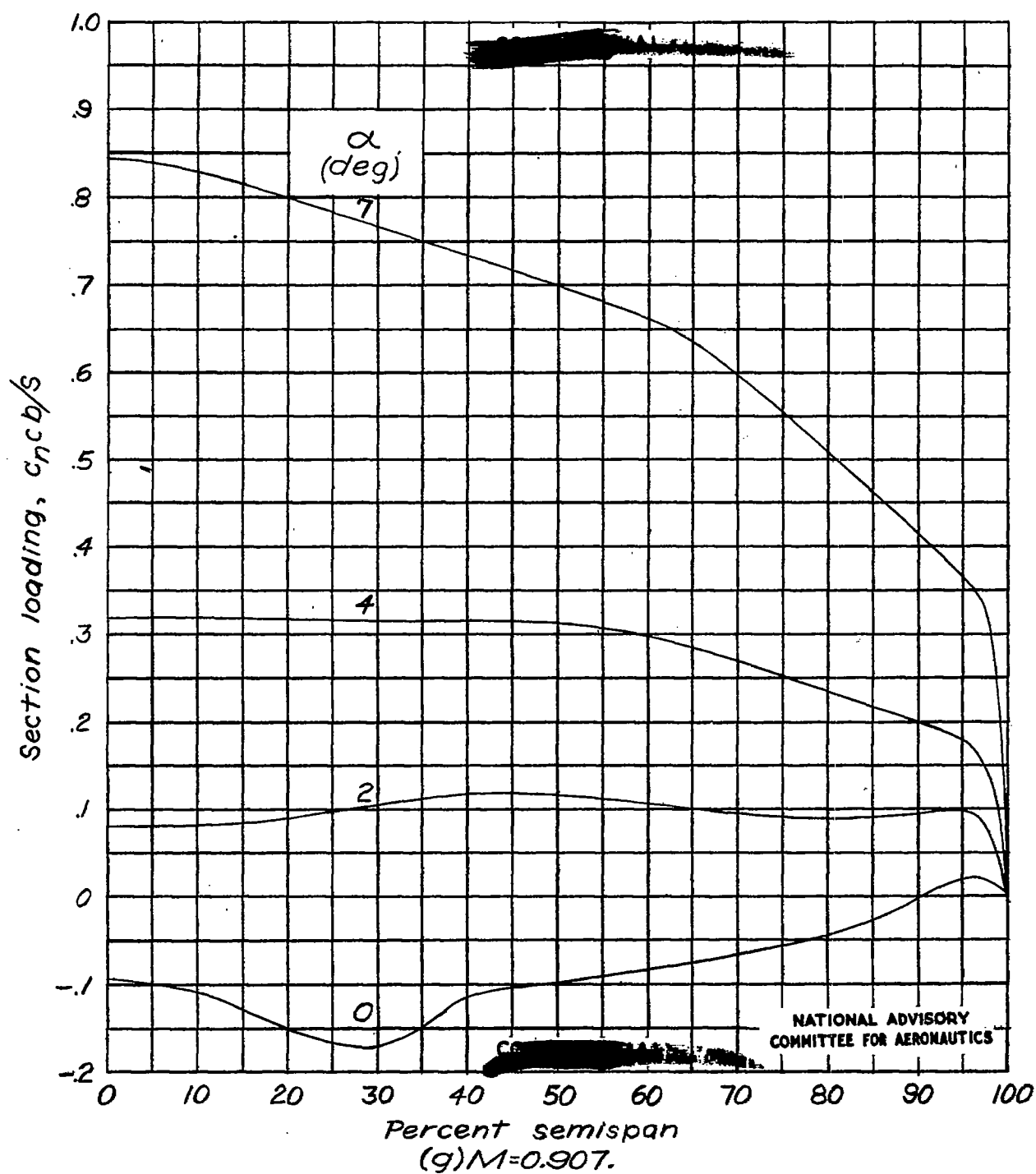


Figure 6.-Continued.

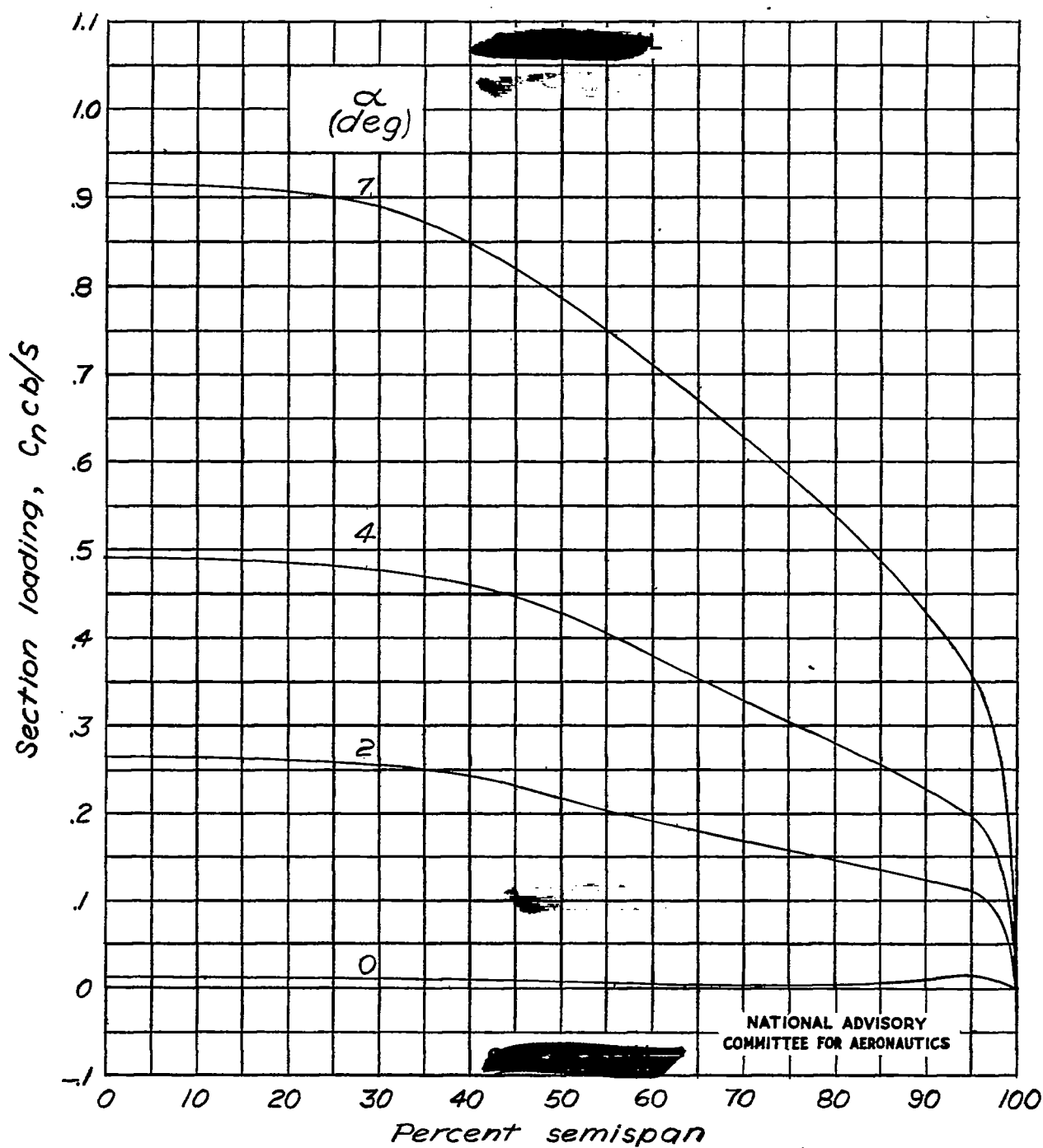


Figure 6 .- Concluded.
(h) $M=0.925$ (uncorrected).

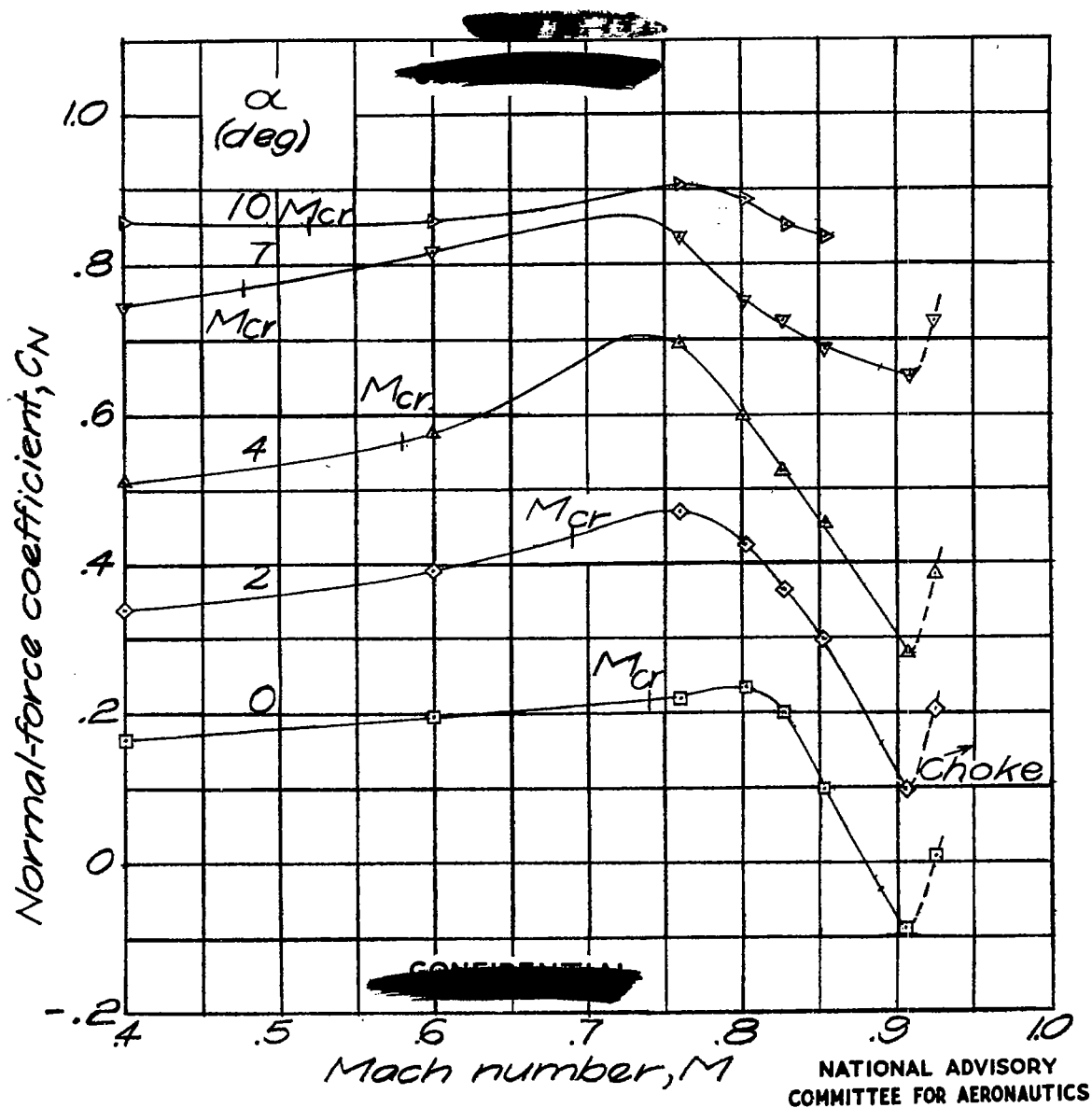


Figure 7. — Variation of wing normal-force coefficient with Mach number.

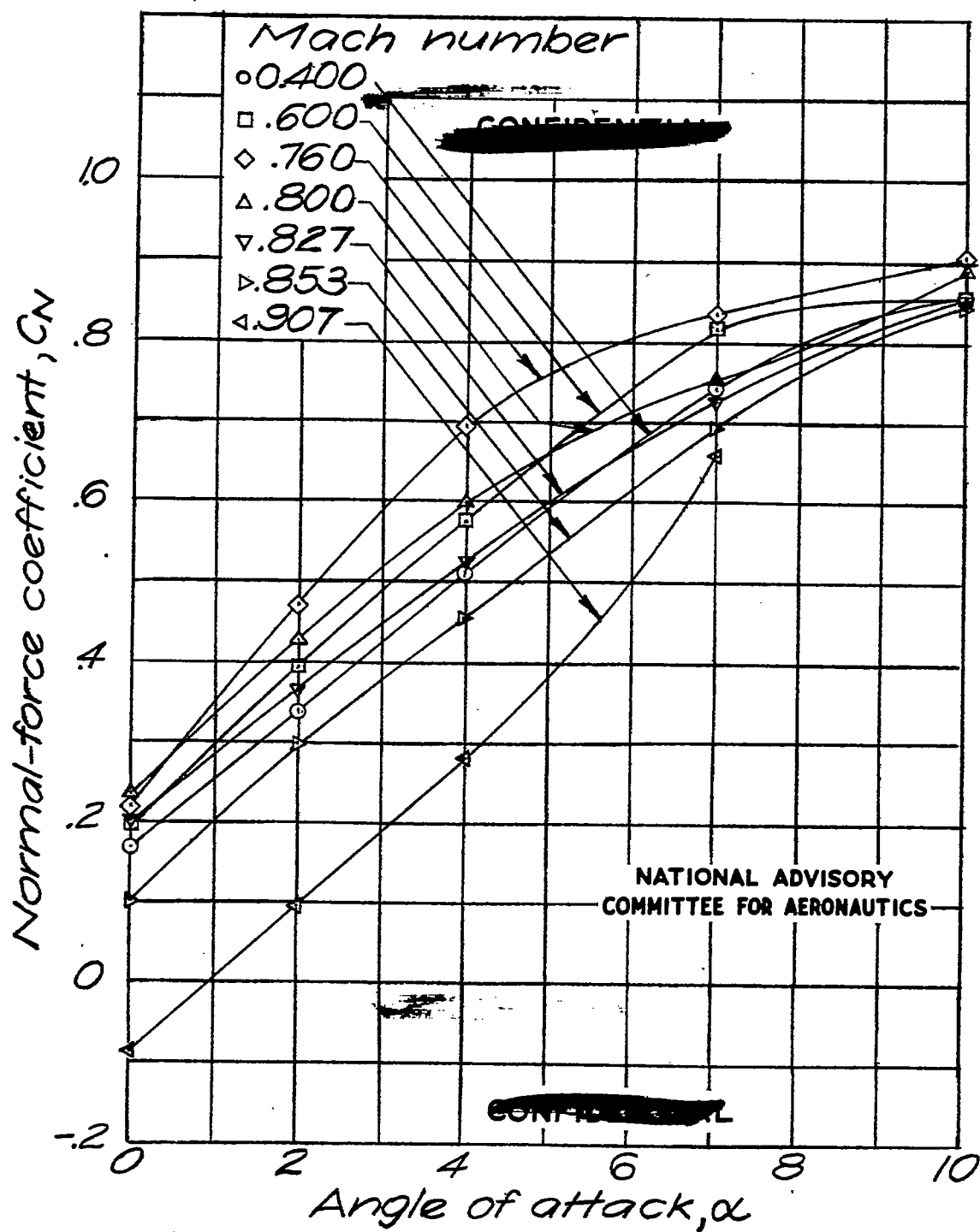


Figure 8.— Variation of normal-force coefficient with angle of attack.

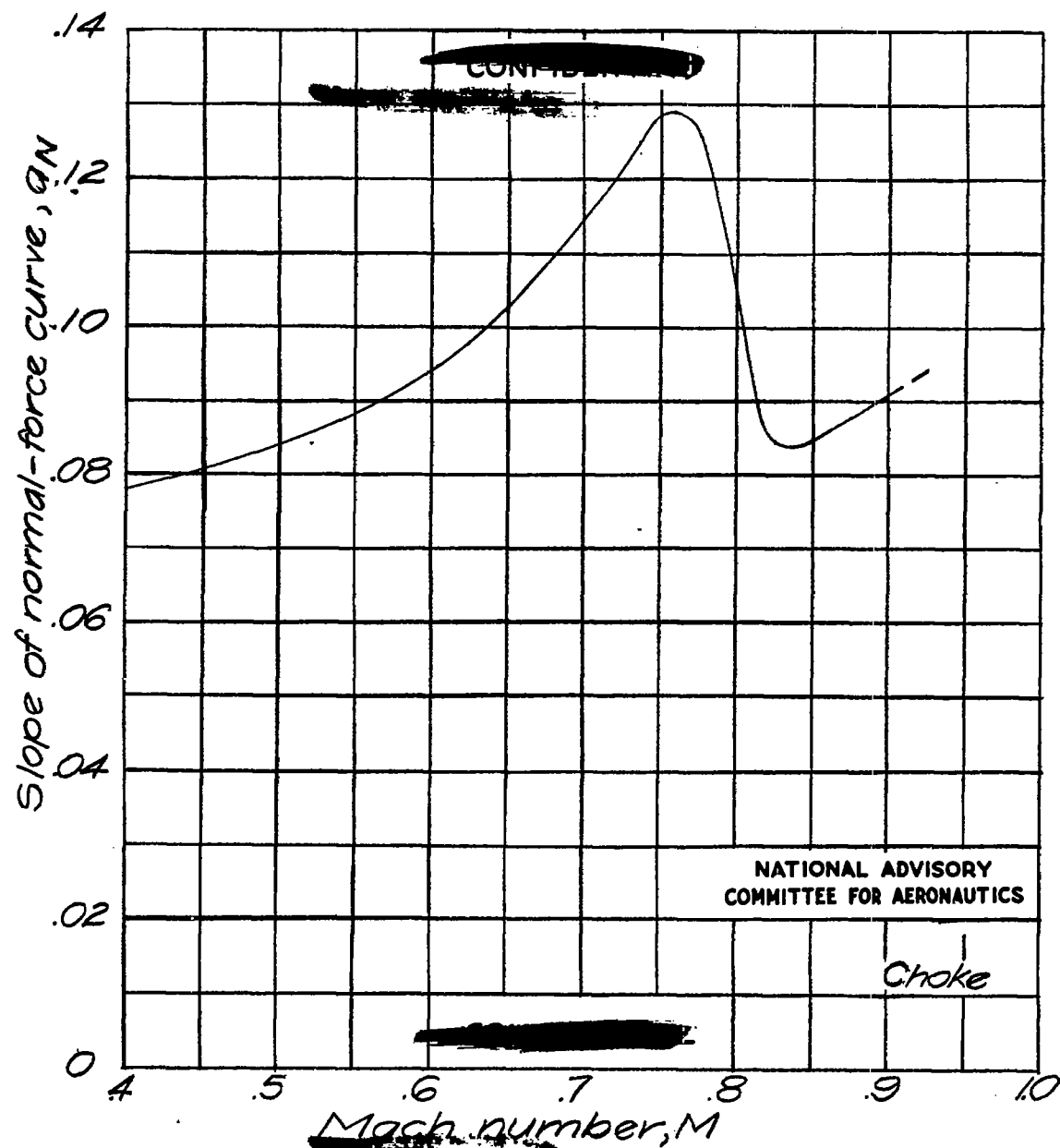


Figure 9.— Slope of normal-force-coefficient curve for 60 pounds per square foot loading at 35,000-foot altitude.

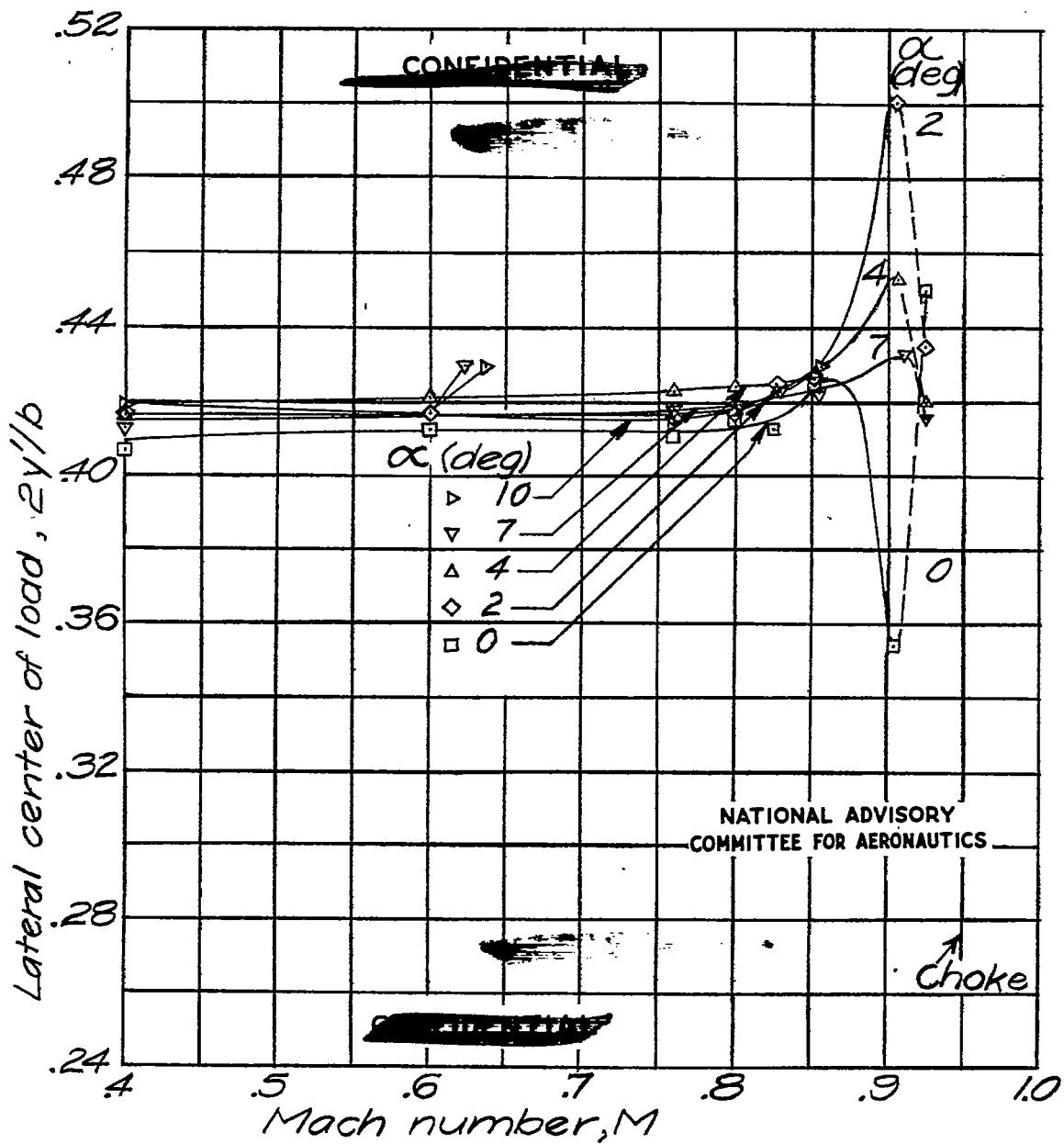


Figure 10. - Variation of center of load on semispan with Mach number.

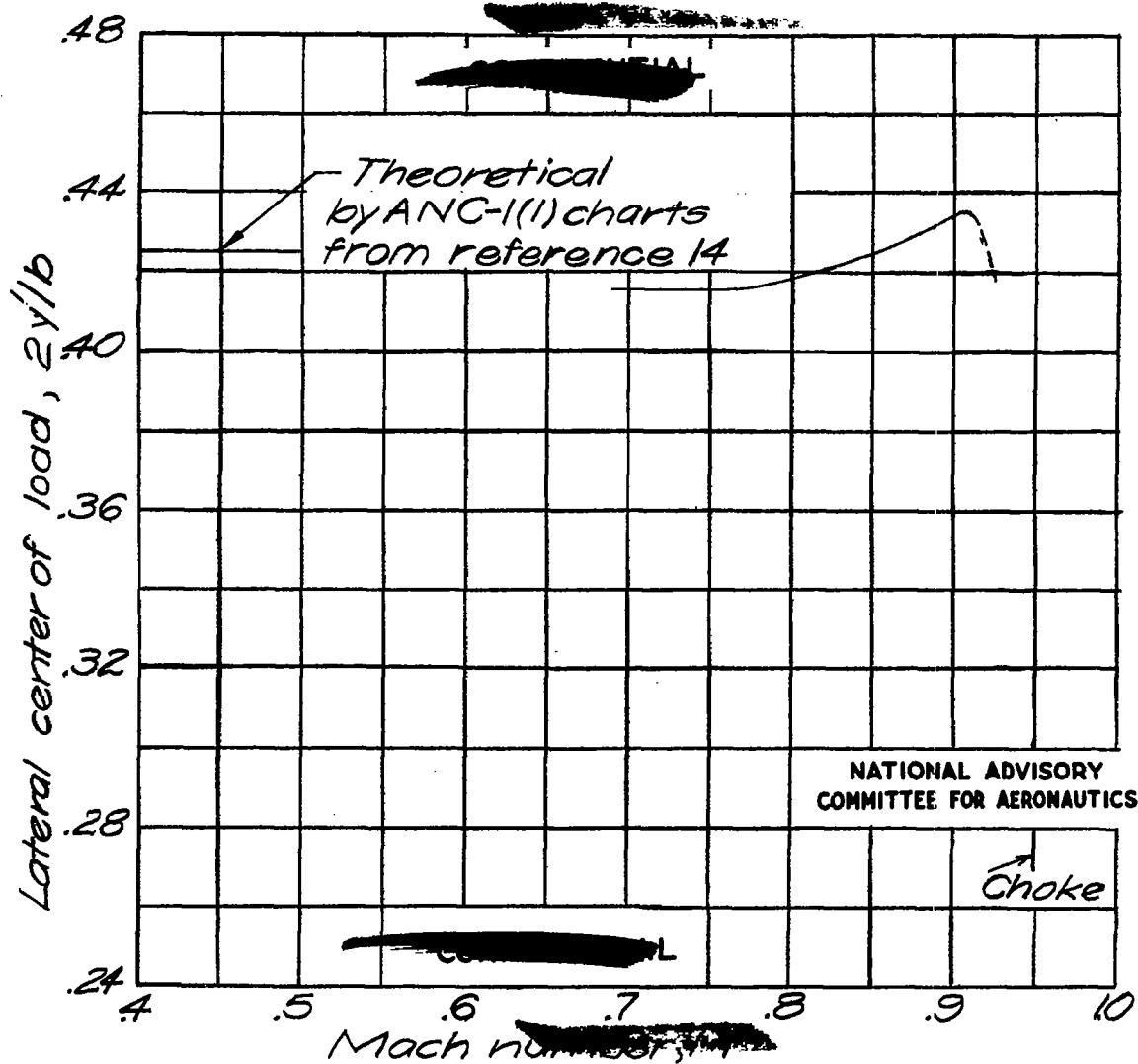


Figure 11. — Variation of wing center of load with Mach number for a wing loading of 180 pounds per square foot at 35,000-foot altitude.

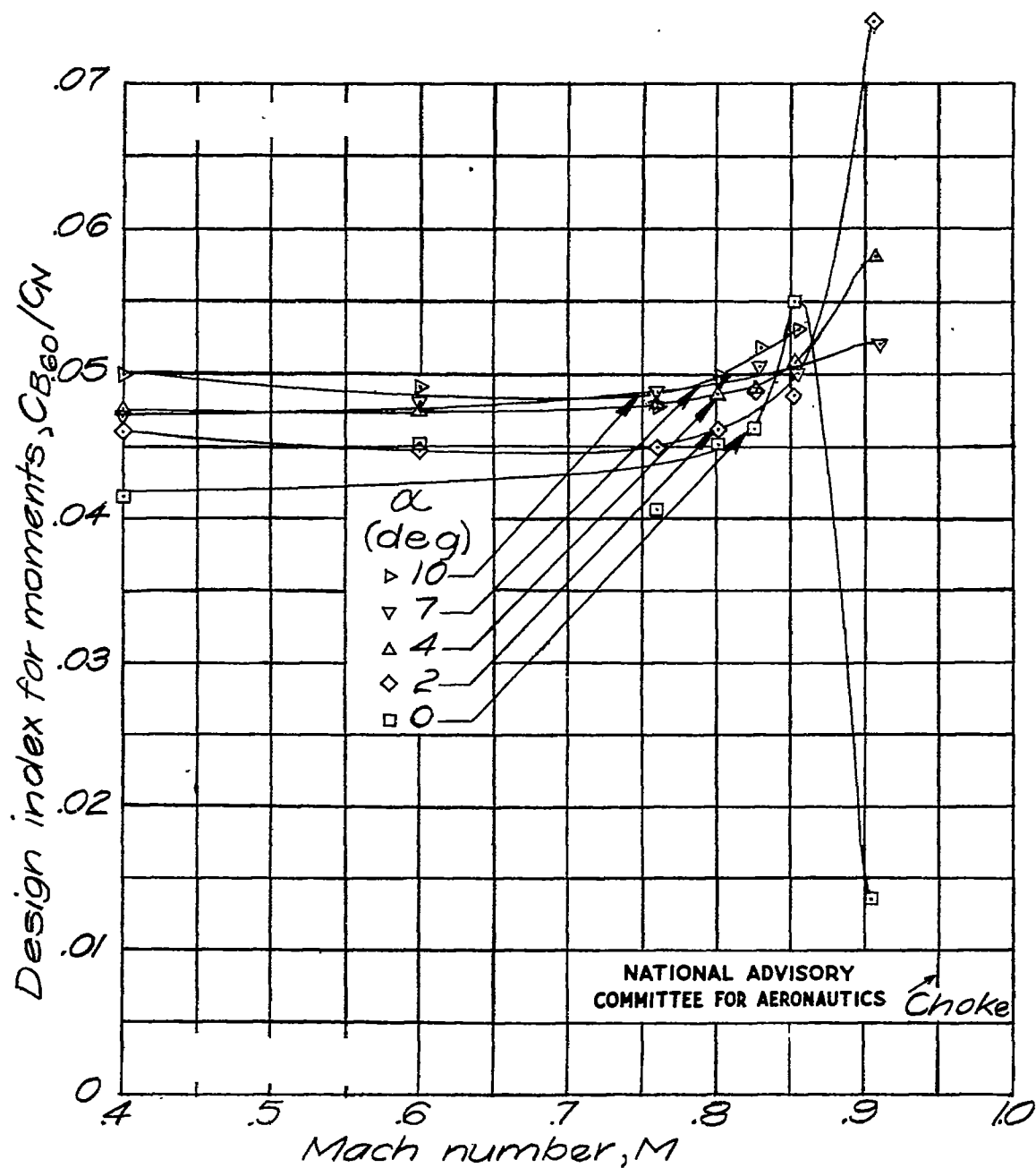


Figure 12. — Variation with Mach number of design indexes for bending moments at the 60-percent-semispan station.

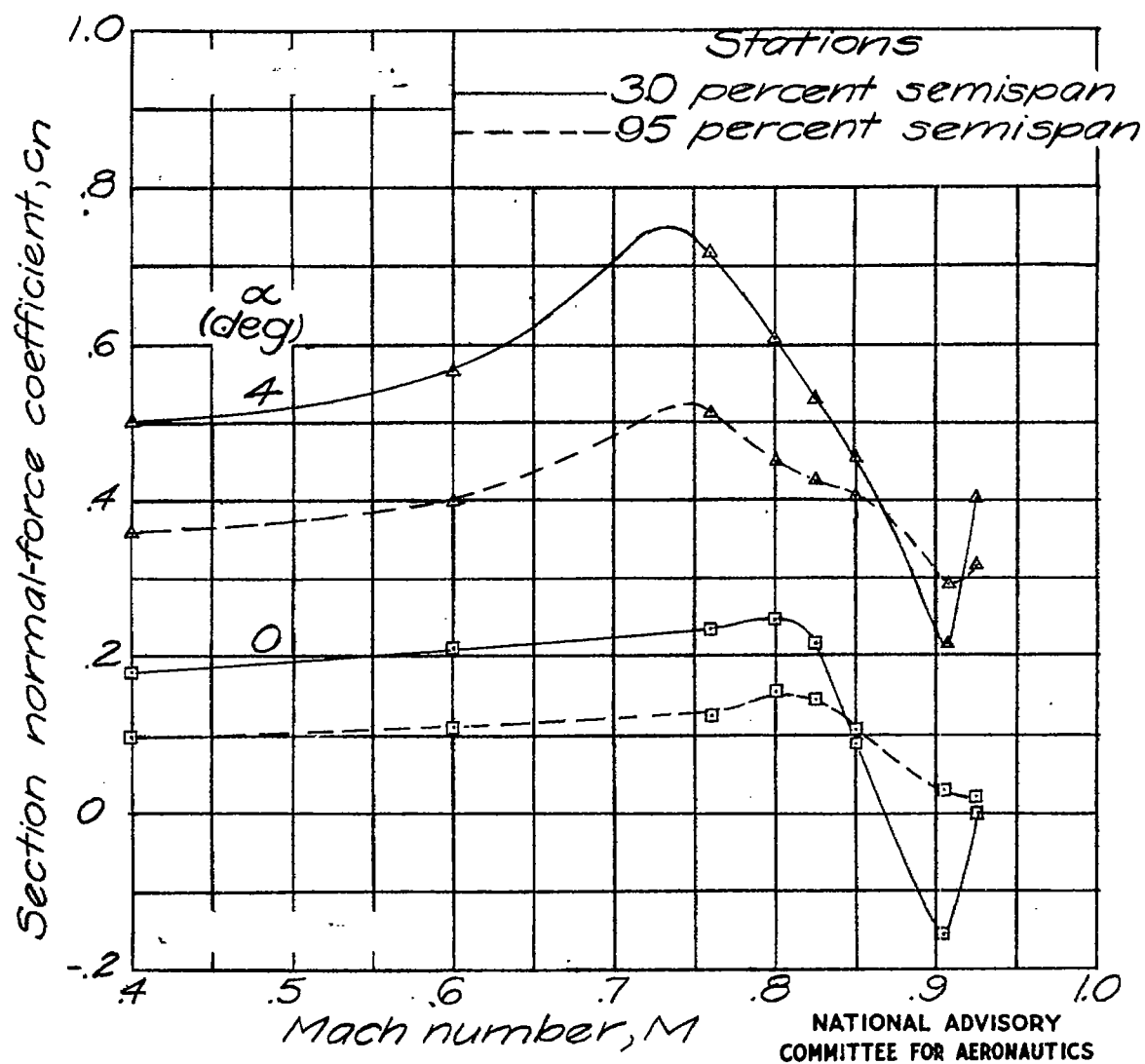


Figure 13. - Variation of section normal-force coefficient with Mach number at two spanwise stations.

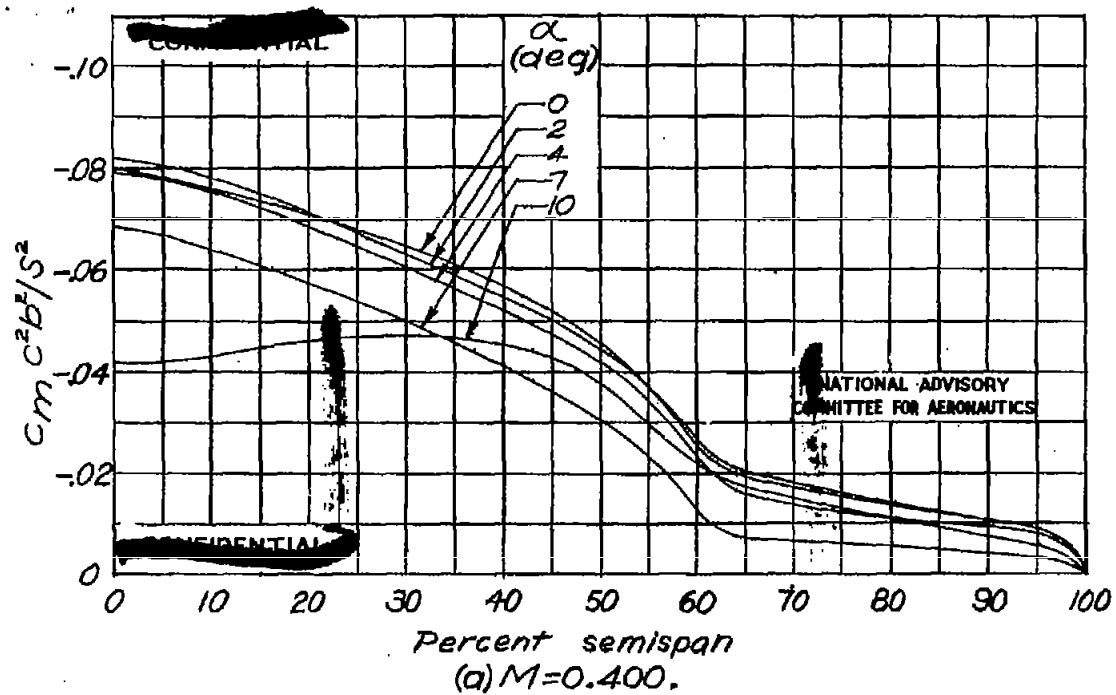


Figure 14.- Spanwise variation in section moment factor.

Fig. 14b

NACA RM No. L6H28a

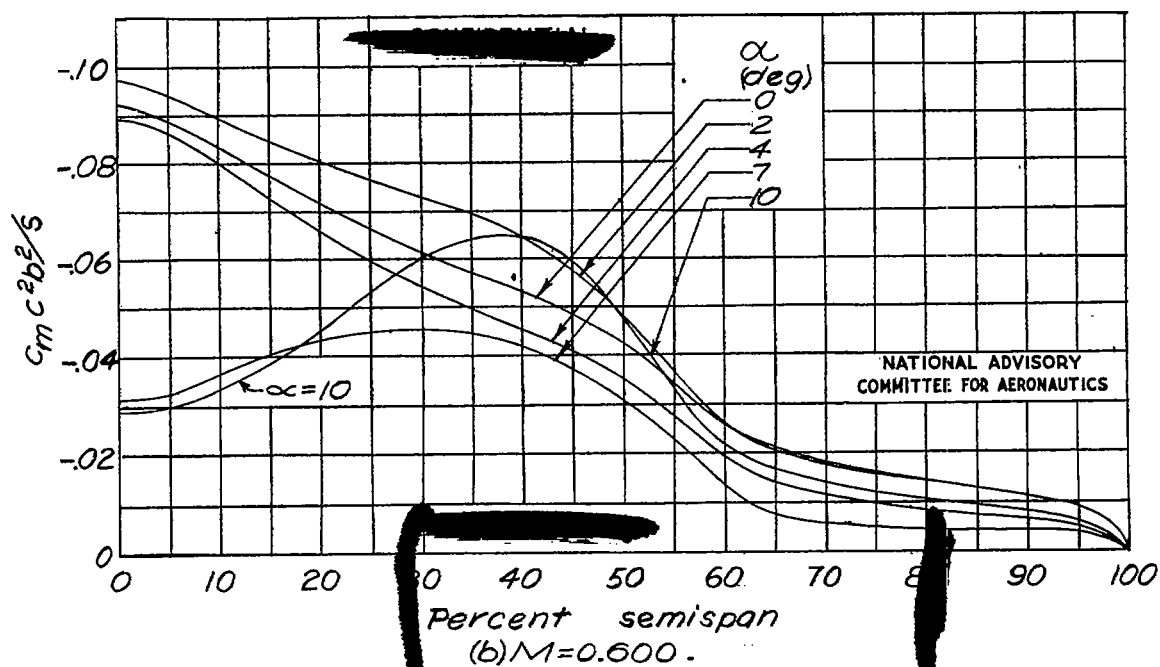


Figure 14.- Continue.

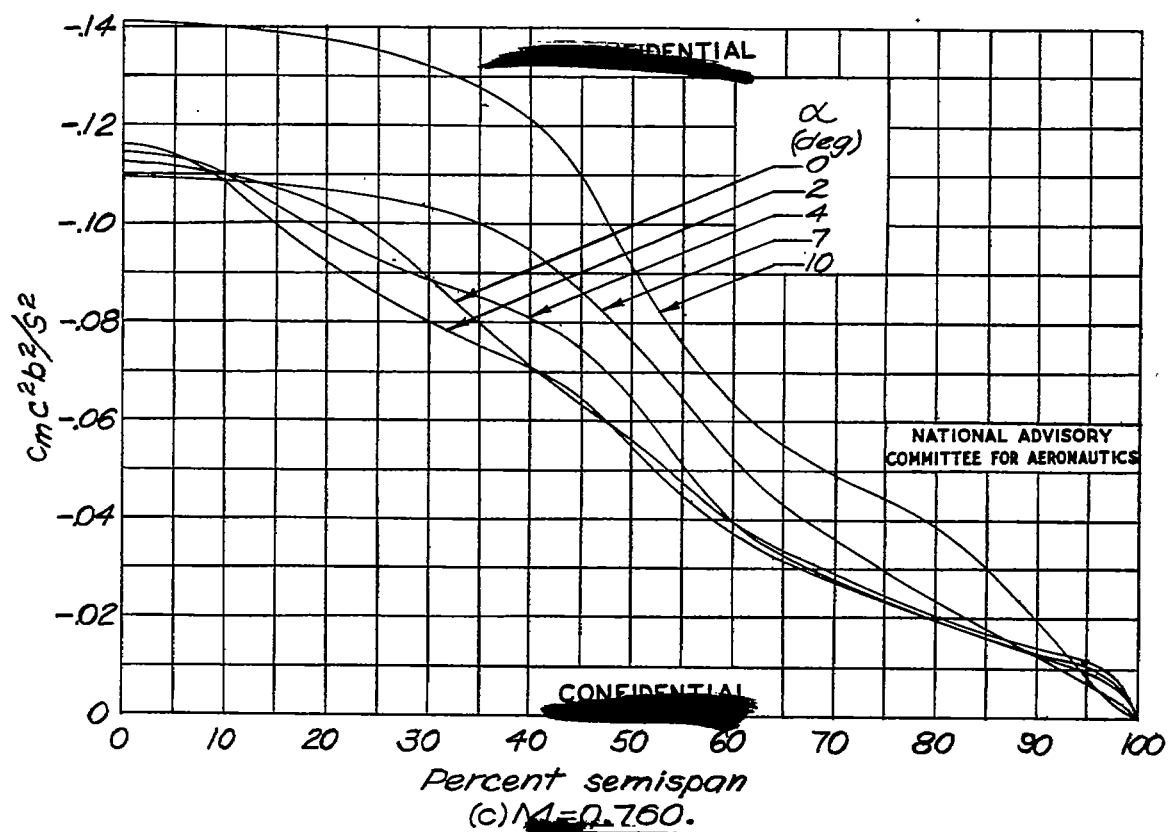


Figure 14.-Continued.

Fig. 14d

NACA RM No. L6H28a

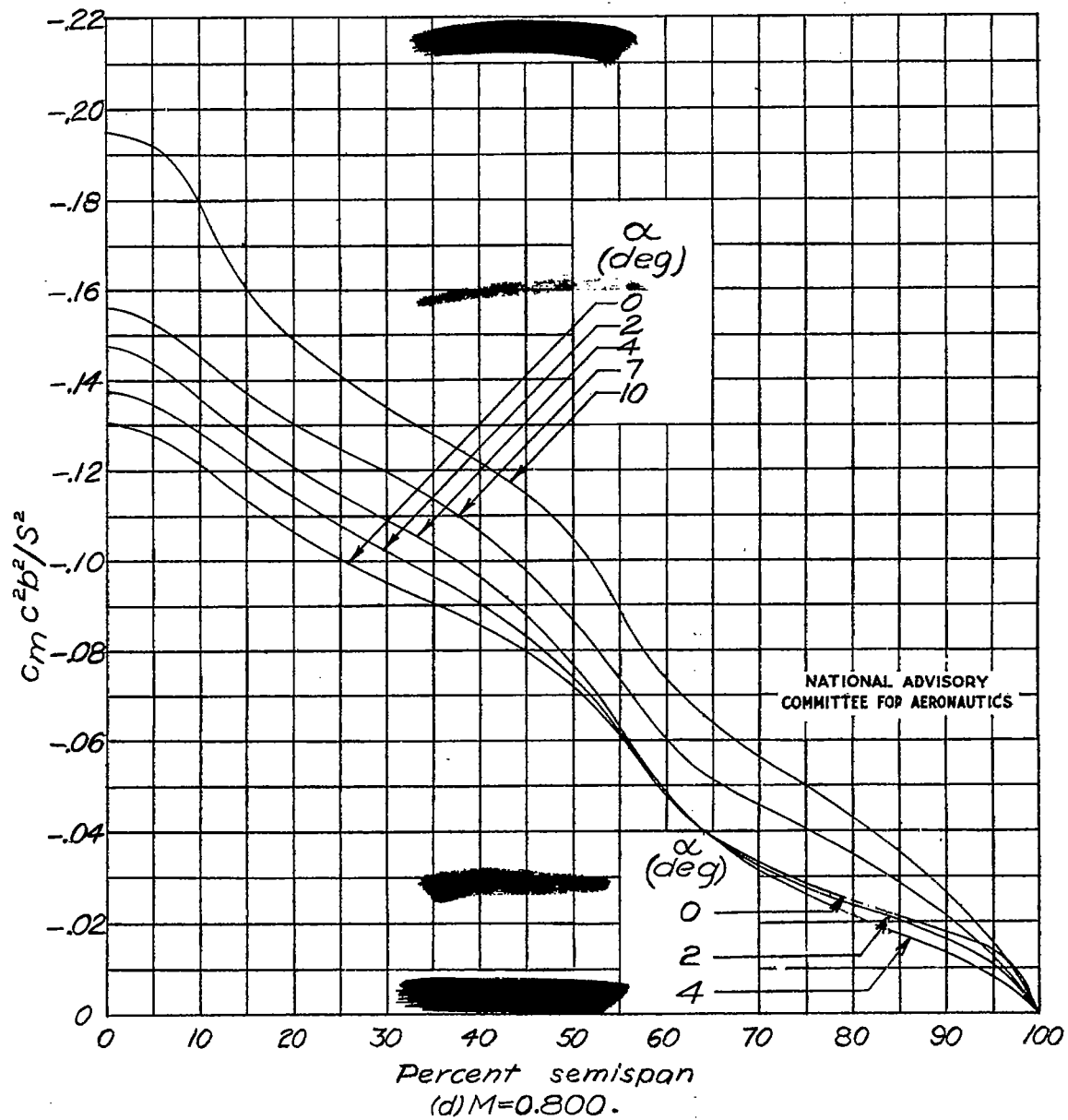


Figure 14.-Continued.

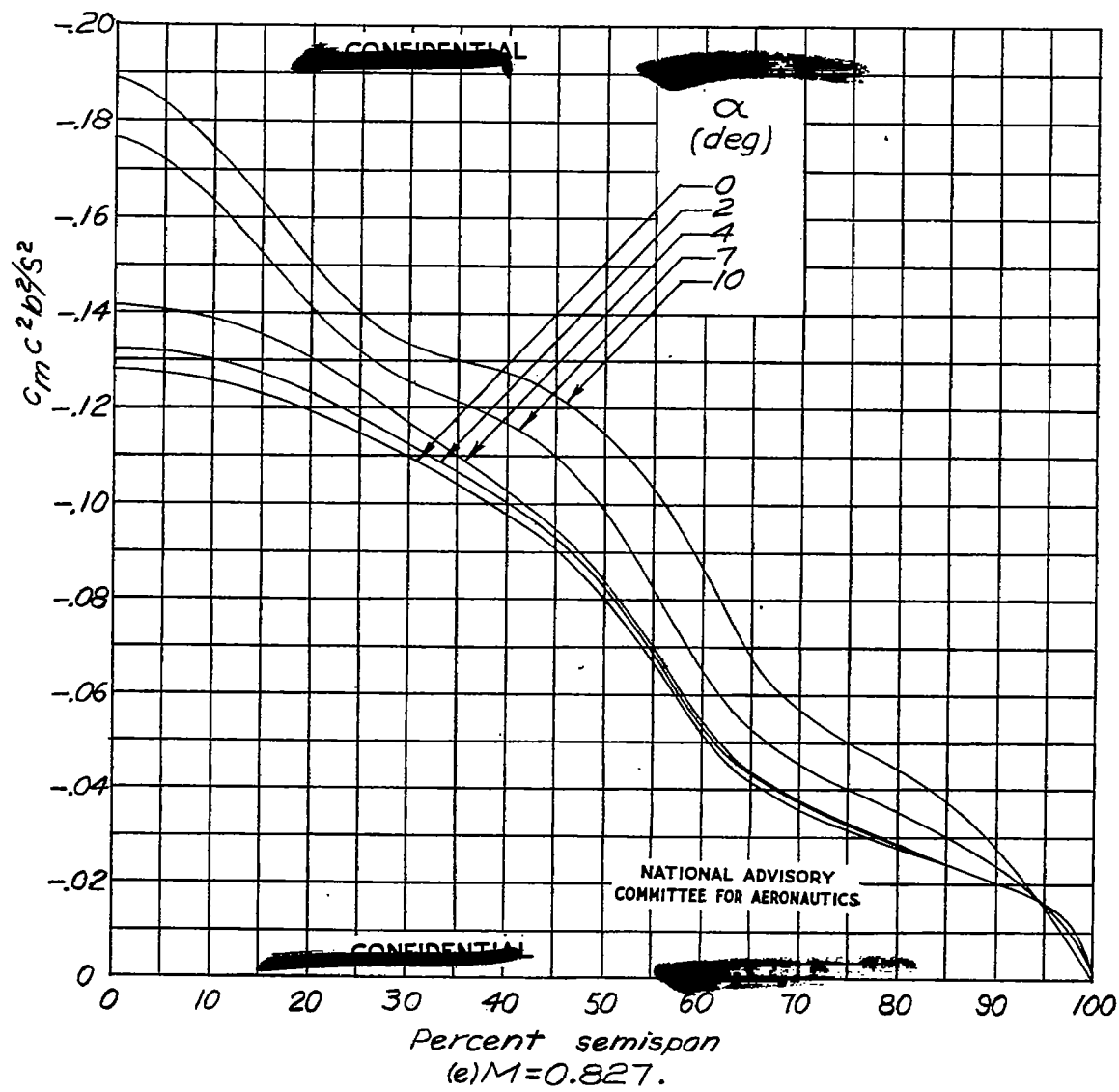


Figure 14.-Continued.

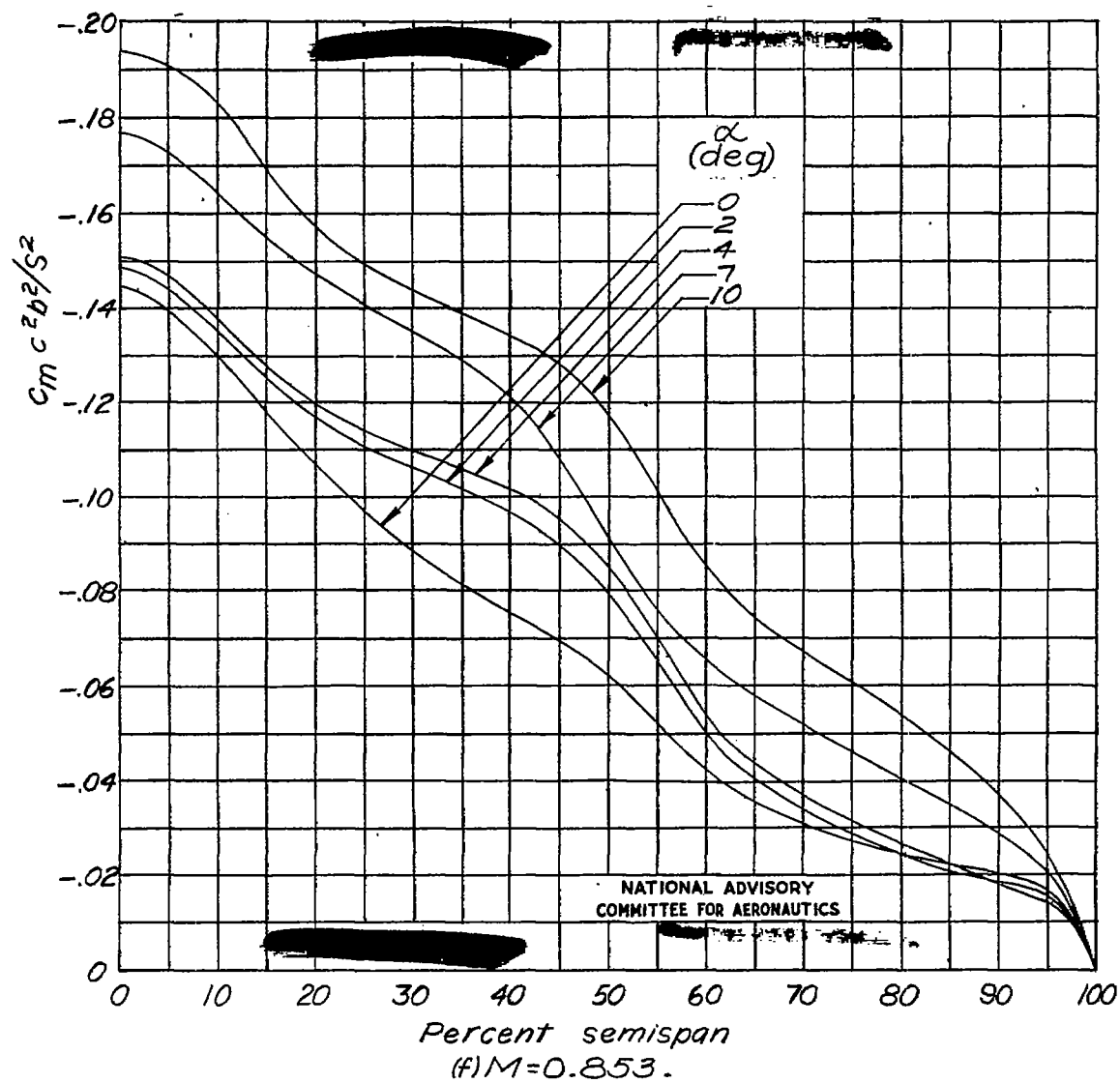


Figure 14.- Continued.

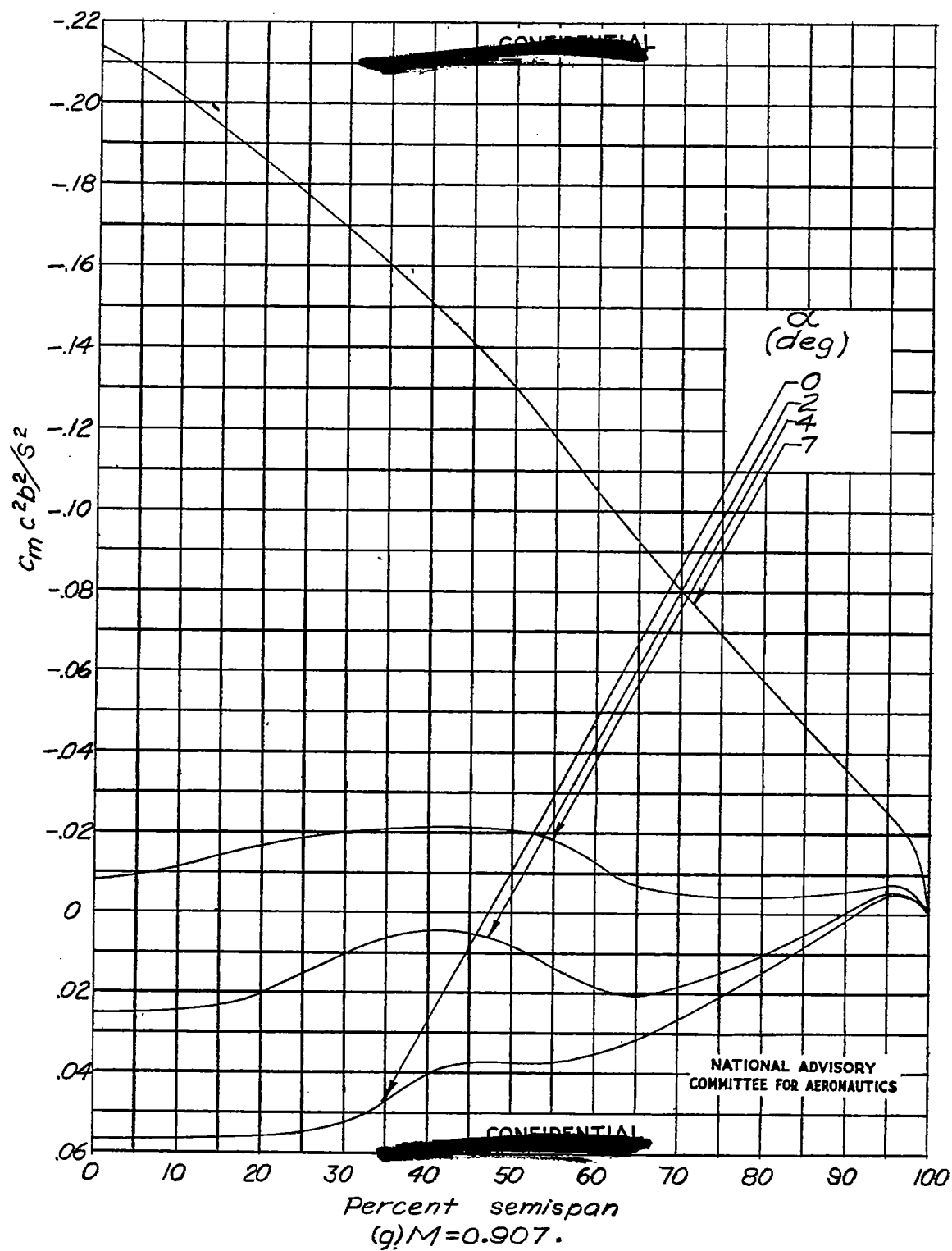


Figure 14.- Continued.

Fig. 14h

NACA RM No. L6H28a

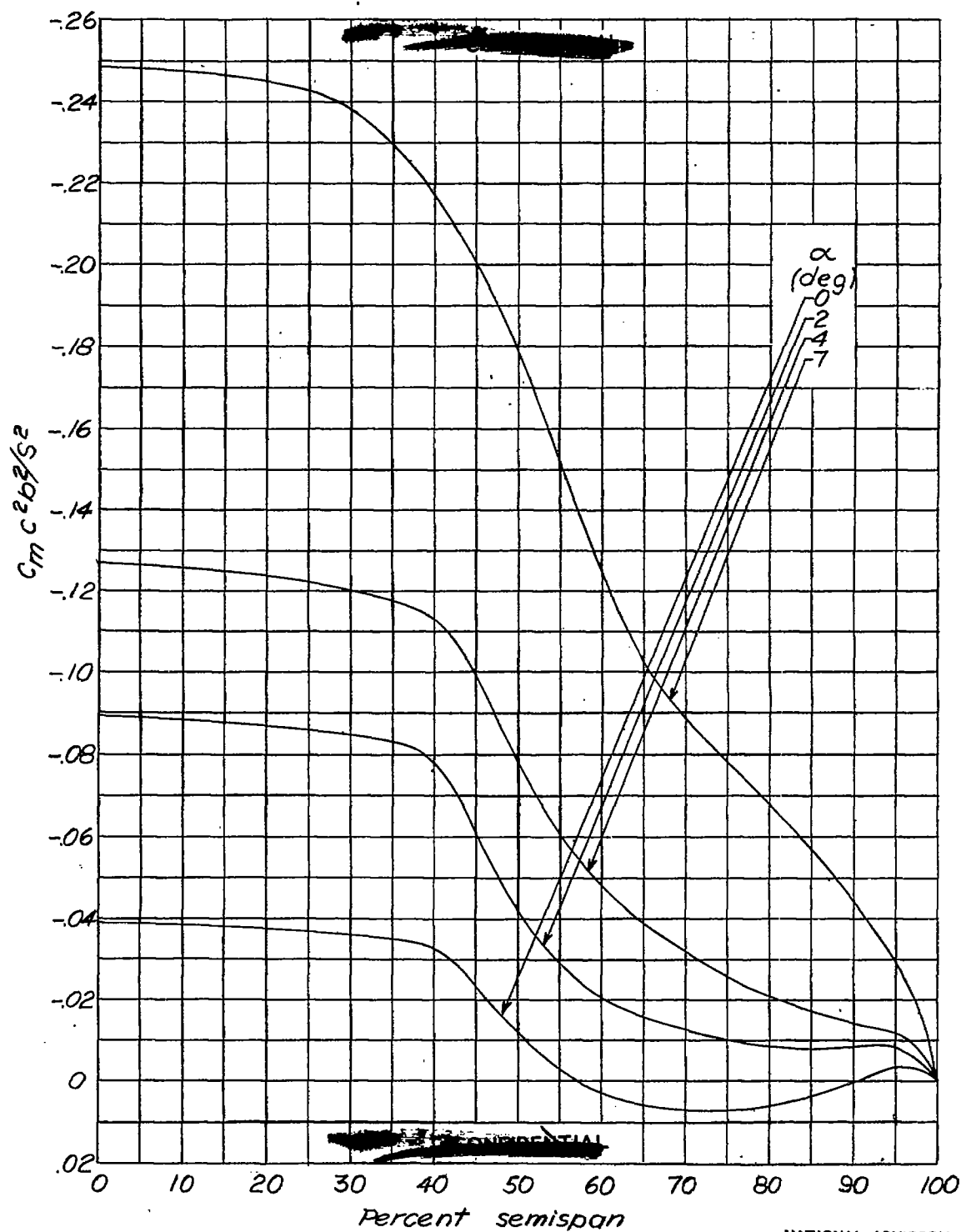


Figure 14.- Concluded.

NATIONAL ADVISORY
COMMITTEE FOR AERONAUTICS

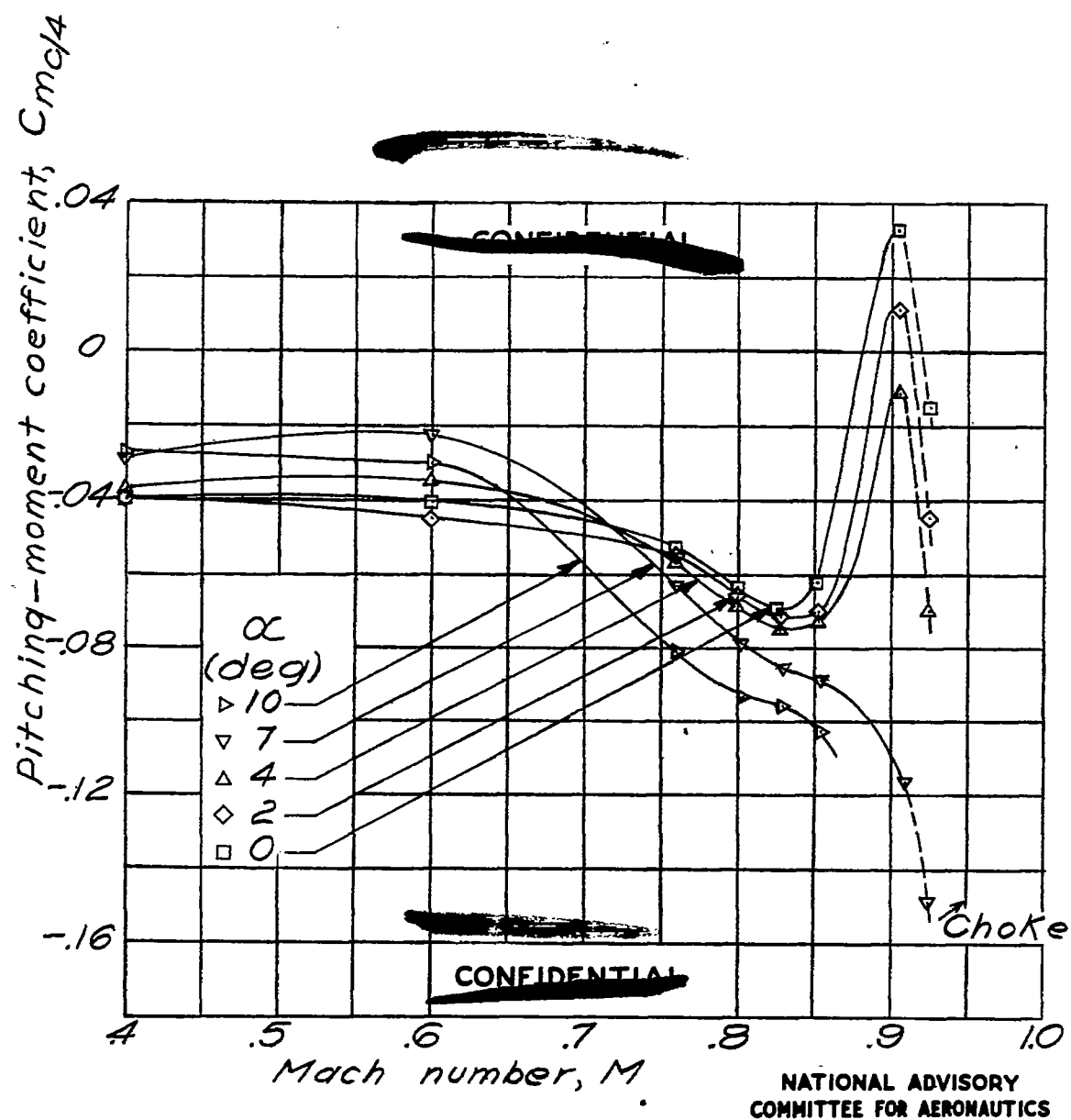


Figure 15.—Variation of wing pitching-moment coefficient with Mach number.

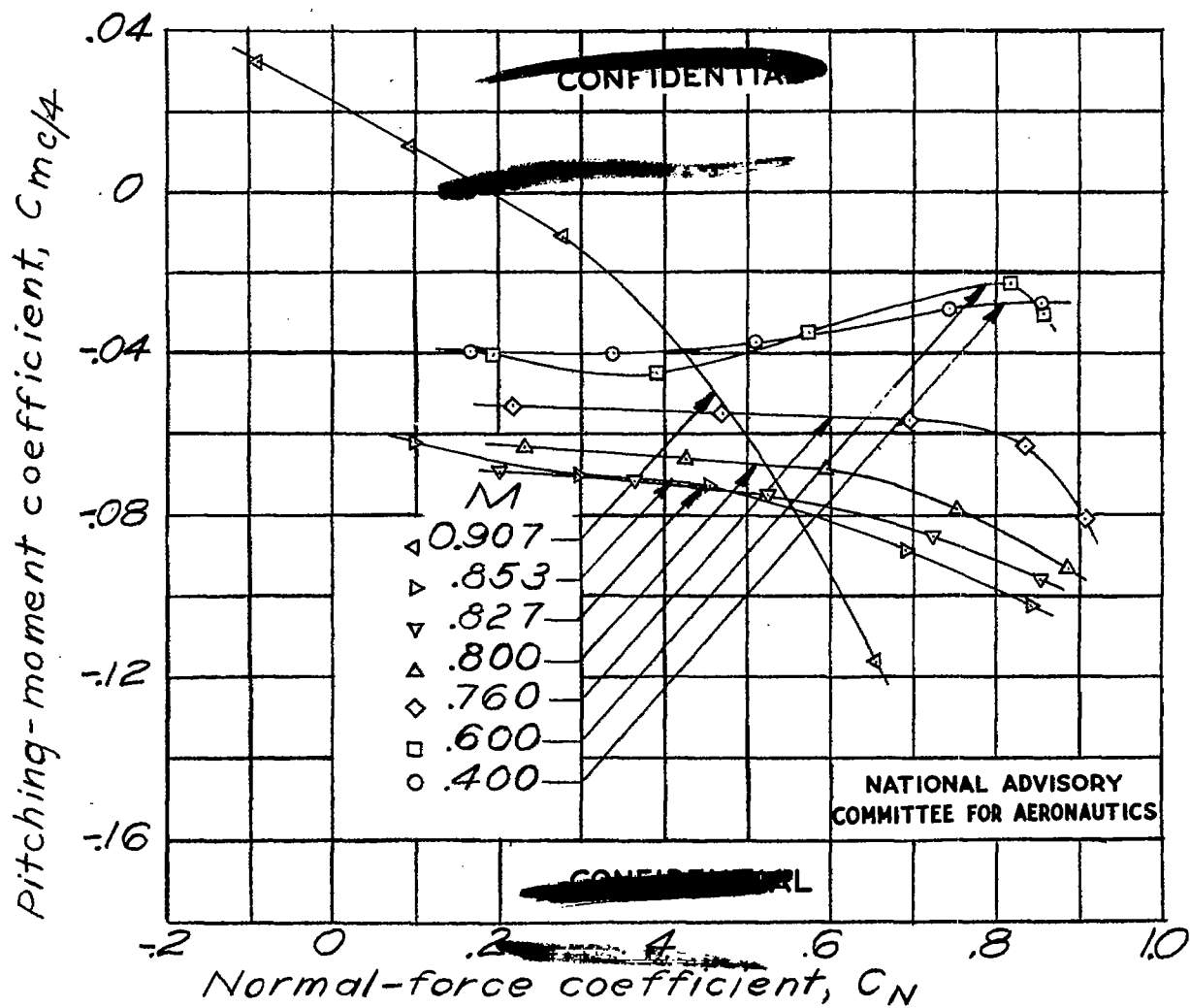


Figure 16.—Variation of wing pitching-moment coefficient with normal-force coefficient.

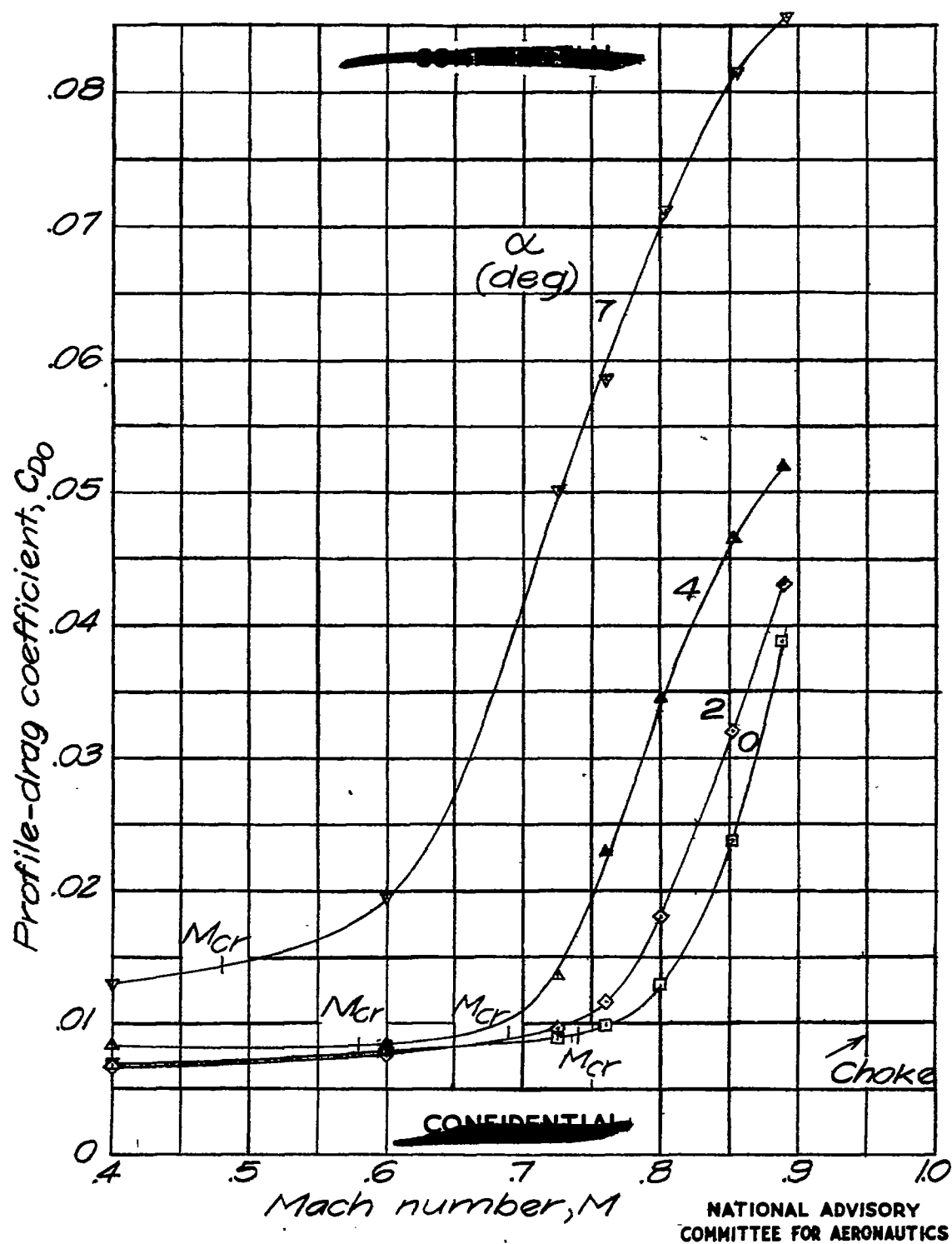


Figure 17.— Variation of wing profile-drag coefficient with Mach number.

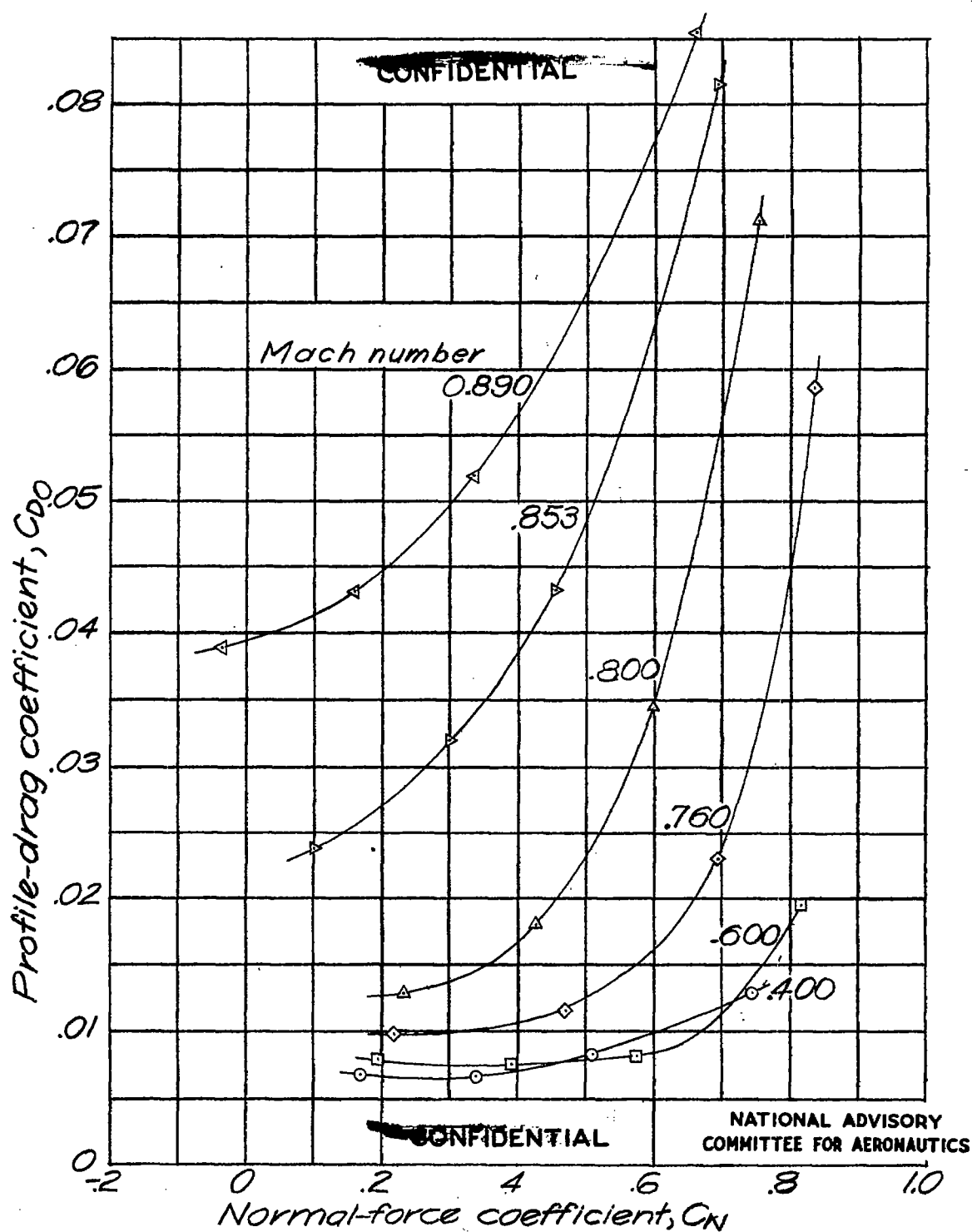


Figure 18.— Variation of wing profile-drag coefficient with normal-force coefficient.

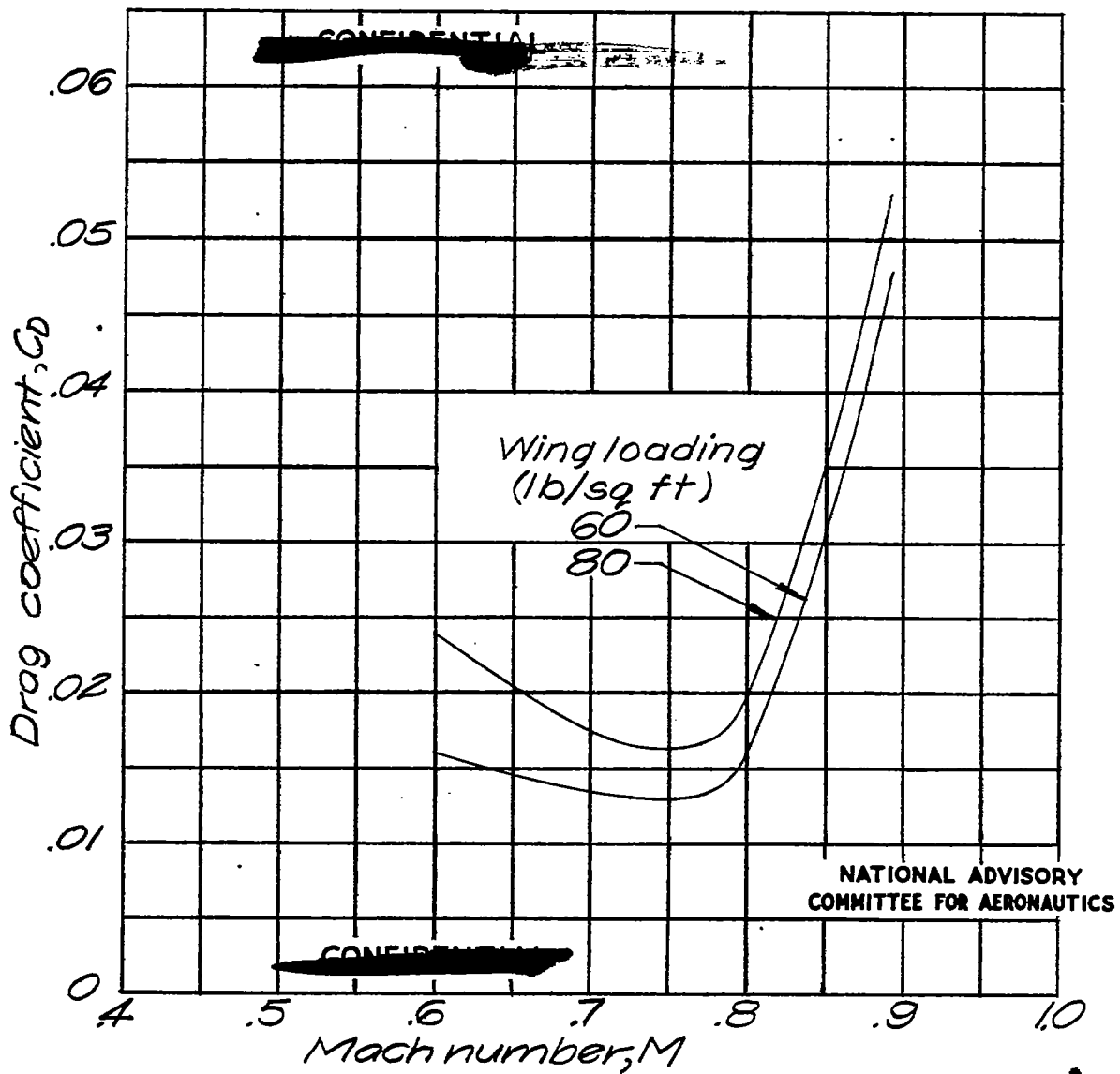


Figure 19.- Variation of drag coefficient with Mach number for wing loadings of 60 and 80 pounds per square foot at 35,000-foot altitude (calculated induced drag included).

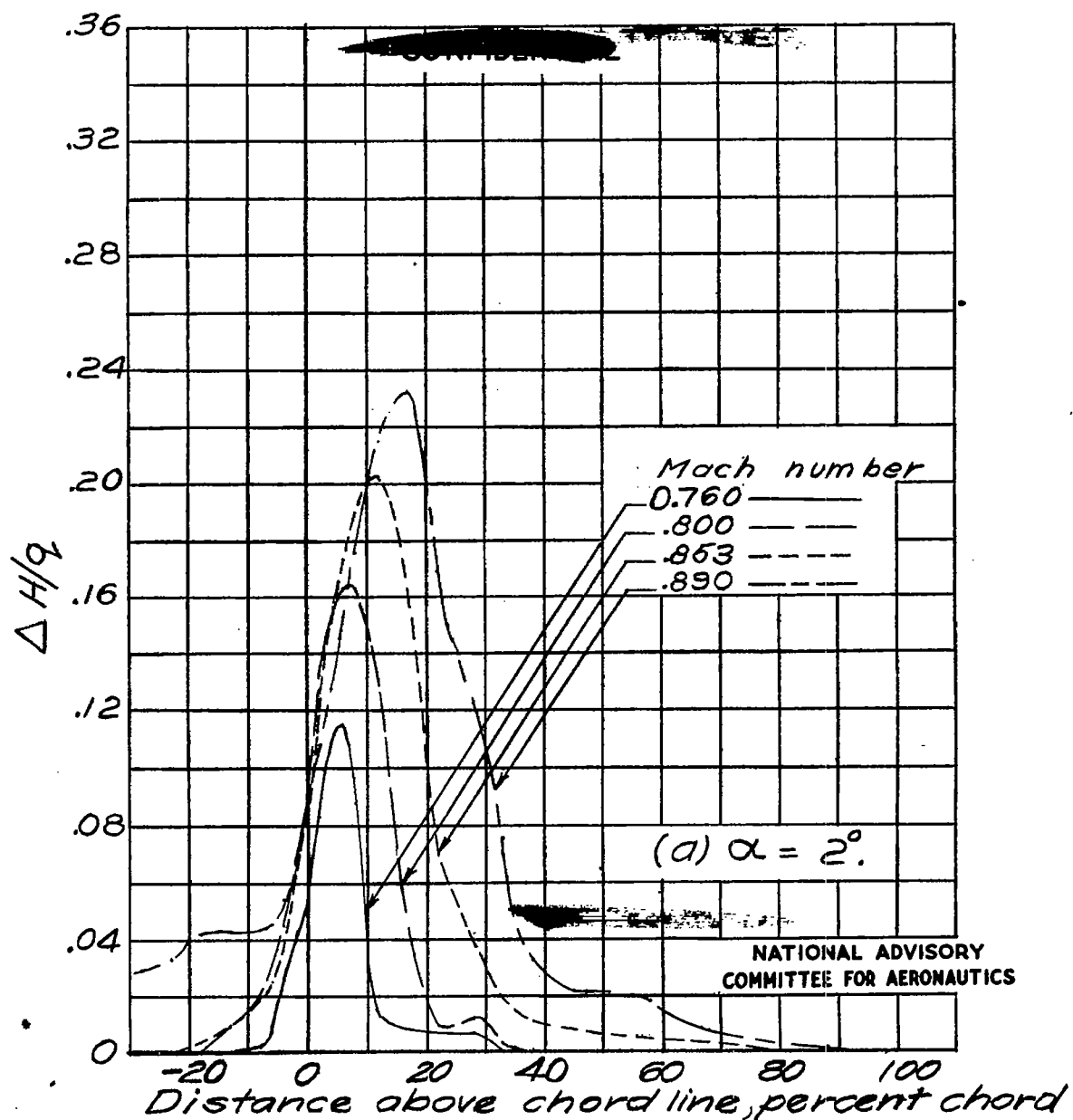


Figure 20.—Wake widths for several Mach numbers 2.82 root chords behind the 25-percent-chord line.

~~CONFIDENTIAL~~

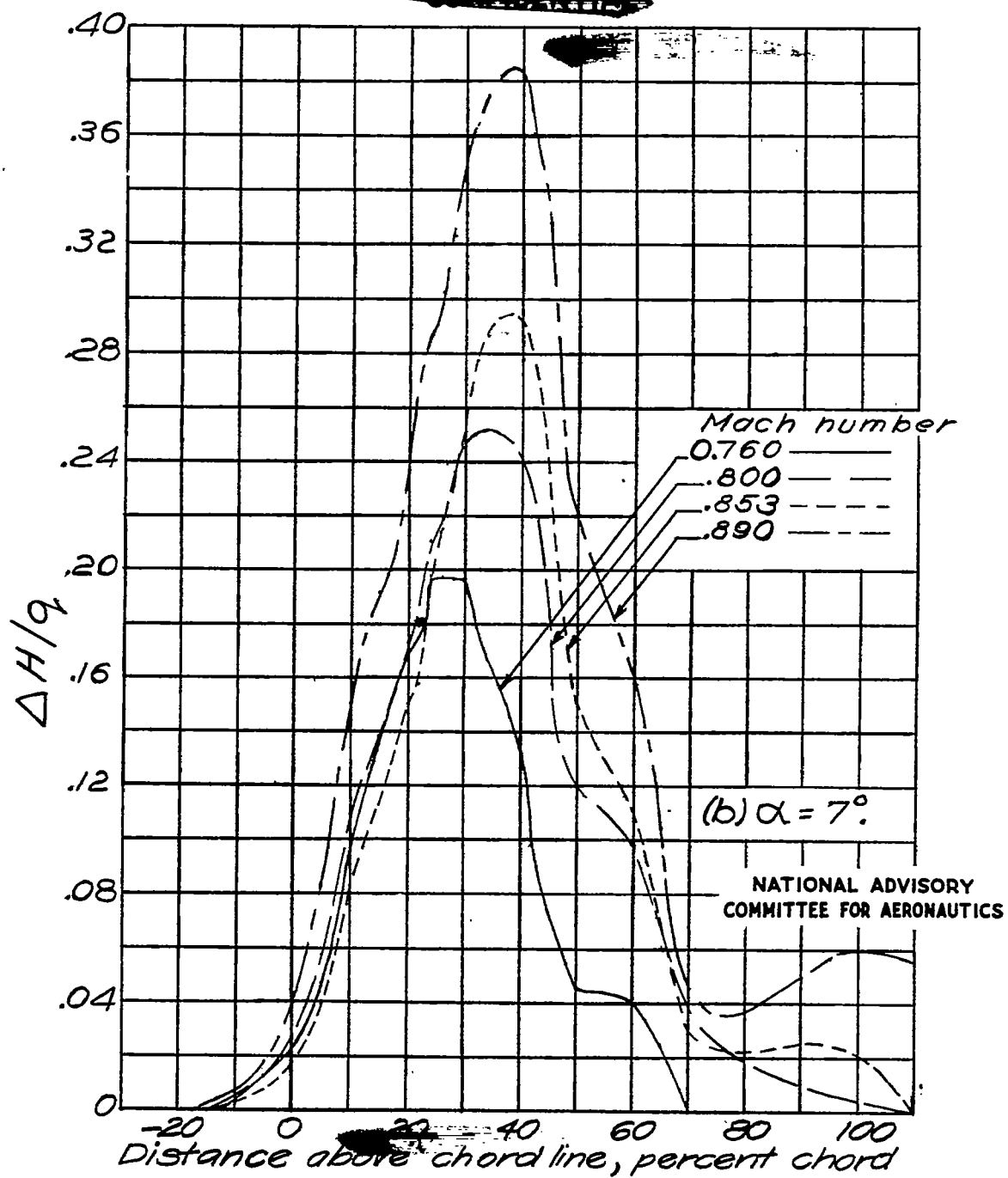
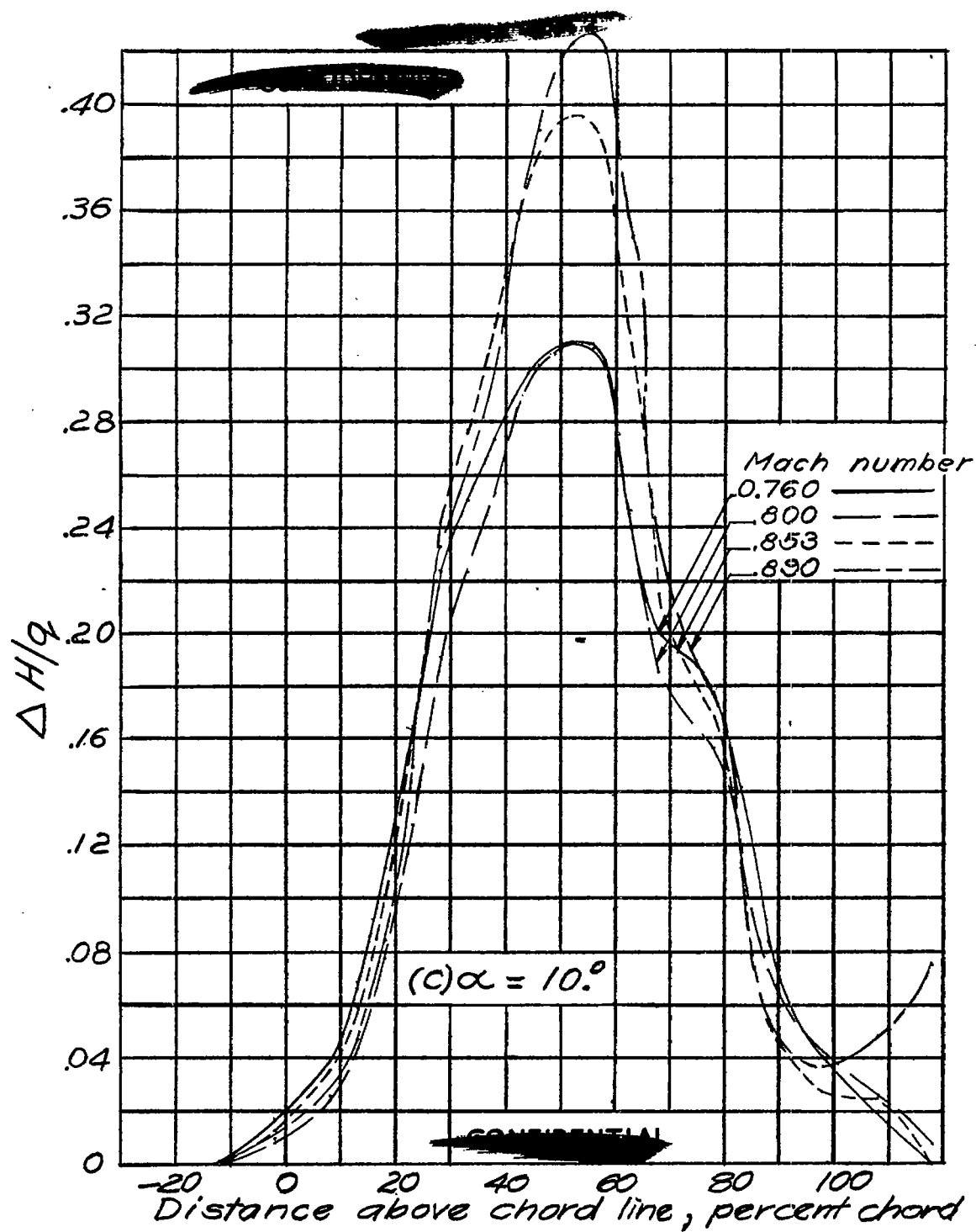


Figure 20 .- Continued.

~~CONFIDENTIAL~~

Figure 20.—~~continued~~.NATIONAL ADVISORY
COMMITTEE FOR AERONAUTICS

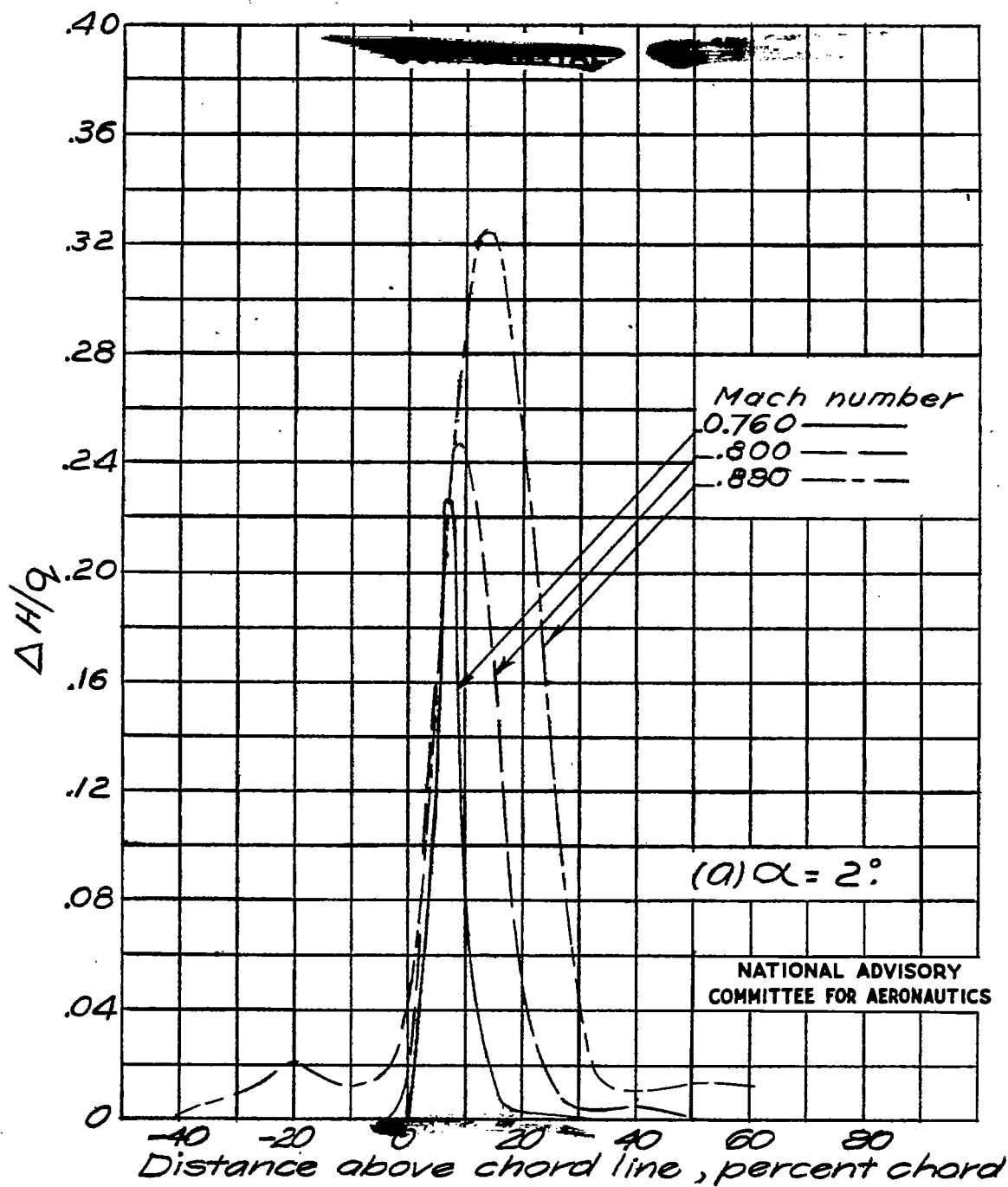


Figure 21 .— Wake widths for several Mach numbers 1.40 root chords behind the 25-percent-chord line.

~~CONFIDENTIAL~~

Fig. 21b

NACA RM No. L6H28a

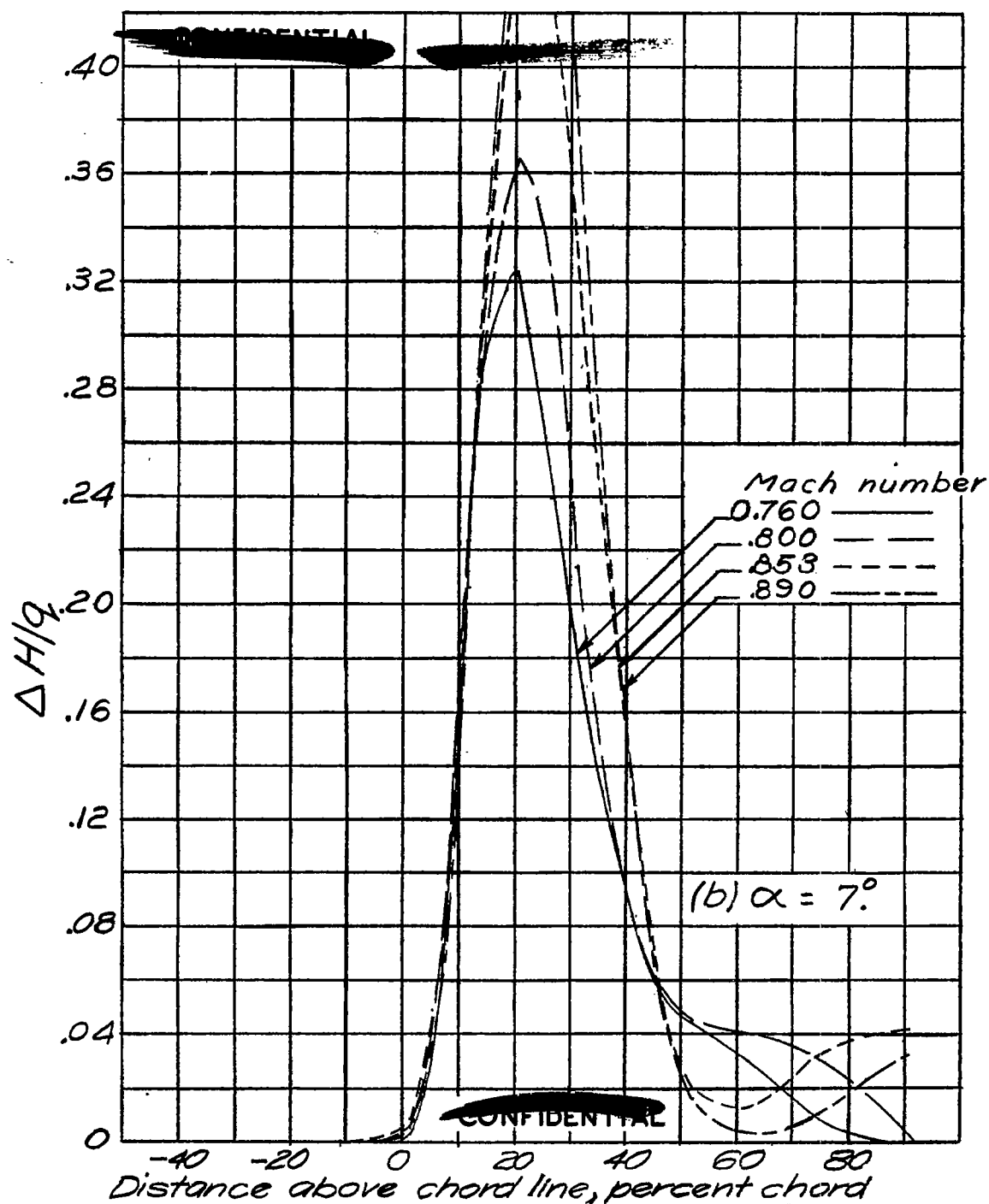


Figure 21 .— Concluded.

NATIONAL ADVISORY
COMMITTEE FOR AERONAUTICS